Quantifying Heatwaves and Seagrass Recovery Dynamics in Aquatic Ecosystems

Spencer John Tassone
Virginia Beach, Virginia

P.B.G.C. Geographic Information Systems, Virginia Commonwealth University, 2019
M.S. Biology, Virginia Commonwealth University, 2017
B.S. Environmental Studies, Virginia Commonwealth University, 2014
A.S. Social Sciences, Tidewater Community College, 2011

A Dissertation presented to the Graduate Faculty
of the University of Virginia in Candidacy for the Degree of
Doctor of Philosophy

Department of Environmental Sciences

University of Virginia
April 2023

Abstract

Increasing climatic variability has amplified the frequency of pulsed disturbance events, including extremes in temperature. These discrete periods of anomalously high temperature, referred to as heatwaves, have gained attention due to their destructive and lasting impacts relative to longer-term increases in mean temperature. Heatwaves in the open and coastal oceans have increased in frequency, duration, and magnitude in recent decades, occasionally producing mass mortality and regime shifts. While positive water temperature trends have been documented in many inland waterways, heatwaves in lotic systems have not been analyzed. In this dissertation, I quantified trends in heatwaves for rivers, estuaries, and coastal sediments. I also conducted a seagrass removal experiment to test seagrass resilience (i.e., recovery rate) to a heatwave-like disturbance event and synthesized related studies on seagrass recovery following disturbance.

Riverine heatwaves increased in frequency throughout the United States over the period 1996-2021. Lotic heatwaves varied based on atmospheric temperature, discharge, stream order, and position relative to a reservoir. There were no significant trends in estuarine heatwaves based on analyses of 17 sites from 1996 to 2019. However, estuarine heatwaves co-occurred with deleterious water quality conditions such as extreme low dissolved oxygen and acidic pH events. Within the Virginia Coastal Reserve (VCR) over the period 1994-2022, coastal sediment heatwaves increased in frequency at a depth of 5 cm and were tightly coupled with water column heatwaves.

Seagrasses were removed from replicated plots at two locations within a large VCR meadow. Seagrass recovery was faster at the meadow interior relative to the edge, likely due to greater hydrodynamic stress at the meadow edge. Seagrass recovered linearly, independent of

position within the meadow, and were facilitated by lateral clonal growth and seedling recruitment. Lastly, the literature synthesis provided evidence that 47% of known seagrass species have been included in English language disturbance-recovery studies but that the majority of studies have occurred in monocultures of the genus *Zostera*. Experimental disturbances were most often conducted on relatively small spatial scales (median = 0.25 m^2), likely overrepresenting the contribution of lateral clonal growth and underrepresenting the effect of hydrodynamics that larger disturbances experience.

This dissertation shows how climate change signals are manifesting in aquatic ecosystems. My findings provide an assessment of heatwaves in rivers, estuaries, and coastal sediments and the largest-scale experimental analysis of seagrass recovery. These studies suggests that key ecosystem services such as maintaining high water quality and high carbon sequestration could be reduced as heatwaves and disturbances become more frequent in coastal areas with a warming climate. Lastly, my dissertation highlights the value of long-term monitoring in establishing baseline assessments that inform ecosystem management.

Acknowledgments

I have many people to thank for their support in helping me achieve my academic goal of producing this dissertation. I am perpetually grateful for the thoughtful guidance that my advisor, Michael Pace, has generously provided me over the years. I have also benefitted from an outstanding Pace Lab cohort, including Alice Besterman, Cal Buelo, Dat Ha, and Jonathan Walter, who have entertained thoughtful academic and ecological discussions and provided levity and encouragement during successes and setbacks – thank you. Thank you to my committee members Karen McGlathery and Patricia Wiberg for their feedback and advice, and Julianne Quinn for serving as my Dean's Representative.

Many thanks to my office mates, along with my colleagues and the faculty in the Virginia Coast Reserve LTER Lagoon Group, whose feedback and companionship have been invaluable. Thank you to the VCR staff (Cora Baird, Amelie Berger, Tom Burkett, Buck Doughty, Donna Fauber, Sophia Hoffman, David Lee, Jonah Morreale) for help with fieldwork and administrative tasks, as well as providing delicious meals and fostering a productive and welcoming environment to work. Thank you to Max Moran and the many REU's that helped collect data for chapters 4 and 5. Thank you Meg Miller, for teaching me how to use the spectrophotometer on more than one occasion and for your candor and kindness. Thank you Clay Ford of UVA Library's StatLab, with help selecting and implementing appropriate statistical methods for various analyses. Thank you to the 60 Stack Overflow users who provided 99 answers to 80 separate R questions I asked while working on this dissertation (special thanks to users: akrun, Ronak Shah, Allan Cameron, and TarJae who collectively answered most of the SO questions I asked). Thank you, Joe Wood and Paul Bukaveckas, for introducing me to scientific research as an undergraduate, fostering my interests in aquatic sciences, encouraging me to pursue graduate

education and exceptional mentorship. Thank you to the Jefferson Scholars Foundation and Kenneth L. Bazzle for supporting the last year of my dissertation.

I am eternally grateful to my family, friends, and loved ones. My parents, Craig and Candice, and my brother Adam have provided unwavering love and support in all aspects of my life, including an enthusiasm for my dissertation research. To my wife Morgan – your perennial love, support, encouragement, and patience throughout the years has been motivating and a consistent source of inspiration, thank you.

Table of Contents

List of Tables

List of Figures

Chapter 1: Introduction to the Dissertation

Disturbances are often recognizable based on their extreme nature and outsized impacts on the physical environment relative to their short duration (e.g., hurricanes, floods, forest fires). However, some disturbances are long-term and persistent (e.g., sea-level rise, land subsidence, climate warming). This distinction between extreme short and long-term disturbances are termed pulse and press disturbance, respectively. Since the 1960s, ecologists have recognized the central role that pulse and press disturbance events play in shaping ecosystem structure and function. In the 1980s the U.S. National Science Foundation established the Long-Term Ecological Research (LTER) network and highlighted disturbance patterns as one of their five core research themes. Improvements in computational and sensor technology (i.e., satellites, low-cost automated sensors) have led to a breadth and depth of theoretical, experimental, and observational research and monitoring efforts that have advanced adaptation, restoration, and management of ecosystem services in relation to disturbance. However, climate change, a global press disturbance, is creating conditions that often lead to more frequent pulse disturbances. Understanding how climate change will impact disturbance attributes and how ecosystem structure and function respond is key to ecosystem management and resilience.

Disturbances are quantified based on temporal characteristics (i.e., duration, frequency), spatial characteristics (i.e., areal extent, pattern at various geographic scales), and event characteristics (e.g., magnitude, severity, onset rate). Globally, over the past five decades, the frequency of pulse disturbance events has increased (WMO 2021). Anthropogenic warming of the atmosphere has been attributed to ~90% of marine heatwave (MHW) disturbance events (i.e., discrete periods of anomalously high water temperature), which doubled in frequency between 1982-2016 (Frölicher et al. 2018; Fox-Kemper et al. 2021). MHWs have received growing

attention due in part to their disproportionate and lasting destructive impacts relative to longer term changes in mean temperature (Easterling et al. 2000; Jentsch et al. 2007). MHWs push organisms to their thermal limits leading to mortality (Roberts et al. 2019; Till et al. 2019; Piatt et al. 2020; Garrabou et al. 2022), cause range contractions (Marba and Duarte 2010; Osland et al. 2013; Smale and Wernberg 2013), and lead to loss of carbon stocks (Arias-Ortiz et al. 2018; Aoki et al. 2021). Furthermore, continued warming of the atmosphere through the end of the 21st century is predicted to increase the frequency of compound disturbance events (i.e., 2+ disturbance events co-occurring at the same location and time) in aquatic ecosystems, which represent times of enhanced stress that will cause enduring changes to ecosystems (Gruber 2011; Collins et al. 2019).

Aquatic heatwaves are one type of pulse disturbance event which can be a catalyst for disturbances in other water quality variables that are temperature dependent. Oxygen solubility in water is inversely proportional to water temperature such that an extreme high water temperature event (i.e., heatwave) can reduce oxygen within the pelagic environment leading to hypoxic conditions. Similarly, ecosystem metabolism (i.e., primary production and respiration) is a temperature dependent process and if conditions allow for respiration to exceed production (e.g., thermal stress of primary producer), respiration can deplete dissolved oxygen in the water column. This process can also promote low pH (i.e., acidic) events depending on buffering conditions via the production of dissolved CO_2 and carbonic acid. However, few studies have considered aquatic heatwaves outside oceanic and lentic ecosystems or within other aqueous mediums such as sediments. Furthermore, few studies have considered the resilience of ecosystems that have been subject to aquatic heatwave events.

Ecosystem resilience incorporates mechanisms of stability as characterized by the ability to resist and recover, facilitating the maintenance of ecosystem goods, services, and structures in the presence of extreme conditions. With ~40% of the world's human population living within 100 km of a coastline (Martínez et al. 2007), coastal ecosystem stability is critical to the provisioning of goods and services, which also serve to protect property and sustain economic activities (Barbier et al. 2011). Seagrass meadows are one vegetated coastal marine ecosystem that provides many ecosystem goods and services (e.g., food production, coastal protection, erosion control, water purification, fisheries maintenance, tourism, recreation, education, research, carbon sequestration). These ecosystems are prone to disturbance due in part to their widespread occurrence, proximity to human dominated coastlines, and climate change, which have contributed to an accelerating global loss (Orth et al. 2006; Waycott et al. 2009; Dunic et al. 2021). Furthermore, seagrass ecosystems are a globally significant carbon sink, accounting for ~10% of annual oceanic carbon burial despite occupying < 0.2% of oceanic surface area (Duarte et al. 2005; Fourqurean et al. 2012). If efforts to manage and restore the services that seagrass ecosystems provide are to be successful in a future characterized by increasing disturbance frequency, then it is critical to develop a better understanding of the resilience properties of these ecosystems.

The goal of this dissertation was to expand the investigation of heatwaves into previously unexplored aquatic ecosystems and measure the stability of seagrass ecosystems to disturbance events. Research on heatwaves has largely been conducted in the atmosphere and in large oceanic regions via the use of satellite-derived datasets. However, remotely sensed temperature datasets have low spatial resolution (1-50 km), limiting their application to aquatic ecosystems with large surface areas. Direct measurements of temperature using *in-situ* thermistors provide

another approach for quantifying heatwaves as these sensors can be deployed in smaller waterways and in sediments that would otherwise be unavailable or contaminated by land using satellite observations. Furthermore, aquatic heatwaves represent an emergent disturbance type for seagrass ecosystems (Arias-Ortiz et al. 2018; Berger et al. 2020; Aoki et al. 2021). While seagrass meadows are stable to a variety of small-scale disturbances, they can undergo state change to an unvegetated bare sediments (Orth et al. 2020). Despite the breadth of seagrass disturbance-recovery studies, there has been little cross-system examination of the resulting patterns. This dissertation expands the investigation of aquatic heatwaves into rivers, estuaries, and shallow coastal sediments by utilizing continuous, long-term monitoring networks. Additionally, seagrass meadow stability was quantified by experimentally inducing a heatwave-like disturbance, and by synthesizing related experimental and observational studies of seagrass recovery following disturbance.

Chapter 2 examines the prevalence of heatwaves in 70 streams and rivers throughout the United States. Specifically, this study, published in *Limnology and Oceanography Letters*, provided a baseline evaluation of heatwave metrics (i.e., frequency, duration, and magnitude), evaluated temporal trends, and if trends varied in relation to season, region, discharge, stream order, and position in the landscape relative to a dam. The frequency of lotic freshwater heatwaves increased throughout the U.S. over the 26-year study period of 1996-2021, with a doubling in the annual mean number of total heatwave days. Riverine heatwave frequency was positively associated with summer and fall seasons, mid- to high-order streams, positions above dams, and where no dam was present. Riverine heatwaves were driven by increases in atmospheric temperature and exacerbated by declines in discharge. These results suggest that

riverine heatwaves will continue proliferating, given climate model projections of rising atmospheric temperature and declining discharge conditions throughout the 21st century.

Chapter 3 examines the prevalence of heatwaves for 12 estuaries along the U.S. Atlantic, Pacific, Gulf of Mexico, and Caribbean coasts, along with their co-occurrence with atmospheric heatwaves, extreme low dissolved oxygen (DO), and acidic pH events. While this study, published in *Estuaries and Coasts*, found no evidence of temporal trends in estuarine heatwave metrics, estuarine heatwaves regularly occurred over the 24-year study period between 1996-2019. Estuarine heatwaves began during an active atmospheric heatwave between 6-71% of the time depending on location. Likewise, low DO or low pH events started during an active estuarine heatwave 2-45% and 0-18% of the time, respectively. The triple co-occurrence of an estuarine heatwave, low DO, and acidic pH event was rare, ranging between 0-7% of all estuarine heatwaves. The frequency and duration of extreme low DO and pH significantly declined over the study period. Overall, these results provided evidence of extensive geographic improvements in estuarine water quality regarding extreme low DO and acidic pH events, along with the first baseline assessment of estuarine heatwaves and their co-occurrence with atmospheric heatwaves and other deleterious water quality conditions.

Chapter 4 tests if MHWs could propagate into surficial coastal sediments and induce a sediment heatwave (SHW). This work was initiated by collecting hourly sediment temperature between June 2020 and October 2022 at a depth of 5 cm (where seagrass rhizomes were most abundant) from two locations within the restored subtidal South Bay seagrass meadow of the Virginia Coast Reserve LTER. Given the relatively short temporal sediment temperature records, a statistical model of sediment temperature was developed for each meadow location (i.e., meadow interior and edge) using multiple-linear regression, along with long-term (1994-2022)

water temperature and water level observations from a nearby National Oceanic and Atmospheric Administration tidal station. Model validation provided strong support for both models, allowing for sediment heatwave analyses. Results suggested that the number of sediment heatwaves significantly increased in frequency as did the total annual number of sediment heatwave days at both meadow locations over the 29-year study period. Sediment heatwaves at both meadow locations co-occurred with a MHW 79-81% of the time, and the top 10% most extreme MHW and sediment heatwaves occurred between November and April. Sediment heatwaves co-occurred with an anomalously long duration MHW in June 2015 that is associated with a 90% decline in seagrass and 20% decline in stored sediment carbon from this system, suggesting that SHWs may have contributed to the observed seagrass and sediment carbon loss. These results provide the first assessment of SHWs in any aquatic ecosystem.

In Chapter 5, I present an experimental removal of seagrass from the meadow interior and edge of South Bay to better understand the processes that support seagrass ecosystem stability. Additionally, I synthesized results from prior English language seagrass disturbance-recovery studies, summarizing spatial scales of experimental and observational research, rates of recovery, and factors related to recovery. Linear recovery occurred within the meadow interior after 24 months, whereas recovery was incomplete at the meadow edge and projected to require 158 months. Differences in recovery times were likely due to storm-driven sediment erosion at the edge sites. At both locations, recovery was facilitated by lateral clonal growth from the disturbance edge and seedling recruitment. The literature synthesis provided evidence that 47% of known seagrass species have been included in disturbance-recovery studies but that the majority of studies have occurred in monocultures of the genus *Zostera*. Experimental disturbances were most often conducted on relatively small spatial scales, likely inflating the

contribution of lateral clonal growth to recovery and limiting scalability by neglecting the impact of hydrodynamic factors on recovery rates that occurs within larger disturbance gaps. The combined results indicate that seagrass meadows are resilient to disturbances large and small and that the seagrass meadow state is stable across a broad set of conditions. Combined, meadow position influences disturbance susceptibility, and the geographic range and species diversity of seagrasses are under-represented in disturbance-recovery studies; possibly due to limiting the literature synthesis to English publications.

Chapter 6 summarizes the main findings of this dissertation and provides future research directions. Specifically, I conclude that like MHWs, riverine heatwaves have significantly increased in frequency in recent decades, that estuarine heatwaves regularly co-occur with extremes in other water quality variables, that MHWs can propagate into coastal sediments and induce SHWs, and that seagrass are resilient to MHW-like disturbances. These results offer insights into characteristics that promote heatwave development in inland and coastal ecosystems and how a threatened aquatic ecosystem, with climate change mitigation potential, recovers following disturbances. This dissertation emphasizes the value of continuous long-term, high-frequency monitoring networks to advance the understanding of how climate change is manifesting in aquatic ecosystems.

References

Aoki, L. R., McGlathery, K. J., Wiberg, P. L., Oreska, M. P. J., Berger, A. C., Berg, P., & Orth, R. J. (2021). Seagrass Recovery Following Marine Heat Wave Influences Sediment Carbon Stocks. *Frontiers in Marine Science*, *7*, 576784. https://doi.org/10.3389/fmars.2020.576784

Arias-Ortiz, A., Serrano, O., Masqué, P., Lavery, P. S., Mueller, U., Kendrick, G. A., Rozaimi, M., Esteban, A., Fourqurean, J. W., Marbà, N., Mateo, M. A., Murray, K., Rule, M. J., & Duarte, C. M. (2018). A marine heatwave drives massive losses from the world's largest seagrass carbon stocks. *Nature Climate Change*, *8*(4), 338–344. https://doi.org/10.1038/s41558-018-0096-y

Barbier, E. B., Hacker, S. D., Kennedy, C., Koch, E. W., Stier, A. C., & Silliman, B. R. (2011). The value of estuarine and coastal ecosystem services. *Ecological Monographs*, *81*(2), 169–193. https://doi.org/10.1890/10-1510.1

Berger, A. C., Berg, P., McGlathery, K. J., & Delgard, M. L. (2020). Long-term trends and resilience of seagrass metabolism: A decadal aquatic eddy covariance study. *Limnology and Oceanography*, *65*(7), 1423–1438. https://doi.org/10.1002/lno.11397

Collins, M., M. Sutherland, L. Bouwer, S.-M. Cheong, H. J. D. Combes, M. K. Roxy, I. Losada, K. McInnes, B. Ratter, E. Rivera-Arriaga, R. D. Susanto, D. Swingedouw, L. Tibig, P. Bakker, C. M. Eakin, K. Emanuel, M. Grose, M. Hemer, L. Jackson, A. Kääb, J. Kajtar, T. Knutson, C. Laufkötter, I. Noy, M. Payne, R. Ranasinghe, G. Sgubin, M.-L. Timmermans, A. Abdulla, M. H. González, and C. Turley. (2019). *IPCC Special Report on the Ocean and Cryosphere in a Changing Climate*: Extremes, Abrupt Changes and Managing Risks 6: 589-655.

Duarte, C. M., J. J. Middelburg, and N. Caraco. (2005). Major role of marine vegetation on the oceanic carbon cycle. *Biogeosciences*, *2*, 1-8. https://doi.org/10.5194/bg-2-1-2005

Dunic, J. C., Brown, C. J., Connolly, R. M., Turschwell, M. P., & Côté, I. M. (2021). Long-term declines and recovery of meadow area across the world's seagrass bioregions. *Global Change Biology*, *27*(17), 4096–4109. https://doi.org/10.1111/gcb.15684

Easterling, D. R., Meehl, G. A., Parmesan, C., Changnon, S. A., Karl, T. R., & Mearns, L. O. (2000). Climate extremes: observations, modeling, and impacts. *Science*, *289*(5487), 2068-2074.

Fourqurean, J. W., Duarte, C. M., Kennedy, H., Marbà, N., Holmer, M., Mateo, M. A., Apostolaki, E. T., Kendrick, G. A., Krause-Jensen, D., McGlathery, K. J., & Serrano, O. (2012). Seagrass ecosystems as a globally significant carbon stock. *Nature Geoscience*, *5*(7), 505–509. https://doi.org/10.1038/ngeo1477

Fox-Kemper, B., H. T. Hewitt, C. Xiao, G. Aðalgeirsdóttir, S. S. Drijfhout, T. L. Edwards, N. R.

Golledge, M. Hemer, R. E. Kopp, G. Krinner, A. Mix, D. Notz, S. Nowicki, I. S. Nurhati, L. Ruiz, J-B. Sallée, A. B. A. Slangen, Y. Yu, (2021). Ocean, Cryosphere and Sea-level Change. In: *Climate Change 2021: The Physical Science Basis. Contribution of Working Group I to the Sixth Assessment Report of the Intergovernmental Panel on Climate Change* [Masson-Delmotte, V., P. Zhai, A. Pirani, S. L. Connors, C. Péan, S. Berger, N. Caud, Y. Chen, L. Goldfarb, M. I. Gomis, M. Huang, K. Leitzell, E. Lonnoy, J.B.R. Matthews, T. K. Maycock, T. Waterfield, O. Yelekçi, R. Yu and B. Zhou (eds.)]. Cambridge University Press. In Press.

Frölicher, T. L., Fischer, E. M., & Gruber, N. (2018). Marine heatwaves under global warming. *Nature*, *560*(7718), 360–364. https://doi.org/10.1038/s41586-018-0383-9

Garrabou, J., Gómez-Gras, D., Medrano, A., Cerrano, C., Ponti, M., Schlegel, R., ... & Harmelin, J. G. (2022). Marine heatwaves drive recurrent mass mortalities in the Mediterranean Sea. *Global Change Biology*, *28*(19), 5708-5725.

Gruber, N. (2011). Warming up, turning sour, losing breath: Ocean biogeochemistry under global change. *Philosophical Transactions of the Royal Society A: Mathematical, Physical and Engineering Sciences*, *369*(1943), 1980–1996. https://doi.org/10.1098/rsta.2011.0003

Jentsch, A., Kreyling, J., & Beierkuhnlein, C. (2007). A new generation of climate-change experiments: events, not trends. *Frontiers in Ecology and the Environment*, *5*(7), 365-374.

Marbà, N., & Duarte, C. M. (2009). Mediterranean warming triggers seagrass (*Posidonia oceanica*) shoot mortality. *Global Change Biology*, *16*(8), 2366–2375. https://doi.org/10.1111/j.1365-2486.2009.02130.x

Martínez, M. L., Intralawan, A., Vázquez, G., Pérez-Maqueo, O., Sutton, P., & Landgrave, R. (2007). The coasts of our world: Ecological, economic and social importance. *Ecological Economics*, *63*(2–3), 254–272. https://doi.org/10.1016/j.ecolecon.2006.10.022

Orth, R. J., Carruthers, T. J. B., Dennison, W. C., Duarte, C. M., Fourqurean, J. W., Heck, K. L., Hughes, A. R., Kendrick, G. A., Kenworthy, W. J., Olyarnik, S., Short, F. T., Waycott, M., & Williams, S. L. (2006). A Global Crisis for Seagrass Ecosystems. *BioScience*, *56*(12), 987. https://doi.org/10.1641/0006-3568(2006)56[987:AGCFSE]2.0.CO;2

Orth, R. J., Lefcheck, J. S., McGlathery, K. S., Aoki, L., Luckenbach, M. W., Moore, K. A., Oreska, M. P. J., Snyder, R., Wilcox, D. J., & Lusk, B. (2020). Restoration of seagrass habitat leads to rapid recovery of coastal ecosystem services. *Science Advances*, *6*(41), eabc6434. https://doi.org/10.1126/sciadv.abc6434

Osland, M. J., Enwright, N., Day, R. H., & Doyle, T. W. (2013). Winter climate change and coastal wetland foundation species: Salt marshes vs. mangrove forests in the southeastern United States. *Global Change Biology*, *19*(5), 1482–1494.

https://doi.org/10.1111/gcb.12126

Piatt, J. F., Parrish, J. K., Renner, H. M., Schoen, S. K., Jones, T. T., Arimitsu, M. L., Kuletz, K. J., Bodenstein, B., García-Reyes, M., Duerr, R. S., Corcoran, R. M., Kaler, R. S. A., McChesney, G. J., Golightly, R. T., Coletti, H. A., Suryan, R. M., Burgess, H. K., Lindsey, J., Lindquist, K., … Sydeman, W. J. (2020). Extreme mortality and reproductive failure of common murres resulting from the northeast Pacific marine heatwave of 2014-2016. *PLOS ONE*, *15*(1), e0226087. https://doi.org/10.1371/journal.pone.0226087

Roberts, S. D., Van Ruth, P. D., Wilkinson, C., Bastianello, S. S., & Bansemer, M. S. (2019). Marine Heatwave, Harmful Algae Blooms and an Extensive Fish Kill Event During 2013 in South Australia. *Frontiers in Marine Science*, *6*, 610. https://doi.org/10.3389/fmars.2019.00610

Smale, D. A., & Wernberg, T. (2013). Extreme climatic event drives range contraction of a habitat-forming species. *Proceedings of the Royal Society B: Biological Sciences*, *280*(1754), 20122829. https://doi.org/10.1098/rspb.2012.2829

Till, A., Rypel, A. L., Bray, A., & Fey, S. B. (2019). Fish die-offs are concurrent with thermal extremes in north temperate lakes. *Nature Climate Change*, *9*(8), 637–641. https://doi.org/10.1038/s41558-019-0520-y

Waycott, M., Duarte, C. M., Carruthers, T. J. B., Orth, R. J., Dennison, W. C., Olyarnik, S., Calladine, A., Fourqurean, J. W., Heck, K. L., Hughes, A. R., Kendrick, G. A., Kenworthy, W. J., Short, F. T., & Williams, S. L. (2009). Accelerating loss of seagrasses across the globe threatens coastal ecosystems. *Proceedings of the National Academy of Sciences*, *106*(30), 12377–12381. https://doi.org/10.1073/pnas.0905620106

WMO. (2021). WMO Atlas of mortality and economic losses from weather, climate, and weather extremes (1970-2019). *World Meteorological Organization*. WMO-No. 1267

Chapter 2: Increasing heatwave frequency in streams and rivers of the United States

Published in *Limnology and Oceanography Letters* (2022) DOI: 10.1002/lol2.10284

Co-Authors: Alice F. Besterman, Cal D. Buelo, Dat T. Ha, Jonathan A. Walter, and Michael L. Pace.

Author Contribution Statement: SJT and MLP designed the study. SJT performed the analysis and wrote the manuscript. AFB, CDB, DTH, JAW, and MLP contributed to improving the analysis and manuscript.

Abstract

Heatwaves are increasing in frequency, duration, and intensity in ocean, coastal, and lake ecosystems. While positive water temperature trends have been documented in many rivers, heatwaves have not been analyzed. This study examined heatwaves in rivers throughout the United States between 1996-2021. Riverine heatwaves increased in frequency over the study period, with the most robust increases occurring in summer and fall, in mid to high order streams, and at free-flowing sites and sites above a reservoir. The increase in heatwave frequency was accompanied by an increase in moderate strength heatwaves as well as a doubling of the annual mean total number of heatwave days at a site. Riverine heatwaves were often associated with normal or below-normal discharge conditions and at sites with a mean annual discharge ≤ 250 m^3 s^{-1}. These results provide the first assessment of heatwaves in rivers for a large geographic area in the United States.

Introduction

Increasing climate variability and rising water temperatures have spurred interest in anomalous extreme high temperature events called heatwaves due to their potentially disproportionate impact relative to a gradual, long-term change in mean temperature (Jentsch et al. 2007; Vasseur et al. 2014). Positive trends in heatwave characteristics, such as frequency (i.e., total events per unit time), duration (i.e., total days an event lasts), and intensity (i.e., the magnitude of an event) have been documented in ocean, coastal, and lake ecosystems (Lima and Wethey 2012, Oliver et al. 2021, Woolway et al. 2021) and have been linked to shifts in ecosystem metabolism (Berger et al. 2020), organism mortality (Till et al. 2019), and poor water quality (Tassone et al. 2022). Lotic water temperatures have been increasing since the mid-20th century (Webb and Nobilis 1995; Kaushal et al. 2010). However, heatwaves in riverine systems have not been considered, providing uncertainty in riverine heatwave distribution and trends.

Aquatic heatwave development is dependent upon vertical diffusive heat flux across the air-water boundary and horizontal advective heat flux (Holbrook et al. 2019; Oliver et al. 2021). In running waters, the primary control on diffusive heat flux is seasonal and spatial variability in atmospheric temperature (Caissie 2006). There are numerous controls on advective heat fluxes in lotic systems and include precipitation and discharge regimes, flow modification by reservoirs, groundwater supply, and stream size (Vannote et al. 1980; Caissie 2006, Haddeland et al. 2014, Hare et al. 2021). With projected climate warming and increasing demand for freshwater, diffusive and advective heat fluxes are expected to intensify throughout the 21st century and increase the frequency, duration, and intensity of extreme high water temperature conditions (Meehl et al. 2007; Wuebbles et al. 2017).

In this study, we document the frequency, duration, and intensity of riverine heatwaves using in-situ water temperature measurements from 1996-2021 for 70 riverine sites located

throughout the U.S. We also compare regional and seasonal patterns in heatwaves and test relationships between heatwave characteristics, atmospheric temperature, precipitation, discharge, stream order, and position relative to reservoirs. We hypothesize that heatwave characteristics will be positively affected by increasing atmospheric temperature as well as declining precipitation and discharge. We also hypothesize that heatwaves will be more likely at sites above reservoirs where dam operations do not ameliorate temperature extremes and in mid to higher stream orders where riparian cover and groundwater contributions that moderate temperatures are reduced.

Methods

Data Sources and Processing

The United States Geological Survey (USGS) conducts surface water monitoring throughout the U.S. as part of its national water information system (https://waterdata.usgs.gov/nwis/; USGS 2016). All sites with daily mean water temperature records available for the 26-year period of 1996-2021 were identified using the R package 'dataRetrieval' version 2.7.6 (De Cicco et al. 2018). Tidally influenced and lake stations were removed prior to analysis. Periods of ice cover and flagged data other than those 'Approved', 'Approved Revised', 'Approved Edited', or 'Provisional' were considered missing values. Sites with < 90% of their daily records were also excluded. Linear interpolation was applied to water temperature gaps ≤ 2 days. For larger gaps, multiple linear regression models were developed using 1 km^2 resolution, daily climate data provided by Daymet version 4 (Thornton et al. 2020) using the R package 'daymetr' version 1.6 (Hufkens et al. 2018). Only those sites with regressions where $R^2 \geq 0.80$ were used in this analysis (mean ± SD $R^2 = 0.91 \pm 0.04$). Of the 70 long-term water temperature sites, 51 had concurrent daily mean discharge that were ≥ 90%

complete after removing flagged data. This resulted in a total of 1,820 station years of air temperature, precipitation (daymetr), and water temperature (USGS); and 1,326 station years of discharge data (USGS) available for analysis.

Site specific variables included region, Strahler stream order, and position in landscape relative to a reservoir. Regional assignment was classified according to historical climatically consistent regions of the U.S. (Figure 2.1; Karl and Koss 1984). Strahler stream order was determined using the USGS NHDPlus High Resolution geospatial database using ESRI ArcMap version 10.8. Categorical assignment of site position relative to a reservoir (i.e., above, below, none) was determined from aerial photographic visual inspection of each sites location relative to the U.S. Army Corps of Engineers National Inventory of Dams (NID) in ArcMap (https://nid.sec.usace.army.mil, see Appendix 1: Supplemental Information).

Heatwave Detection

Riverine heatwaves were identified following the Hobday et al. (2016) definition for marine heatwaves as those periods when daily mean water temperature exceeds a local, seasonally varying 90^{th} percentile threshold for a period ≥ 5 days. Similarly, heatwaves were classified based on their peak intensity relative to multiples of the 90^{th} percentile difference from the long-term climatology (Hobday et al. 2018). Heatwave identification and classification were obtained using the 'heatwaveR' R package version 0.4.4 (Schlegel and Smit 2018). For each heatwave, we quantified event duration and cumulative intensity above the 90^{th} percentile. For each site, heatwave frequency was determined as the annual number of heatwave events. Each event was assigned according to northern hemisphere meteorological seasons (winter = Dec-Feb, spring = March-May, summer = June-Aug, fall = Sept-Nov; NOAA 2016) which have been used

in estuarine and atmospheric studies of a similar spatial scale (Lau and Nath 2012; Tassone et al. 2022).

High and low discharge was determined as the difference between each site's observed daily mean discharge and an expected daily mean discharge (hereafter referred to as 'residual discharge'). The expected daily mean discharge was determined using the 'heatwaveR' R package which calculates a centered 11-day mean discharge climatology based on day of year (i.e., Jan 1 = 1, Dec 31 = 365) which is then smoothed using a 31-day moving average (Schlegel and Smit 2018). Residual discharge values > 0 and < 0 indicated above and below normal discharge respectively.

Statistical Analyses

Long-term trends in monthly mean air and water temperature, discharge, and total precipitation (all forms converted to water equivalent), were determined using Seasonal-Kendall test with Sen's slope estimates ('wql' R package version 0.4.9; Jassby and Cloern 2017). Trends in heatwave characteristics were conducted on annual timeseries as heatwaves are rare events and often span monthly boundaries. Annual trends were determined using Mann-Kendall tests ('Kendall' R package version 2.2; McLeod 2011) with Sen's slope estimates ('trend' R package version 1.1.4; Pohlert 2020). These non-parametric trend analyses are robust to outliers and have been used in similar studies of long-term change in water temperature (Hirsch et al. 1982; Kaushal et al. 2010) and heatwaves (Perkins and Alexander 2013; Tassone et al. 2022). To reduce Type 1 errors that could arise from multiple comparisons, a 15% false discovery rate was applied to the heatwave analysis prior to determining statistical significance (Benjamini and Hochberg 1995; McDonald 2014). Annual mean discharge was normalized by site to examine

relative trends. Data collection and analyses were performed in the R statistical environment (R Core Team 2020).

Results

Season

There was a total of 3,984 riverine heatwave events (35,360 days) between 1996-2021 for the 70 sites (664,300 daily observations) considered in this analysis. The mean frequency, duration, and maximum intensity above the 90th percentile threshold for heatwaves were 2 events yr^{-1}, 9 days, and 1.7 °C respectively, and ranged up to 12 events yr^{-1}, 103 days, and 9.0 °C (SI Figure 2.1). Summer heatwaves made up 28% of all heatwaves, followed by spring (26%), fall (24%), and winter (22%). Overall, riverine heatwave frequency significantly increased over time (0.06 events yr^{-1}, p-value = 0.004) and for the summer (0.03 events yr^{-1}, p-value = 0.004) and fall seasons (0.02 events yr^{-1}, p-value = 0.029, Table 2.1). The increased frequency of heatwaves was accompanied by significant increases in moderate strength events (3.4 events yr^{-1}, p-value = 0.003; Figure 2.2a). Similarly, moderate strength events significantly increased in duration (30.1 days yr^{-1}, p-value = 0.002; Figure 2.2b) and maximum intensity (10.5 °C yr^{-1}, p-value = 0.01; Figure 2.2c). There was a significant increase in and approximate doubling of the annual mean total number of heatwave days at a site from 11 in 1996 to 25 in 2021 (slope = 0.53 days yr^{-1}, p-value = 0.015).

During riverine heatwaves, discharge generally was at or below normal discharge conditions (SI Figure 2.2a). Some heatwaves occurred when discharge was at or above normal conditions, particularly between November-February. However, those heatwaves that occurred between March-October, which includes North American summer, were associated with periods of low discharge. The annual total number of heatwave events was greatest in rivers that had an

annual daily mean discharge ≤ 250 $m^3 s^{-1}$ (SI Figure 2.2b). The cumulative intensity above the 90th percentile threshold of riverine heatwaves was lowest between July-September and greatest between October-June (SI Figure 2.3).

Region

The south had the largest median (61 events $site^{-1}$) and maximum (76 events) number of riverine heatwave events over the study period. Conversely, the southwest had the lowest median (44 events $site^{-1}$) and minimum number of events (39 events). There were significantly more riverine heatwaves in the northeast (mean ± SD = 60 ± 7), southeast (59 ± 6), and south (65 ± 10) regions compared to the southwest (47 ± 9; p-values ≤ 0.038). Heatwave frequency trends were positive at 49% of sites, with significant positive trends (n = 19) ranging from 0.06 events yr^{-1} in the southwest to 0.20 events yr^{-1} in the northwest (Figure 2.3a). Regional heatwave duration trends were predominantly positive (61%), with 11 statistically significant positive trends ranging from 0.13 to 0.46 days yr^{-1} (Figure 2.3b). Similarly, cumulative intensity trends were positive for 60% of sites, with 4 statistically significant trends ranging from 0.15-0.22 °C days yr^{-1} (Figure 2.3c). Heatwave frequency, duration, and cumulative intensity trends were negative at 6% (n = 4), 13% (n = 9), and 20% (n = 20) of sites respectively.

There was a positive relationship between annual mean air and water temperature trends (slope ± SE = 0.43 ± 0.19, R^2 = 0.07, p-value = 0.024), with the southeast region having the greatest mean increase in air temperature trend (0.04 °C yr^{-1}; SI Figure 2.4a) and greatest range of water temperature trends (-0.06-0.06 °C yr^{-1}; SI Figure 2.4b). Precipitation and discharge trends were positively correlated (slope ± SE = 0.73 ± 0.20, R^2 = 0.21, p-value < 0.001) with all significant precipitation declines being limited to the northwest (SI Figure 2.4c). The northwest, west, and southwest all had significant declines in discharge trends, ranging from -4.28-0.01 m^3

s^{-1} yr^{-1} (SI Figure 2.4d). Annual total precipitation and normalized annual mean discharge were significantly positively correlated in all regions (slope range = 0.01-0.27 %, p-values ≤ 0.01) except for the west and west north central. Normalized annual mean discharge was significantly negatively correlated with annual mean water temperature in the south (slope = -0.005 °C, p-value = 0.026), southeast (slope = -0.007 °C, p-value < 0.001), and southwest (slope = -0.004 °C, p-value < 0.001).

Stream Order

Riverine heatwave frequency significantly increased in mid (order 4-5) to high (order 8-9) order streams (range = 0.06-0.10 events yr^{-1}, all p-value ≤ 0.018; Table 2.1). The mean duration of 5^{th} order riverine heatwave events increased (slope = 0.08 days yr^{-1}, p-value = 0.038, Table 2.1) however, this result should be interpreted with caution as the p-value exceeds the 15% false discovery rate threshold for statistical significance.

Reservoir Position

The frequency of riverine heatwaves significantly increased at free-flowing sites with no reservoir (0.06 events yr^{-1}, p-value = 0.008) and at sites above a reservoir (0.09 events yr^{-1}, p-value = 0.012, Table 2.1). Similarly, heatwave duration increased at sites above a reservoir (0.06 days yr^{-1}, p-value = 0.017). There was not a statistically significant difference in the total number of heatwave events per site with reservoir position, although the median number of riverine heatwaves at sites above a reservoir was greater ($median_{Above}$ = 62) than those below or with no reservoir present (each 56).

Discussion

Heatwaves are Increasing

Riverine heatwaves increased in frequency (0.06 events yr^{-1}) over the study period, with significant increases during summer (June-Aug; 0.03 events yr^{-1}) and fall (Sept-Nov; 0.02 events yr^{-1}). Thus, the frequency of discrete, extended (≥ 5 days) periods of extremely high water temperatures is increasing when water temperature is at its annual peak. However, summer heatwaves generally had the lowest cumulative intensities relative to other times of the year. We did not observe a significant difference in riverine heatwave duration among months, suggesting that the departure from seasonally-adjusted water temperature is greatest during fall, winter, and spring. Of the top 1% most extreme and severe heatwaves observed, 92% occurred between December and April, with 8% occurring in July and August. Furthermore, heatwave frequency increased in mid to high order streams (range = 0.06-0.10 events yr^{-1}) and doubled the average annual total heatwave days from 11 days in 1996 to 25 days in 2021. Sites with an annual daily mean discharge ≤ 250 $m^3 s^{-1}$ experienced the greatest annual number of heatwave events, indicating smaller gaged streams maybe regularly exposed to heatwaves. The increasing frequency of riverine heatwaves represents an emergent climate change signal outside of linear warming trends, as has been observed in other climate related variables (Trenberth et al. 2014; Lee 2021).

Riverine heatwaves are increasing in frequency above reservoirs (0.09 events yr^{-1}) as well as in free-flowing rivers (0.06 events yr^{-1}) but not below reservoirs, suggesting that reservoirs are mitigating increases in heatwave frequency in downstream reaches. This may reflect release of cool hypolimnetic waters that develop during summer thermal stratification and release of relatively warm waters during winter that develop due to flow reduction and lack of reservoir shading (Ren et al. 2020). Likewise, the mean duration of riverine heatwaves increased at sites above reservoirs (0.06 days yr^{-1}). This increasing duration of heatwaves above reservoirs is

likely, in part, due to reduced reservoir discharge and longer hydraulic residence times during periods of drought which have increased in frequency and severity due to climate change (Mosley 2015). Nonetheless, dams provide a management option for reducing extreme high water temperatures in tailwaters by increasing discharge and hypolimnetic release (to the limit of hypolimnetic volume).

We did not observe any significant increasing trends in the frequency, duration, or intensity of riverine heatwaves among regions of the U.S. Nevertheless, riverine heatwaves regularly occurred in all regions, with sites experiencing an average of 2 ± 2 heatwaves yr^{-1}. Furthermore, riverine water temperature is increasing significantly throughout the U.S. at a rate of 0.01-0.06 °C yr^{-1}, similar to previous riverine (Kaushal et al. 2010), estuarine (Tassone et al. 2022), and lake studies (O'Reilly et al. 2015), yet exceeding the global ocean (Garcia-Soto et al. 2021).

In inland systems, elevated water temperature increases mobilization of contaminants (i.e., heavy metals, pesticides) within the aquatic food web (Patra et al. 2015) which subsidize riparian and terrestrial consumers (Walters et al. 2008; Moy et al. 2016). As a consequence, fish are likely to carry a larger contaminant burden as freshwater temperatures increase (Patra et al. 2015), leading to stricter advisories on human fish consumption and a greater burden on subsistence fishing communities. Furthermore, extreme high water temperatures interrupt migration (Keefer et al. 2009) and contribute to mass-mortality events (Lynch and Risley 2003, Keefer et al. 2010). Riverine heatwaves represent an emerging climate change threat with potential to impact adjacent ecosystems, exacerbate known stressors, and induce lethal and sublethal damage.

Discharge and Precipitation Influence Heatwaves

Daily mean discharge was often at or below the expected daily mean discharge during riverine heatwaves. Furthermore, the annual total number of heatwaves was greatest at sites with an annual daily mean discharge ≤ 250 m^3 s^{-1}. These results support model projections and meta-analyses of synchrony between higher water temperature and periods of low flow (Arismendi et al. 2013; van Vliet et al. 2013) and highlight the important effect of discharge on riverine thermal conditions, including extremes. Climate change and anthropogenic activities have altered discharge by: influencing precipitation and low flow timing and intensity, altering snowmelt timing (Mosley 2015; Dudley et al. 2017), increasing water withdrawal, changing seasonal patterns due to impoundment, and altering land cover (Caissie 2006; Jame and Bowling 2020). These collective impacts favor the development of riverine heatwaves.

Normalized annual mean discharge and annual total precipitation were positively correlated across all regions with the northeast ($R^2 = 0.49$), east north central ($R^2 = 0.47$), and south ($R^2 = 0.43$) having the strongest relationships (all other $R^2 \leq 0.40$). Annual mean water temperature and normalized annual mean discharge were negatively correlated across all regions, except for Alaska, and were generally weak ($R^2 \leq 0.22$) yet significant in the southeast, south, and southwest. This suggests that during years of low precipitation, discharge is reduced, resulting in a lower volume of water that is easier to warm. Climate warming has increased extremes in precipitation such that droughts have become more frequent (Arismendi et al. 2013; Chiang et al. 2021). While we did not consider intraannual precipitation variability in this analysis, increasing summer synchrony in drought, low discharge, and peak air temperature would increase the risk for riverine heatwave development by promoting warm water conditions. Increasing riverine water temperature is driven, in part, by rising atmospheric temperature however, water temperature trends at 39% of the sites exceeded the magnitude of atmospheric

temperature trends suggesting additional drivers of rising water temperature. Similar results have been reported for some regions of the U.S. (Isaak et al. 2012; Jastram and Rice 2015), Europe (Michel et al. 2020), Great Britain (Orr et al. 2015), and Japan (Ye and Kameyama 2021) which have implicated hydrology, watershed landcover change, and large-scale climatic oscillations as additional drivers of rising river water temperatures. Furthermore, Hare et al. (2021) suggested that U.S. streams with shallow groundwater contributions, approximately 40% of streams, are warming faster than deep groundwater streams. Our results provide evidence of an indirect relationship between precipitation and water temperature via discharge, and that riverine heatwaves were often associated with normal or below-normal discharge conditions. Interannual variability in precipitation can enhance or reduce heatwave development during wet and dry years respectively with relation to discharge. Similarly, intraannual variability in precipitation may have contributed to the increasing frequency of summer and fall heatwaves. While atmospheric warming and landcover change will continue to increase riverine water temperature, actions that reduce surface water discharge, such as reduced precipitation, surface water abstraction, and groundwater withdrawal are likely to exacerbate riverine warming trends and heatwave frequency.

Ecosystem Management

Water temperature influences many water quality variables which in the U.S. are regulated by the Clean Water Act. Restoration and antidegradation requirements for water quality criteria will be detrimentally affected by heatwaves potentially resulting in increased violations and failure to reach improvement goals. Broader spatial coverage, greater representation of stream types, and continuous sub-daily long-term data collection will be essential to track heatwave conditions. Furthermore, these improved monitoring efforts will help

identify and prioritize restoration of waterways that are exceeding water temperature standards and provide protection for those currently meeting standards (Palmer et al. 2009).

Conclusions

Based on the period covered by the data synthesized in this study, riverine heatwave frequency is increasing throughout the U.S., doubling the average annual number of heatwave days between 1996-2021. These heatwaves are driven by increases in atmospheric temperature and exacerbated by declines in discharge. Sites most susceptible to riverine heatwaves include those either above a dam or free-flowing, and with an annual daily mean discharge ≤ 250 m^3 s^{-1}. Similarly, heatwaves were often associated with normal or below-normal discharge conditions. Heatwave frequency significantly increased in summer and fall however, heatwaves were most intense in the winter and spring. Climate models project rising atmospheric temperature throughout the 21st century (Meehl et al. 2007; Wuebbles et al. 2017) along with low discharge conditions (Milly et al. 2005, van Vliet 2013) indicating that riverine heatwaves will continue proliferating. Managing river temperatures will be of increased importance in the future and expanded temperature monitoring should be a priority.

References

Arismendi, I., Safeeq, M., Johnson, S.L., Dunham, J.B. and Haggerty, R., 2013. Increasing synchrony of high temperature and low flow in western North American streams: double trouble for coldwater biota?. *Hydrobiologia*, *712*(1), 61-70.

Benjamini, Y., and Hochberg, Y. 1995. Controlling the False Discovery Rate: A Practical and Powerful Approach to Multiple Testing. *Journal of the Royal Statistical Society: Series B (Methodological)*, *57*(1), 289–300. https://doi.org/10.1111/j.2517-6161.1995.tb02031.x

Berger, A. C., Berg, P., McGlathery, K. J., and Delgard, M. L. 2020. Long-term trends and resilience of seagrass metabolism: A decadal aquatic eddy covariance study. *Limnology and Oceanography*, *65*(7), 1423–1438. https://doi.org/10.1002/lno.11397

Caissie, D. 2006. The thermal regime of rivers: A review. *Freshwater Biology*, *51*(8), 1389–1406. https://doi.org/10.1111/j.1365-2427.2006.01597.x

Chiang, F. Mazdiyasni, O., and AghaKouchak, A. 2021. Evidence of anthropogenic impacts on global drought frequency, duration, and intensity. *Nature Communications*, *12*, 2754. https://doi.org/10.1038/s41467-021-22314-w

De Cicco, L. A., Hirsch, R. M., Lorenz, D., Watkins, W. D. 2022, dataRetrieval: R packages for discovering and retrieving water data available from Federal hydrologic web services, v.2.7.11, doi:10.5066/P9X4L3GE

Dudley, R. W., Hodgkins, G. A., McHale, M. R., Kolian, M. J., and Renard, B. (2017). Trends in snowmelt-related streamflow timing in the conterminous United States. *Journal of Hydrology*, *547*, 208–221. https://doi.org/10.1016/j.jhydrol.2017.01.051

Garcia-Soto, C., Cheng, L., Caesar, L., Schmidtko, S., Jewett, E.B., Cheripka, A., Rigor, I., Caballero, A., Chiba, S., Báez, J.C. and Zielinski, T., 2021. An overview of ocean climate change indicators: Sea surface temperature, ocean heat content, ocean pH, dissolved oxygen concentration, arctic sea ice extent, thickness and volume, sea-level and strength of the AMOC (Atlantic Meridional Overturning Circulation). *Frontiers in Marine Science*, *8*, 642372. https://doi.org/10.3389/fmars.2021.642372

Haddeland, I., Heinke, J., Biemans, H., Eisner, S., Flörke, M., Hanasaki, N., Konzmann, M., Ludwig, F., Masaki, Y., Schewe, J., Stacke, T., Tessler, Z. D., Wada, Y., and Wisser, D. 2014. Global water resources affected by human interventions and climate change. *Proceedings of the National Academy of Sciences*, *111*(9), 3251–3256. https://doi.org/10.1073/pnas.1222475110

Hare, D.K., Helton, A.M., Johnson, Z.C., Lane, J.W. and Briggs, M.A., 2021. Continental-scale analysis of shallow and deep groundwater contributions to streams. Nature Communications, 12(1), 1-10. https://doi.org/10.1038/s41467-021-21651-0

Hirsch, R. M., Slack, J. R., and Smith, R. A. 1982. Techniques of trend analysis for monthly water quality data. *Water Resources Research*, *18*(1), 107–121. https://doi.org/10.1029/WR018i001p00107

Hobday, A. J., Alexander, L. V., Perkins, S. E., Smale, D. A., Straub, S. C., Oliver, E. C. J.,

Benthuysen, J. A., Burrows, M. T., Donat, M. G., Feng, M., Holbrook, N. J., Moore, P. J., Scannell, H. A., Sen Gupta, A., and Wernberg, T. 2016. A hierarchical approach to defining marine heatwaves. *Progress in Oceanography, 141*, 227–238. https://doi.org/10.1016/j.pocean.2015.12.014

Hobday, A., Oliver, E., Sen Gupta, A., Benthuysen, J., Burrows, M., Donat, M., Holbrook, N., Moore, P., Thomsen, M., Wernberg, T., and Smale, D. 2018. Categorizing and Naming Marine Heatwaves. *Oceanography*, *31*(2). https://doi.org/10.5670/oceanog.2018.205

Holbrook, N.J., Scannell, H.A., Sen Gupta, A., Benthuysen, J.A., Feng, M., Oliver, E.C., Alexander, L.V., Burrows, M.T., Donat, M.G., Hobday, A.J. and Moore, P.J., 2019. A global assessment of marine heatwaves and their drivers. *Nature Communications, 10*(1), 1-13. https://doi.org/10.1038/s41467-019-10206-z

Hufkens, K., Basler, D., Milliman, T., Melaas, E. K., and Richardson, A. D. 2018. An integrated phenology modelling framework in R. *Methods in Ecology and Evolution*, *9*(5), 1276-1285. https://doi.org/10.1111/2041-210X.12970

Isaak, D. J., Wollrab, S., Horan, D., and Chandler, G. 2012. Climate change effects on stream and river temperatures across the northwest U.S. from 1980–2009 and implications for salmonid fishes. *Climatic Change*, *113*(2), 499–524. https://doi.org/10.1007/s10584-011-0326-z

Jame, S. A., and Bowling, L. C. 2020. Groundwater Doctrine and Water Withdrawals in the United States. *Water Resources Management*, *34*(13), 4037–4052. https://doi.org/10.1007/s11269-020-02642-0

Jassby, A. D., and Cloern, J. E. 2017. wq: Some tools for exploring water quality monitoring data. R package version 0.4.9 https://cran.r-project.org/package=wq

Jastram, J. D., and Rice, K. C., 2015, Air- and stream-water-temperature trends in the Chesapeake Bay region, 1960–2014: U.S. Geological Survey Open-File Report 2015–1207, 28 p., http://dx.doi.org/10.3133/ofr20151207.

Jentsch, A., Kreyling, J., and Beierkuhnlein, C. 2007. A new generation of climate-change experiments: events, not trends. *Frontiers in Ecology and the Environment*, 5(7), 365-374.

Karl, T. R., and Koss, W. J. 1984. Regional and national monthly, seasonal, and annual temperature weighted by area, 1895-1983. Historical Climatology Series 4-3, National Climatic Data Center, Asheville, NC, 38 pp.

Kaushal, S. S., Likens, G. E., Jaworski, N. A., Pace, M. L., Sides, A. M., Seekell, D., Belt, K. T., Secor, D. H., and Wingate, R. L. 2010. Rising stream and river temperatures in the United States. *Frontiers in Ecology and the Environment*, *8*(9), 461–466. https://doi.org/10.1890/090037

Keefer, M. L., Peery, C. A., and High, B. 2009. Behavioral thermoregulation and associated mortality trade-offs in migrating adult steelhead (Oncorhynchus mykiss): Variability among sympatric populations. *Canadian Journal of Fisheries and Aquatic Sciences*, *66*(10), 1734–1747. https://doi.org/10.1139/F09-131

Keefer, M. L., Taylor, G. A., Garletts, D. F., Gauthier, G. A., Pierce, T. M., and Caudill, C. C. 2010. Prespawn mortality in adult spring Chinook salmon outplanted above barrier dams: Chinook salmon prespawn mortality. *Ecology of Freshwater Fish*, *19*(3), 361–372. https://doi.org/10.1111/j.1600-0633.2010.00418.x

Lau, N. C., and Nath, M. J. 2012. A Model Study of Heat Waves over North America: Meteorological Aspects and Projections for the Twenty-First Century. *Journal of Climate*, *25*(14), 4761–4784. https://doi.org/10.1175/JCLI-D-11-00575.1

Lee, C. C. 2022. Weather whiplash: Trends in rapid temperature changes in a warming climate. *International Journal of Climatology*, *42*(8), 4214-4222.

Lima, F. P., and Wethey, D. S. 2012. Three decades of high-resolution coastal sea surface temperatures reveal more than warming. *Nature Communications*, *3*(1), 704. https://doi.org/10.1038/ncomms1713

Lynch, D. D. and Risley, J. C. 2003. Klamath River Basin hydrologic conditions prior to the September 2002 die-off of salmon and steelhead: U.S. Geological Survey Water-Resources Investigations Report 03–4099, 10 p. https://doi.org/10.3133/wri034099

McDonald, J. H. 2014. Handbook of Biological Statistics (3rd ed., pp. 254-260). Baltimore, MD: sparky house publishing.

McLeod, A. I. 2011. Kendall: Kendall rank correlation and Mann-Kendall trend test. R package version 2.2. https://CRAN.R-project.org/package=Kendall

Meehl, G.A., T.F. Stocker, W.D. Collins, P. Friedlingstein, A.T. Gaye, J.M. Gregory, A. Kitoh, R. Knutti, J.M. Murphy, A. Noda, S.C.B. Raper, I.G. Watterson, A.J. Weaver and Z.-C. Zhao, 2007: Global Climate Projections. In: Climate Change 2007: The Physical Science Basis. Contribution of Working Group I to the Fourth Assessment Report of the Intergovernmental Panel on Climate Change [Solomon, S., D. Qin, M. Manning, Z. Chen, M. Marquis, K.B. Averyt, M. Tignor and H.L. Miller (eds.)]. Cambridge University Press, Cambridge, United Kingdom and New York, NY, USA.

Michel, A., Brauchli, T., Lehning, M., Schaefli, B., and Huwald, H. 2020. Stream temperature and discharge evolution in Switzerland over the last 50 years: Annual and seasonal behaviour. *Hydrology and Earth System Sciences*, *24*(1), 115–142. https://doi.org/10.5194/hess-24-115-2020

Milly, P. C. D., Dunne, K. A., and Vecchia, A. V. 2005. Global pattern of trends in streamflow and water availability in a changing climate. *Nature*, *438*(7066), 347–350. https://doi.org/10.1038/nature04312

Mosley, L. M. 2015. Drought impacts on the water quality of freshwater systems; review and integration. *Earth-Science Reviews*, *140*, 203–214. https://doi.org/10.1016/j.earscirev.2014.11.010

Moy, N. J., Dodson, J., Tassone, S. J., Bukaveckas, P. A., and Bulluck, L. P. 2016. Biotransport of Algal Toxins to Riparian Food Webs. *Environmental Science and Technology*, *50*(18), 10007–10014. https://doi.org/10.1021/acs.est.6b02760

NOAA National Centers for Environmental Information. 2016. Meteorological versus

astronomical seasons. https://www.ncei.noaa.gov/news/meteorological-versus-astronomical-seasons

Oliver, E. C. J., Benthuysen, J. A., Darmaraki, S., Donat, M. G., Hobday, A. J., Holbrook, N. J., Schlegel, R. W., and Sen Gupta, A. 2021. Marine Heatwaves. *Annual Review of Marine Science*, *13*(1), 313–342. https://doi.org/10.1146/annurev-marine-032720-095144

O'Reilly, C. M., S. Sharma, D. K. Gray, S. E. Hampton, J. S. Read, R. J. Rowley, P. Schneider, J. D. Lenters, P. B. McIntyre, B. M. Kraemer, G. A. Weyhenmeyer, D. Straile, B. Dong, R. Adrian, M. G. Allan, O. Anneville, L. Arvola, J. Austin, J. L. Bailey, J. S. Baron, J. D. Brookes, E. Eyto, M. T. Dokulil, D. P. Hamilton, K. Havens, A. L. Hetherington, S. N. Higgins, S. Hook, L. R. Izmest'eva, K. D. Joehnk, K. Kangur, P. Kasprzak, M. Kumagai, E. Kuusisto, G. Leshkevich, D. M. Livingstone, S. MacIntyre, L. May, J. M. Melack, D. C. Mueller-Navarra, M. Naumenko, P. Noges, T. Noges, R. P. North, P. Plisnier, A. Rigosi, A. Rimmer, M. Rogora, L. G. Rudstam, J. A. Rusak, N. Salmaso, N. R. Samal, D. E. Schindler, S. G. Schladow, M. Schmid, S. R. Schmidt, E. Silow, M. E. Soylu, K. Teubner, P. Verburg, A. Voutilainen, A. Watkinson, C. E. Williamson, and G. Zhang. 2015. Rapid and highly variable warming of lake surface waters around the globe. *Geophysical Research Letters 42*(24): 10773-10781.

Orr, H. G., Simpson, G. L., Clers, S., Watts, G., Hughes, M., Hannaford, J., Dunbar, M. J., Laizé, C. L. R., Wilby, R. L., Battarbee, R. W., and Evans, R. 2015. Detecting changing river temperatures in England and Wales. *Hydrological Processes*, *29*(5), 752–766. https://doi.org/10.1002/hyp.10181

Palmer, M. A., Lettenmaier, D. P., Poff, N. L., Postel, S. L., Richter, B., and Warner, R. 2009. Climate Change and River Ecosystems: Protection and Adaptation Options. *Environmental Management*, *44*(6), 1053–1068. https://doi.org/10.1007/s00267-009-9329-1

Patra, R. W., Chapman, J. C., Lim, R. P., Gehrke, P. C., and Sunderam, R. M. 2015. Interactions between water temperature and contaminant toxicity to freshwater fish: Temperature effects on toxicity of pesticides to fish. *Environmental Toxicology and Chemistry*, *34*(8), 1809–1817. https://doi.org/10.1002/etc.2990

Perkins, S. E., and Alexander, L. V. 2013. On the Measurement of Heat Waves. *Journal of Climate*, *26*(13), 4500–4517. https://doi.org/10.1175/JCLI-D-12-00383.1

Pohlert, T. 2020. trend: Non-Parametric Trend Tests and Change-Point Detection. R package version 1.1.4. https://CRAN.R-project.org/package=trend

R Core Team. 2020. R: A language and environment for statistical computing. R Foundation for Statistical Computing, Vienna, Austria. https://www.R-project.org/.

Ren, L., Song, C., Wu, W., Guo, M., and Zhou, X. 2020. Reservoir effects on the variations of the water temperature in the upper Yellow River, China, using principal component analysis. *Journal of Environmental Management*, *262*, 110339. https://doi.org/10.1016/j.jenvman.2020.110339

Schlegel, R. W., and A. J. Smit. 2018. heatwaveR: A central algorithm for the detection of heatwaves and cold-spells. *Journal of Open Source Software* 3(27): 821

Tassone, S. J., Besterman, A. F., Buelo, C. D., Walter, J. A., and Pace, M. L. 2022. Co-occurrence of Aquatic Heatwaves with Atmospheric Heatwaves, Low Dissolved Oxygen, and Low pH Events in Estuarine Ecosystems. *Estuaries and Coasts, 45*(3), 707–720. https://doi.org/10.1007/s12237-021-01009-x

Thornton, M.M., R. Shrestha, Y. Wei, P.E. Thornton, S. Kao, and B.E. Wilson. 2020. Daymet: Daily Surface Weather Data on a 1-km Grid for North America, Version 4. ORNL DAAC, Oak Ridge, Tennessee, USA. https://doi.org/10.3334/ORNLDAAC/1840

Till, A., Rypel, A. L., Bray, A., and Fey, S. B. 2019. Fish die-offs are concurrent with thermal extremes in north temperate lakes. *Nature Climate Change, 9*(8), 637–641. https://doi.org/10.1038/s41558-019-0520-y

Trenberth, K.E., Dai, A., Van Der Schrier, G., Jones, P.D., Barichivich, J., Briffa, K.R. and Sheffield, J. 2014. Global warming and changes in drought. *Nature Climate Change, 4*(1), 17-22.

U.S. Geological Survey. 2016. National Water Information System data available on the World Wide Web (USGS Water Data for the Nation) http://dx.doi.org/10.5066/F7P55KJN

Vannote, R.L., Minshall, G.W., Cummins, K.W., Sedell, J.R. and Cushing, C.E. 1980. The river continuum concept. *Canadian journal of fisheries and aquatic sciences, 37*(1), 130-137.

van Vliet, M. T. H., Franssen, W. H. P., Yearsley, J. R., Ludwig, F., Haddeland, I., Lettenmaier, D. P., and Kabat, P. 2013. Global river discharge and water temperature under climate change. *Global Environmental Change*, *23*(2), 450–464. https://doi.org/10.1016/j.gloenvcha.2012.11.002

Vasseur, D. A., DeLong, J. P., Gilbert, B., Greig, H. S., Harley, C. D. G., McCann, K. S., Savage, V., Tunney, T. D., and O'Connor, M. I. 2014. Increased temperature variation poses a greater risk to species than climate warming. *Proceedings of the Royal Society B: Biological Sciences*, *281*(1779), 20132612. https://doi.org/10.1098/rspb.2013.2612

Walters, D. M., Fritz, K. M., and Otter, R. R. 2008. The dark side of subsidies: adult stream insects export organic contaminants to riparian predators. *Ecological Applications, 18*(8), 1835-1841.

Webb, B. W., and Nobilis, F. 1995. Long term water temperature trends in Austrian rivers. *Hydrological Sciences Journal*, *40*(1), 83–96. https://doi.org/10.1080/02626669509491392

Woolway, R. I., Jennings, E., Shatwell, T., Golub, M., Pierson, D. C., and Maberly, S. C. 2021. Lake heatwaves under climate change. *Nature*, *589*(7842), 402–407. https://doi.org/10.1038/s41586-020-03119-1

Wuebbles, D. J., Fahey, D. W., Hibbard, K. A., DeAngelo, B., Doherty, S., Hayhoe, K., Horton, R., Kossin, J. P., Taylor, P. C., Waple, A. M., and Yohe, C. P. 2017. *Executive summary. Climate Science Special Report: Fourth National Climate Assessment, Volume I*. U.S. Global Change Research Program. https://doi.org/10.7930/J0DJ5CTG

Ye, F., and Kameyama, S. 2021. Long-term nationwide spatiotemporal changes of freshwater temperature in Japan during 1982–2016. *Journal of Environmental Management*, *281*, 111866. https://doi.org/10.1016/j.jenvman.2020.111866

Table 2.1 Riverine heatwave trends vary by season, stream order, and landscape position. Reported slopes are Sen's slope estimates from Mann-Kendall (M-K) trend analysis. Units for the frequency slope are heatwave events yr^{-1} while the average duration slope is days yr^{-1}. The 15% false discovery rate (FDR) values are the adjusted critical values used to determine statistical significance after multiple comparisons testing to control for type 1 errors. Only statistically significant results are reported. Italicized values have a p-value < 0.05 but are greater than the adjusted critical value and should be interpreted with caution.

Test Type	Variable	Category	Slope (yr^{-1})	M-K p-value	15% FDR
Time	Frequency		0.06	0.004	0.050
Season	Frequency	Summer	0.03	0.004	0.008
		Fall	*0.02*	*0.029*	0.025
Stream Order	Frequency	3	*0.06*	*0.048*	0.038
		4	0.10	< 0.001	0.006
		5	0.07	0.018	0.025
		8	0.06	0.015	0.019
		9	0.08	0.007	0.013
	Avg. Duration	5	*0.08*	*0.038*	0.031
Reservoir	Frequency	None	0.06	0.008	0.017
		Above	0.09	0.012	0.033
	Avg. Duration	Above	0.06	0.017	0.050

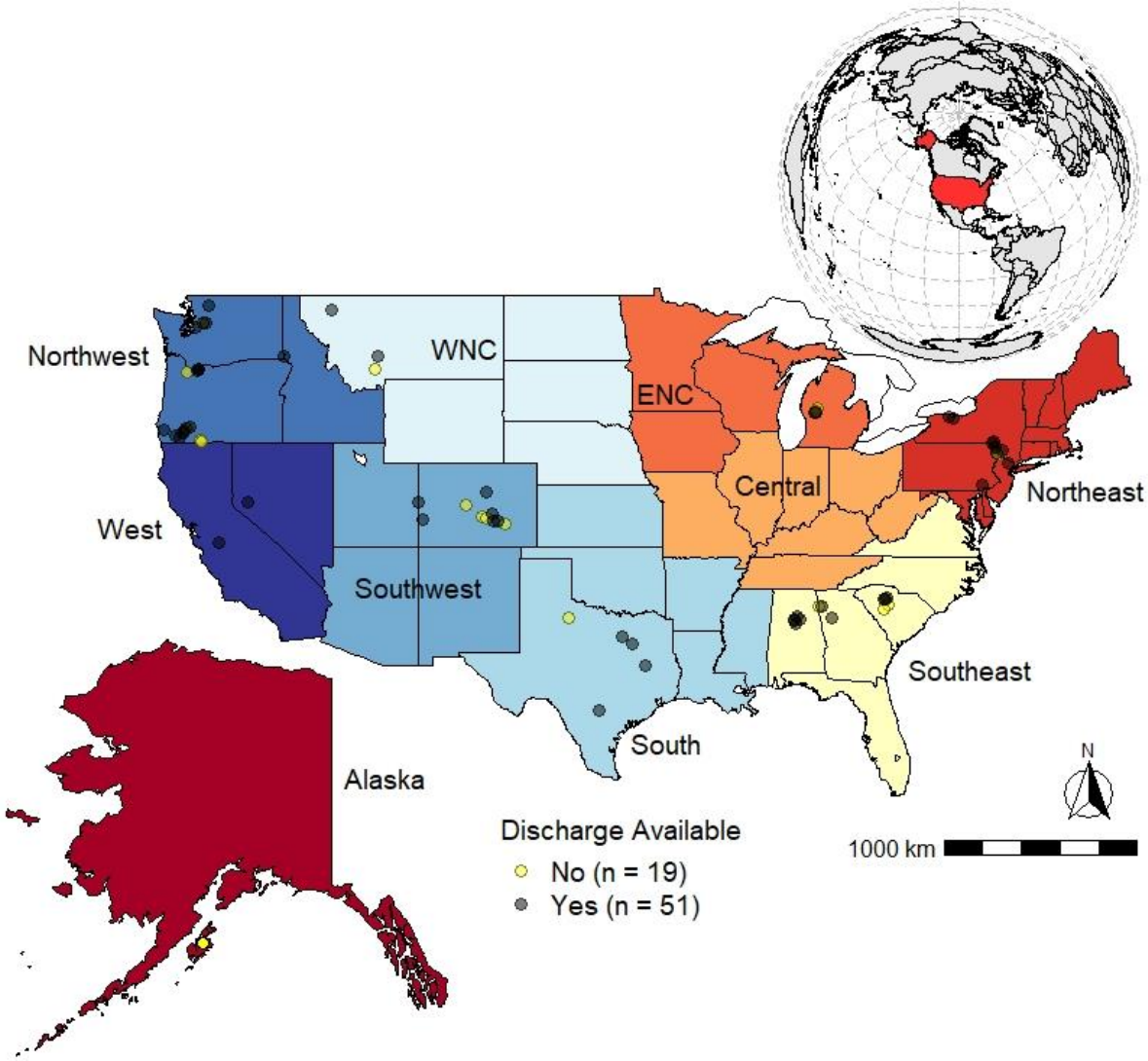

Figure 2.1 Study site locations throughout regions of the U.S. All 70 sites, as represented by a dot, had daily mean water temperature data available between 1996-2021 however not all sites had daily mean discharge data available. Sites with discharge are represented by black dots while those without are yellow dots. WNC = West North Central, ENC = East North Central.

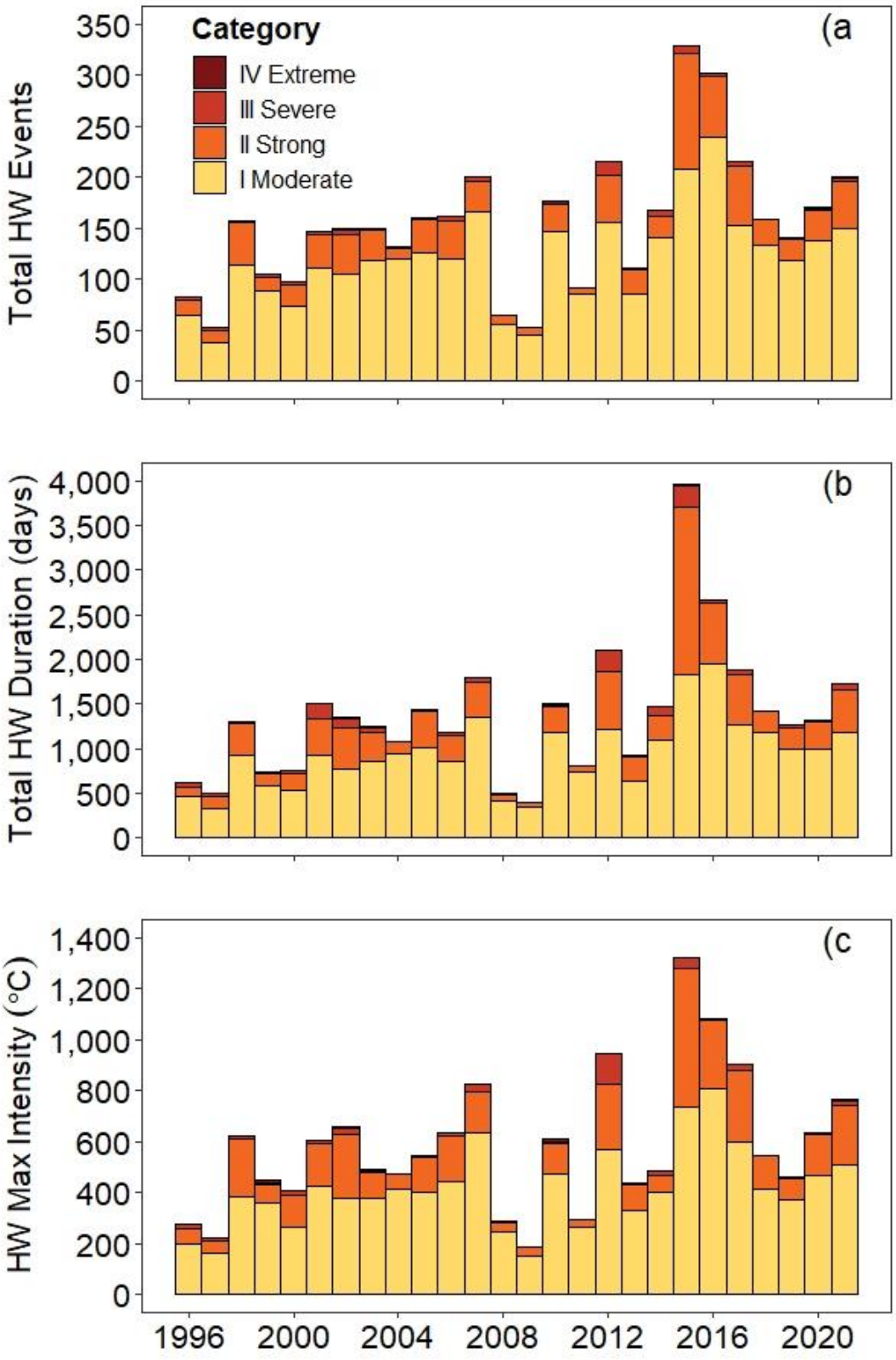

Figure 2.2 Severity classification of the annual total number of riverine heatwaves for all 70 sites throughout the U.S. (a) along with the total duration of all heatwave days per year (b) and the cumulative maximum intensity of all heatwaves events per year (c).

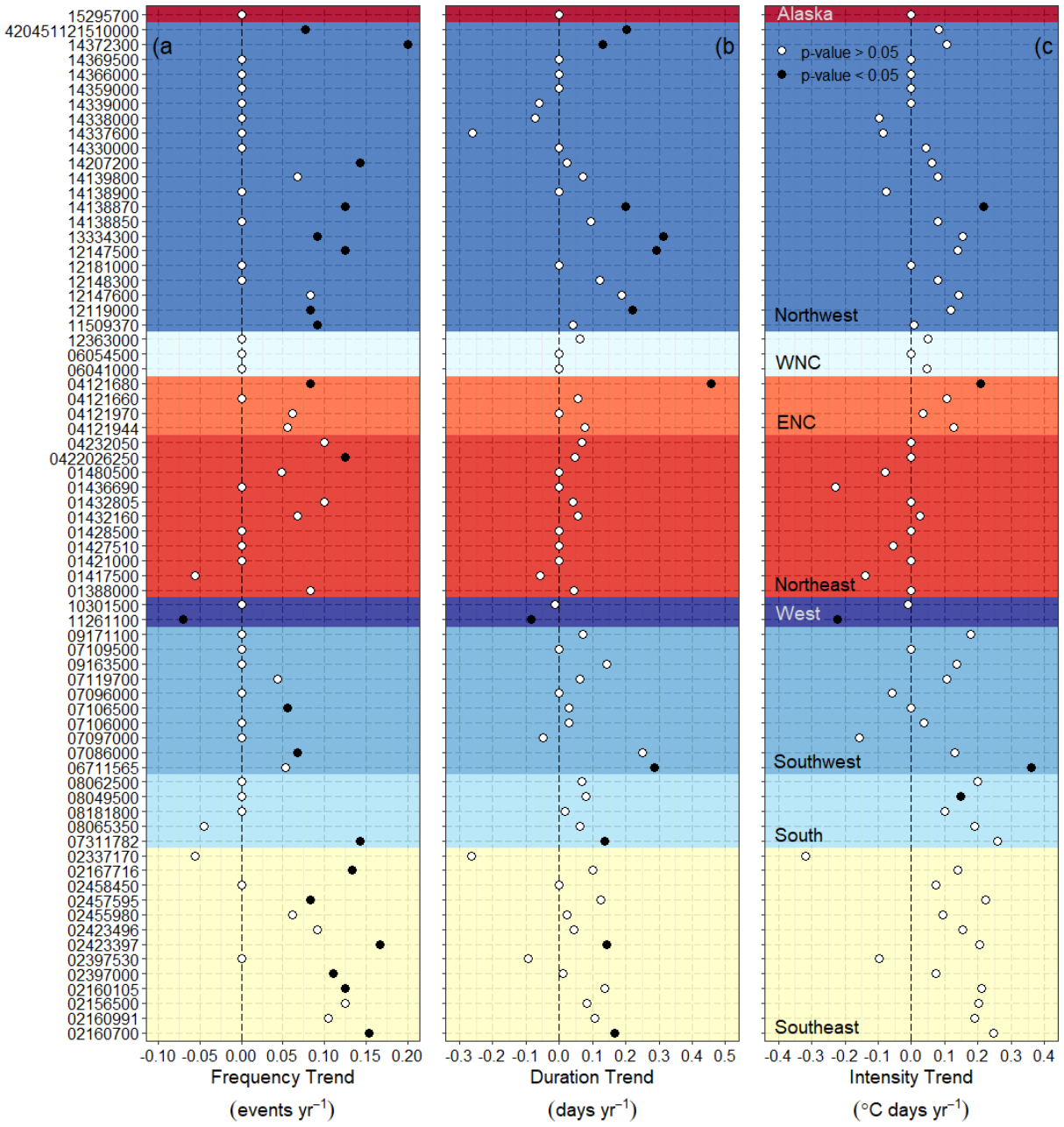

Figure 2.3 Heatwave frequency trends as determined by Sen's slope estimate for all 70 sites (USGS site numbers on y-axis) throughout the U.S. (a) along with heatwave duration trends (b) and cumulative intensity trends (c). Colors within the plots denote U.S. regions from Figure 1. Black dots represent statistically significant (p-value < 0.05) trends as determined using Mann-Kendall tests, while white dots represent non-statistically significant trends (p-value > 0.05). WNC = West North Central, ENC = East North Central.

Chapter 3: Co-occurrence of aquatic heatwaves with atmospheric heatwaves, low dissolved oxygen, and low pH events in estuarine ecosystems

Published in *Estuaries and Coasts* (2022) DOI: 10.1007/s12237-021-01009-x

Co-Authors: Alice F. Besterman, Cal D. Buelo, Jonathan A. Walter, and Michael L. Pace.

Author Contribution Statement: SJT and MLP designed the study. SJT performed the analysis and wrote the manuscript. AFB, CDB, JAW, and MLP contributed to improving the analysis and manuscript.

Abstract

Heatwaves are increasing in frequency, duration, and intensity in the atmosphere and marine environment with rapid changes to ecosystems occurring as a result. However, heatwaves in estuarine ecosystems have received little attention despite the effects of high temperatures on biogeochemical cycling and fisheries and the susceptibility of estuaries to heatwaves given their low volume. Likewise, estuarine heatwave co-occurrence with extremes in water quality variables such as dissolved oxygen (DO) and pH have not been considered and would represent periods of enhanced stress. This study analyzed 1,440 station years of high-frequency data from the National Estuarine Research Reserve System (NERRS) to assess trends in the frequency, duration, and severity of estuarine heatwaves and their co-occurrences with atmospheric heatwaves, low DO, and low pH events between 1996-2019. Estuaries are warming faster than the open and coastal ocean, with an estuarine heatwave mean annual occurrence of 2 ± 2 events, ranging up to 10 events per year, and lasting up to 44 days (mean duration = 8 days). Estuarine heatwaves co-occur with an atmospheric heatwave 6-71% of the time, depending on location, with an average estuarine heatwave lag range of 0-2 days. Similarly, low DO or low pH events co-occur with an estuarine heatwave 2-45% and 0-18% of the time, respectively, with an average low DO lag of 3 ± 2 days and low pH lag of 4 ± 2 days. Triple co-occurrence of an estuarine heatwave with a low DO and low pH event was rare, ranging between 0-7% of all estuarine

heatwaves. Amongst all the stations, there have been significant reductions in the frequency, intensity, duration, and rate of low DO event onset and decline over time. Likewise, low pH events have decreased in frequency, duration, and intensity over the study period, driven in part by reductions in all severity classifications of low pH events. This study provides the first baseline assessment of estuarine heatwave events and their co-occurrence with deleterious water quality conditions for a large set of estuaries distributed throughout the U.S.

Introduction

Greenhouse gas concentrations are expected to continue to increase in the atmosphere throughout the first half of the 21st century, which will lead to climate warming and an increase in water temperatures (Hoegh-Guldberg et al. 2014). As aquatic systems absorb excess heat, a higher frequency, duration, intensity, and spatial extent of discrete extreme warm-water periods known as heatwaves is expected (Frölicher et al. 2018; Oliver et al. 2018; Collins et al. 2019; Oliver et al. 2021). Many physiological, ecological, and biogeochemical processes are temperature-dependent, so extremes in temperature, especially at the higher end, can compound other stressors within aquatic ecosystems. The solubility of dissolved gasses is inversely related to temperature, such that as temperature increases, dissolved oxygen (DO) concentration decreases. Furthermore, ecosystem respiration is a temperature-dependent process that consumes DO and produces carbon dioxide (CO_2) which when mixed with water forms carbonic acid, potentially resulting in lower pH depending on buffering conditions. Aquatic heatwaves push organisms past their thermal tolerance (Madeira et al. 2012) and may trigger multiple stressors in aquatic ecosystems such as low DO and low pH events, which are known to cause local population extinction (Llansó 1992, Baird et al. 2004), regional mass mortality (Garrabou et al. 2009), and trophic cascades (Piatt et al. 2020).

While many studies have reported positive temperature trends for aquatic environments, only recently have studies examined extremes in water temperature referred to in coastal and oceanic environments as marine heatwaves. Marine heatwaves (MHWs) have a standardized definition as discrete periods when water temperature is above a seasonally referenced 90th percentile for five or more consecutive days (Hobday et al. 2016). These relatively short-lived, extreme events have attracted research interest, in part because of their potential for

disproportionate impacts on ecosystems (Easterling et al. 2000, Jentsch et al. 2007) and because future warming is likely to increase the frequency, intensity, duration, and spatial extent of heatwaves. MHWs cause shifts in habitat-forming keystone species (e.g., seagrass, salt marshes, and mangroves), non-native species invasions, and regime shifts (Lima and Wethey 2012; Marbà and Duarte 2010; Osland et al. 2013; Smale and Wernberg 2013; Sorte et al. 2013; Wernberg et al. 2016; Aoki et al. 2021). Relative to coastal and oceanic ecosystems, little attention has been given to heatwaves within estuaries despite their vulnerability due to lower water volume and greater heat exchange by tidal, atmospheric, and fluvial forces.

Many organisms use habitat in the river-estuary-coastal ocean continuum and are sensitive to seasonal extremes in these different locations. This variation among habitats requires better understanding of when, where, and how aquatic heatwaves are changing with implications for species distributions, fisheries management, and conservation. Prior studies of MHWs have relied on satellite-derived sea surface temperature (SST) for broad-scale analysis however, satellite-derived SST measures have limitations. Remotely sensed SST measures are collected at daily to monthly time intervals, are limited by cloud cover, and have low spatial resolution (1-50 km) limiting their use to large bodies of water with low land contamination (i.e., land cover within pixel < 50%; Lima and Wethey 2012). Direct measurements of temperature using in-situ thermistors provide another approach for measuring heatwaves and have the benefit of high temporal resolution (minutes to hours) that allow study of site-specific changes in smaller waterways that would otherwise be contaminated by land using satellite observations, are measured in conjunction with other water quality variables, and can be extrapolated to broad scales through monitoring networks. This study 1) provides a baseline assessment of estuarine heatwaves (EHWs) using in-situ water temperature measurements from the last 24 years (1996-

2019) made at U.S. National Estuarine Research Reserve Sites, 2) examines temporal relationships between atmospheric heatwaves (AHWs) and EHWs, and 3) examines the degree to which EHWs and extremes of low DO and pH co-occur.

Methods

Study Sites

The U.S. National Oceanic and Atmospheric Administration's (NOAA) National Estuarine Research Reserve System (NERRS) maintains a system-wide monitoring program that measures meteorological and water quality conditions using high-frequency automated sensors throughout North America. Of the 29 reserves managed by NERRS, we identified 12 reserves (Figure 3.1) with the longest and most complete meteorological station and water quality station records, beginning in 2002 and 1996, respectively (NOAA 2020). The selected reserves occur on both coasts of the contiguous U.S., including the Gulf of Mexico and Puerto Rico and represent five distinct estuarine habitat types (open water, submerged aquatic vegetation (SAV), upland, marsh, and mangrove) as described in earlier NERRS publications (Wenner et al. 2001; Sanger et al. 2002). Each reserve maintains a minimum of four water quality monitoring stations; within the 12 reserves, we identified 17 water quality monitoring stations with water temperature, dissolved oxygen, and pH records from 1996-2019 that had relatively few missing data (max data gap < 4.2% of timeseries; Table 3.1). Each reserve follows standard operating procedures and QAQC protocols that allow for comparison across the reserve system. Automated atmospheric and water quality stations collect samples at 30-minute (prior to 2007) and 15-minute intervals (post 2007). YSI water quality sondes (model 6600 until 2013, EXO2 thereafter) are calibrated every 1-4 weeks depending on site and season to reduce sensor drift and

cleaned to reduce data loss due to biofouling. All data were accessed using the NERRS Centralized Data Management Office's Advanced Query System (http://cdmo.baruch.sc.edu/).

Extreme Event Detection

Atmospheric and water quality data flagged during the QC protocol as outside sensor range, missing, rejected, or suspect were removed from the analysis. Tidal and diurnal signals in the high-frequency water quality data were removed using Fourier transform (aka transform filter) as a low-pass filter (Walters and Heston 1982; Thomson and Emery 2014). This was done to account for advective fluxes from tidal processes that may impact the water quality time series. Gibbs' phenomenon was suppressed using a three-point taper between the pass-band and stop-band (Forbes 1988; Thomson and Emery 2014). Inspection for Gibbs' phenomena contamination in the filtered data did not reveal any obvious introduced spurious oscillations. Daily averages for each parameter were then calculated from the low-pass filtered, high-frequency data if ≥ 75% of a day's high-frequency observations were present using the R package 'openair' version 2.8-3 (Carslaw and Ropkins 2012). The resulting 216 station years of daily average air temperature and 408 station years of daily average water temperature, DO concentration, and pH were then used to identify extreme events using the R package 'heatwaveR' version 0.4.4 (Schlegel and Smit 2018; R Core Team 2020). While the datasets used in our analysis do not provide the recommended 30 consecutive years of data suggested for this sort of analysis (Hobday et al. 2016), the data are the best available source of high-frequency measures of several estuarine water quality variables for over two-decades across broad geographic regions. In addition, Schlegel et al. (2019) presented a sensitivity analysis of the heatwave algorithm which demonstrated that time series as short as 10-years provided event duration and intensity measures similar to 30-year time series.

Estuarine heatwaves followed the Hobday et al. (2016) definition of marine heatwaves as those times when the daily mean water temperatures exceeded the seasonally adjusted 90^{th} percentile threshold (e.g., the upper-tail of the water temperature distribution) for a period ≥ 5 days without a drop below the threshold for ≥ 2 days. Extreme low DO and pH events followed the same definition as estuarine heatwaves, with the exception that these extremes were those times when DO or pH were below the 10^{th} percentile. We identified low pH (i.e., more acidic) rather than high pH conditions of interest given future projections of ocean acidification (Doney et al. 2020). Atmospheric heatwaves were defined similar to estuarine heatwaves, with the exception that atmospheric heat waves last for a period ≥ 3 consecutive days (i.e., no daily gaps below the seasonal threshold during an event; Perkins and Alexander 2013) relative to EHW which last ≥ 5 days and that allow for ≤ 2 gap days below the seasonal threshold during an event (Hobday et al. 2016). These definitions follow convention in the two fields and are related to the greater atmospheric temperature variability relative to water. An EHW was classified as co-occurring with an AHW when the EHW event started while there was an active AHW event occurring. Similarly, low DO and low pH events co-occurred with an EHW if they started while there was an active EHW. Our approach to identifying co-occurrence is conservative given the potential for lags among the variables, but in using this approach we avoided the problem of specifying lags, which likely vary. Since the AHW timeseries was shorter relative to the EHW's, the co-occurrence and lag analyses were assessed between 2002-2019. As EHW and extreme water quality conditions had the same timeseries length, their co-occurrence and lag analyses spanned the entire 1996-2019 timeseries. Severity classification (moderate, strong, severe, extreme) of each extreme event followed the Hobday et al. (2018) method which is based on

event peak intensity and multiples of the 90th percentile difference from the seasonally adjusted mean.

Statistical Analysis

When extreme events were identified, we also quantified event duration, cumulative intensity above the 90th percentile (or below the 10th percentile for DO and pH), rate of event onset, and event decline rate. Event frequency, defined here as the annual sum of events per station, was derived to examine long-term changes in extreme events. Events were further categorized based on reserve region, season (winter = Dec-Feb, spring = March-May, summer = June-Aug, fall = Sept-Nov), and mean salinity during the event (freshwater = 0-0.5 g kg^{-1}, oligohaline = 0.5-5 g kg^{-1}, mesohaline = 5-18 g kg^{-1}, polyhaline = 18-30 g kg^{-1}, seawater = 30+ g kg^{-1}) to identify spatial, seasonal, and salinity-based patterns. While these seasonal definitions may have limitations given differences in season length between regions, they represent Northern hemisphere meteorological seasons (NOAA 2016) and have been used in estuarine and atmospheric studies of a similar spatial scale (Caffrey 2004; Lau and Nath 2012). Annual trends among events with regard to category and variable of interest were calculated using the non-parametric Mann-Kendall trend test with Sen's slope estimator, which are robust against outliers and non-normally distributed data, and have been used in other long-term trend analyses (Hirsch et al. 1982; Webb and Nobilis 1995; Kaushal et al. 2010; Perkins and Alexander 2013). For reserves with two stations, we present averages and associated range. Due to the multiple comparisons, a 10% False Discovery Rate (FDR, also referred to as Benjamini-Hochberg correction) was applied to reduce type 1 errors upon statistical inference (Benjamini and Hochberg 1995). All analyses were performed in the R environment for statistical computing (R

Core Team 2020) with code available on GitHub (https://github.com/spencer-tassone/EstuarineHeatwaves).

Results

Co-Occurrence and Lag-Time of Events

Relatively low intensity, low duration AHW events are able to produce EHWs when water temperature is near its 90th percentile threshold (Figure 3.2a,b). Estuaries can retain this excess heat and, in some cases, trigger the co-occurrence of a low DO event (Figure 3.2c) and low pH event (Figure 3.2d). The proportion of triple co-occurrence of stressful water quality conditions where there was a low DO event and low pH event that began during an EHW was rare, occurring on average (± SD) in only 2 ± 2% of EHWs but ranging up to 7% at some stations. The proportion of EHW that co-occurred during an active AHW event averaged 36% across all stations and ranged between 6-71% (Figure 3.3). The Mid-Atlantic and Northeast regions had the greatest proportional co-occurrences of atmospheric and estuarine heatwaves, averaging 51 ± 3% and 39 ± 21%, respectively. On average, 17 ± 11% of EHWs had co-occurring low DO events, and 6 ± 5% of EHWs had co-occurring low pH events (Figure 3.3). Amongst co-occurring events, the average lag-time between an AHW and the onset of an EHW ranged between 0-2 days (Figure 3.4). Similarly, the average lag-time between co-occurring EHW and the onset of both low DO and low pH events was 3 ± 2 and 4 ± 2 days respectively.

Atmospheric Heatwaves (AHWs)

Between 2002-2019, across NERRS reserves the number of AHW events did not increase over time. During the 18 years observed, the 12 NERRS reserves had a total of 899 AHW events, with a mean reserve total of 75 ± 11 AHWs (Figure 3.5). Similarly, during the 2002-2019 period, there was a larger number of AHW than EHW or low DO and low pH events. The 18-year mean

air temperature trend among the reserves ranged from -0.10 to 0.12 $^{\circ}$C year^{-1} with 8 of the 12 reserves having positive trends. The trend in annual standard deviation was lower than that of the mean air temperature, ranging from -0.03 to 0.05 $^{\circ}$C year^{-1} with 6 of the 12 reserves having positive increases (SI Figure 3.1a).

Estuarine Heatwaves (EHWs)

Among the 17 water quality stations, there was a total of 900 EHW events between 1996-2019 (Table 3.1) with a mean station total number of EHWs of 53 ± 8 (Table 3.1). The mean annual frequency and duration of EHWs ranged between 1-4 events year^{-1} and 6-12 days respectively. The average onset rate of EHWs declined by -0.01 $^{\circ}$C day^{-1} year^{-1} (p-value = 0.001; Table 3.2) among the NERRS stations. There has been no significant trend in severity classification of EHW events (Figure 3.6a), although there has been a non-significant increasing trend in the total number of EHW days (Figure 3.6d). The 24-year mean water temperature trend among the reserves ranged between -0.07-0.09 °C year^{-1} which was greater than the trend in the annual standard deviation (-0.02-0.04 $^{\circ}$C year^{-1}; SI Figure 3.1b). Patterns in mean EHW duration, total number of events, and event frequency as a function of mean depth, mean tidal range, and habitat type were non-significant (SI Figure 3.2).

Low Dissolved Oxygen Events

The frequency (-0.05 events year^{-1}, p-value = 0.008), average cumulative intensity (-0.20 mg L^{-1} days year^{-1}, p-value = 0.031), average duration (-0.12 days year^{-1}, p-value = 0.003), onset and decline rates (-0.01 mg L^{-1} day^{-1} year^{-1}, p-value = 0.003, -0.02 mg L^{-1} day^{-1} year^{-1}, p-value = 0.003 respectively) of low DO events decreased over time throughout the NERRS stations (Table 3.2). There has been a decrease in the total number of low DO events driven by reductions in the strong, severe, and extreme severity classifications (Figure 3.6b). Similarly, there has been a

significant reduction in total low DO days, decreasing by 11.9 days $year^{-1}$ (Figure 3.6e). Regionally, the Northeast had significant declines in average cumulative intensity (-0.37 mg L^{-1} days $year^{-1}$, p-value = 0.001) and event duration (-0.20 days $year^{-1}$, p-value = 0.004). Likewise, the Northeast and Mid-Atlantic had decreased average onset (both -0.01 mg L^{-1} day^{-1} $year^{-1}$, p-value ≤ 0.012) and decline rates of low DO events (-0.02 mg L^{-1} day^{-1} $year^{-1}$, p-value = 0.011, -0.04 mg L^{-1} day^{-1} $year^{-1}$, p-value < 0.001 respectively). The frequency (-0.03 events $year^{-1}$, p-value < 0.001), average duration (-0.14 days $year^{-1}$, p-value = 0.005), and average decline rate (-0.02 pH $days^{-1}$ $year^{-1}$, p-value = 0.012) declined significantly throughout the summer. Patterns in mean low DO duration, total number of events, and event frequency as a function of mean depth, mean tidal range, and habitat type were mostly non-significant (SI Figure 3.3).

Low pH Events

The frequency (-0.09 events $year^{-1}$, p-value ≤ 0.001), average duration (-0.13 days $year^{-1}$, p-value = 0.04), and average cumulative intensity (-0.07 pH days $year^{-1}$, p-value = 0.006) of low pH events significantly decreased over time (Table 3.2). Likewise, there has been a decrease in the total number of low pH events driven by significant reductions in all categories of extreme event classification (Figure 3.6c). Similarly, there has been a significant reduction in total low pH days, decreasing by 24.9 days $year^{-1}$ (Figure 3.6f). All seasons had declines in the frequency of low pH events, with spring and summer reduced by -0.03 events $year^{-1}$ (p-values ≤ 0.008) and fall and winter reduced by -0.02 events $year^{-1}$ (p-values ≤ 0.012). Furthermore, the average cumulative intensity (-0.12 pH days $year^{-1}$, p-value = 0.001) and duration (-0.29 days $year^{-1}$, p-value = 0.004) of low pH events decreased in the Spring. The onset rate of low pH events was reduced in the fall (-0.004 pH day^{-1} $year^{-1}$, p-value = 0.016). Among salinity gradients, the frequency of low pH events declined at the salinity end-members (tidal fresh = -0.08 events $year^{-}$

^{1}, p-value = 0.009; Seawater = -0.10 events year^{-1}, p-value = 0.003). Mesohaline, polyhaline, and seawater segments had significant declines in the average cumulative intensity of low pH events (slopes between -0.11 and -0.08 pH days year^{-1}, p-values ≤ 0.011). Furthermore, the average duration (-0.27 days year^{-1}, p-value = 0.027) and decline rate (-0.004 pH day^{-1} year^{-1}, p-value = 0.007) of low pH events were reduced in the seawater end-member. Regionally, the West coast (-0.20 events year^{-1}), Northeast, Mid-Atlantic (both slopes = -0.10 events year^{-1}), and Southeast (-0.09 events year^{-1}) had significant reductions in low pH event frequency (all p-values ≤ 0.03). Similarly, the West coast, Northeast, and Southeast regions had reduced average cumulative intensity (slopes between -0.10 and -0.06 pH days year^{-1}, p-values ≤ 0.027) and average decline rates (slopes between -0.01 and -0.002 pH day^{-1} year^{-1}, p-values ≤ 0.014). The Northeast region was the only region to have reduced average low pH event onset rate (-0.002 pH day^{-1} year^{-1}, p-value = 0.027). Patterns in mean low pH duration, total number of events, and event frequency as a function of mean depth, mean tidal range, and habitat type were non-significant (SI Figure 3.4).

Discussion

The co-occurrence of and lag-time between extreme events (i.e., EHW, low DO, and low pH) potentially compounds the stressful conditions that a single event may cause. Atmospheric and estuarine heatwaves had the greatest proportion of co-occurrence (6-71%; Figure 3.3) and shortest lag-time (average = 1 ± 1 day; Figure 2.4), suggesting that AHW can push estuaries into heatwave conditions rapidly. Given the relatively high proportion of co-occurrence of AHW and EHW and their short lag times, estuarine heatwaves may interact nonlinearly with ecosystem processes as has been observed in other aquatic ecosystems (Stenseth and Mysterud 2002; Caissie 2006; Wilhelm and Adrian 2008). Estuarine heatwave and low DO co-occurrence were

twice as likely throughout the Atlantic coast (average = 20 ± 9%) relative to the Pacific, Gulf of Mexico, and Caribbean (average = 8 ± 2%; Figure 3.3). Estuarine heatwave and low pH co-occurrence were relatively low and similar across all regions (6 ± 4%). Warm water temperatures stimulate metabolic activity that can cause diel fluctuations in pH (Duarte et al. 2013) however watershed inputs of bicarbonate alkalinity have been increasing in many rivers (Kaushal et al. 2013), increasing the buffering capacity of receiving water bodies against low pH events including those brought on by relatively short-lived extreme EHW events. Likewise, increased production during periods of elevated water temperature could reduce low pH stress in estuaries that are experiencing increased loading of acidic waters, or reduced watershed loading via drought or water withdrawals. The average lag-time between an EHW and low DO or low pH was 3 ± 2 days and 4 ± 2 days respectively, suggesting a possible connection between extreme warm water conditions and ecosystem respiration. The triple co-occurrence of an estuarine heatwave, low DO, and low pH event was low amongst most stations, averaging 2 ± 2%, however Tivoli South Bay, Hudson River, NY had a 7% rate of triple co-occurrence. The relatively high co-occurrence of EHW and low pH events, as well as triple co-occurrences at Tivoli South Bay are likely due this station being connected to a tidal freshwater swamp. The co-occurrence of low DO and low pH appears to have both additive and synergistic negative effects on fish and bivalves (Gobler and Baumann 2016; Chan et al. 2019). These low DO and low pH conditions have become more common in stratified coastal zones due in part to rising water temperature (Gruber 2011; Doney et al. 2012). The NERRS datasets do not allow us to determine if stratification is present in these shallow estuaries (mean water column depth range between 0.68-5.51 meters) as measurements are collected at a single fixed position in the water column. The water quality data produced by NERRS come from ‘bottom waters’ as the water

quality sondes are fixed in elevation above the sediment surface between 0.15-1.0 meters depending on station (1.7 m for APAES which is the lone 'surface water' station). If stratification were present, the AHW-EHW co-occurrence results presented herein are likely conservative estimates given the position of the thermistor sensor in the water column. Stratification may also cause the EHW and low DO/pH events to be conservative estimates again due to sensor position as surface and bottom waters are not exchanged (i.e., surface water experiencing an EHW while bottom water is not). Nonetheless, our results represent observed estuarine water quality conditions where the triple co-occurrence of extreme events was not frequent at most stations. However, these relatively rare periods represent times of enhanced stress where potentially large and enduring changes may occur.

Heating and cooling trends of annual estuarine water temperature were observed throughout the 408 station years available. Of the 17 stations examined in this analysis, 10 showed positive trends in annual water temperature with four being significant (p-value < 0.05) ranging from 0.03-0.09 $^{\circ}C\ year^{-1}$. These warming rates are similar to what others have observed in streams, rivers, and lakes throughout the U.S. (Kaushal et al. 2010; Ding and Elmore 2015; O'Reilly et al. 2015) and greater than warming rates observed in coastal and open ocean studies (Burrows et al. 2011; Lima and Wethey 2012). This suggests that inland aquatic ecosystems, including estuaries, are among the most vulnerable to warming and extreme temperature events which can cause shifts in habitat-forming keystone species (e.g., seagrass, salt marshes, and mangroves), possibly alter greenhouse gas production, local extinction events, non-native species invasions, and regime shifts (Borges et al. 2016; Lima and Wethey 2012; Marbà and Duarte 2010; Marotta et al. 2014; Osland et al. 2013; Smale and Werberg 2013; Bartosiewicz et al. 2016; Wernberg et al. 2016; Kendrick et al. 2019). The standard deviation in annual estuarine

water temperature increased at 13 of the 17 stations (SI Figure 3.1b), suggesting that water temperature variability is increasing at the upper-tail of the water temperature distribution (i.e., distribution width increasing). Reserves in the lower Northeast, Mid-Atlantic, and Northern West coast had trends in annual water temperature standard deviation increasing quicker than the mean. Similar results have been observed for atmospheric heatwaves in Europe (Schär et al. 2004). Throughout the U.S., estuaries will continue to experience extremely high water temperatures, driven in part by projected increases in atmospheric and marine heatwave frequency, intensity, duration, and spatial extent (Lau and Nath 2012, Collins et al. 2019). Additional long-term data from additional sites are needed to refine quantitative relationships between habitats, heatwaves, and water quality variables. The NERRS dataset provides a valuable long-term record and a baseline for future analyses of extreme temperature impacts on these ecosystems.

All significant trends in extreme low DO events were negative, suggesting an improvement in estuarine water quality. Low DO events in estuaries are, in general, decreasing in frequency, mean cumulative intensity, mean duration, and rates of onset and decline (Table 3.2). There has been a significant reduction in the total number of annual low DO events (Figure 3.6b) and the number of low DO days (Figure 6e) with significant reductions in strong, severe, and extreme classifications of low DO events. Significant management improvements in total nitrogen runoff and wastewater treatment have been attributed to improvements in water quality including rising DO concentrations (Tomaso and Najjar 2015; Whitney and Vlahos 2021); however, climate forecasts indicate these improvements in DO will be reduced given lower oxygen solubility and increased respiration under warming estuarine conditions (Whitney and Vlahos 2021). Of the 846 low DO events that were observed in our analysis, 54.7% reached

hypoxia ($\leq$ 2.0 mg L^{-1}) with oxygen dropping to essentially zero (< 0.01 mg L^{-1}) in some cases. Similarly, the mean low DO event duration was 9 days but ranged up to 52 days. While extreme low DO events in estuaries are becoming less frequent, intense and shorter in duration, they co-occur with EHWs in some cases. Improvements in water quality conditions might be reversed in the future if water temperature continues to increase leading to more co-occurring extremes. Likewise, if projections of increase precipitation led to increased freshwater run-off and salinity stratification, then low DO events could become more frequent in bottom water sites increasing the probability of co-occurring water quality extremes.

Similar to the trends in low DO events, all significant trends related to low pH events were negative thereby providing further evidence of improvements in estuarine water quality. In general, low pH events are decreasing in frequency, duration, and intensity over time within U.S. estuaries with frequencies being reduced during all seasons (Table 3.2). Furthermore, there have been significant reductions in all severity classifications of low pH events (Figure 3.6c) and a significant reduction in the total number of low pH days (Figure 3.6f). However, there is regional heterogeneity in low pH frequency with all regions except the Gulf of Mexico showing significant reductions. Similarly, the West coast, Northeast, and Southeast were the only regions to have significant annual declines in mean cumulative intensity and mean decline rate while the Northeast was the only region to have reduced mean low pH event onset rates. Of the 815 low pH events observed in our analysis 46.4% had a pH < 7.0, with some reaching a pH of 6.0, and lasting up to 97 days (mean duration = 12 days). While atmospheric CO_2 emissions continue to push pH in the marine environment lower (Doney et al. 2009), estuarine pH is controlled by many complex interactions, including watershed export of alkalinity (via carbonate lithology, acid deposition, topography, land use/cover, and wastewater effluent), organic matter, CO_2,

nutrient inputs, stratification, and metabolic rates of production and respiration (Cai et al. 2011; Kaushal et al. 2013; Duarte et al. 2013). We show that EHWs co-occur with extreme low pH conditions relatively rarely (≤ 13% of EHWs) for most NERRS stations, but not for all (max co-occurrence = 18% for Tivoli South Bay, Hudson River, NY). Our results provide evidence of improvements in estuarine water quality via reductions in the frequency, duration, and severity of low pH (i.e., acidic) conditions on a broad scale.

Atmospheric heatwaves at the NERRS reserves had no significant trends in heatwave characteristics (Table 3.2). However, there were 899 AHWs observed between 2002-2019 at the 12 NERRS reserves, with West coast and Gulf of Mexico reserves having the greatest number of AHWs relative to the number of reserves in those regions (88 and 82 events reserve^{-1}). AHW events were relatively frequent, with a mean annual occurrence of 4 ± 3 events, ranging up to 18 events year^{-1}, and lasting up to 15 days (mean duration = 4 days). Seasonally, AHW were on average most frequent in the summer and least frequent in the winter however, winter cumulative intensity was greater on average than summer cumulative intensity (2.14 and 1.28 °C days respectively). Likewise, simple linear regression of mean annual air temperature did show significant increases in air temperature, with positive slopes at 8 of the 12 reserves (SI Figure 3.1a). These findings follow prior studies of North American atmospheric temperature trends that have shown a lengthening of the growing season driven in part by warming fall temperatures since the mid-twentieth century (Piao et al. 2008; Burrows et al. 2011; Barichivich et al. 2012). A warming atmosphere will increase diffusive thermal fluxes across the atmosphere-surface water boundary leading to increased temperature stress within estuaries.

Estuarine heatwaves had no significant trends in EHW characteristics across a broad scale with the exception of reduced average onset rate (Table 3.2). This lack of significant trends

is in contrast to studies of the coastal and open oceans that have reported increasing frequencies and durations of marine heatwaves (Lima and Wethey 2012; Frölicher et al. 2018; Oliver et al. 2018). Nonetheless, EHWs occurred relatively frequently, with a mean annual occurrence of 2 ± 2 events, ranging up to 10 events $year^{-1}$, and lasting up to 44 days (average duration = 8 days). Trends in estuarine heatwaves along salinity gradients were non-significant however, there were between 81-268 total events among the salinity segments over the study period with an average duration spanning 7-9 days. Several complex interactions between estuarine attributes (i.e., freshwater discharge, oceanic exchange, depth, residence time, geomorphology, latitude, salinity), catchment characteristics (i.e., riparian cover, impervious surface area, wastewater effluent), and regional climate (i.e., cloud cover, precipitation regime) influence the thermal properties of estuaries, which lead to estuarine segments experiencing differential thermal conditions (Scanes et al. 2020). The onset rate of estuarine heatwaves declined over the study period, suggesting that estuarine heatwaves are reaching peak heatwave intensity less rapidly. This reduction in event onset rate may benefit organisms as it suggests the change from non-heatwave conditions to peak heatwave conditions is becoming more gradual (i.e., less abrupt change). Estuarine heatwaves will likely accelerate due to increased diffusive air-water boundary heat flux and horizontal advective thermal fluxes from a warming coastal ocean and fluvial discharge. This will have cascading impacts on estuarine ecosystem function and services, including ecologically and commercially important organisms.

This study provides the first baseline assessment of estuarine heatwaves and their co-occurrence with low DO and pH for the NERRS sites with the longest records. Future studies should consider the three-dimensional structure of aquatic heatwave events as studies have been limited to surface waters (i.e., satellite data) or fixed water depths (i.e., current study).

Understanding the depth profile and the spatial areal extent of these disturbance events would help resolve their impacts on species' movement and range dynamics, as extreme events can cause barriers to migration if they extend through the whole water column (Major and Mighell 1967, Cairns 1971) and eliminate or severely limit thermal refuges. Similarly, water circulation (i.e., residence time) and stratification are known to influence water quality conditions. Further analysis of EHWs should consider estuary specific residence time and salinity stratification as potential drivers of EHW characteristics. Likewise, this study considered a single tidal filtering approach however, further analyses should consider other tidal filters (i.e., weighted regression) that could be applied to high frequency estuarine measures (Beck et al. 2015). Additionally, benthic sediments are considered thermally stable relative to the overlying water column; however, benthic respiration increases with temperature, and it remains unclear if EHWs increase sediment temperature possibly affecting carbon storage. Developing a thorough understanding of depth profiles during heatwaves would benefit resource managers working to restore aquatic ecosystems, conserve fisheries, limit non-native species introductions, and model carbon sources and sinks from shallow aquatic ecosystems (Caissie 2006; Aoki et al. 2021). Furthermore, water temperatures are increasing in streams and rivers driven in part by a warming climate, discharge regulation, and increased impervious surface area (Webb and Nobilis 1995; Kaushal et al. 2010; Ding and Elmore 2015), yet there is a lack of understanding regarding the frequency, intensity, and duration of aquatic heatwaves in these inland lotic ecosystems that affect thermal inputs to estuaries. Lastly, comparisons among in-situ studies and those utilizing satellite-derived SST may provide an opportunity for a thorough characterization of aquatic heatwaves events in space and time as heatwaves are often short-lived, intense, and occurring at varying spatial scales. Combining in-situ and satellite temperature offers the opportunity to

document more events with coordinated study of impacts as the heating of estuaries increases in the future.

References

Aoki, L. R., K. J. McGlathery, P. L. Wiberg, M. P. J. Oreska, A. C. Berger, P. Berg, R. J. Orth. 2021. Seagrass recovery following marine heat wave influences sediment carbon stocks. *Frontiers in Marine Science* 7: 1170.

Baird, D., R. R. Christian, C. H. Peterson, and G. A. Johnson. 2004. Consequences of hypoxia on estuarine ecosystem function: energy diversion from consumers to microbes. *Ecological Applications* 14(3): 805–822.

Barichivich, J., K. R. Briffa, T. J. Osborn, T. M. Melvin, and J. Caesar. 2012. Thermal growing season and timing of biospheric carbon uptake across the Northern Hemisphere. *Global Biogeochemical Cycles* 26(4): GB4015

Bartosiewicz, M., I. Laurion, F. Clayer, and R. Maranger. 2016. Heat-Wave Effects on Oxygen, Nutrients, and Phytoplankton Can Alter Global Warming Potential of Gases Emitted from a Small Shallow Lake. *Environmental Science & Technology* 50(12): 6267–6275.

Beck, M. W., J. D. Hagy III, M. C. Murrell. 2015. Improving estimates of ecosystem metabolism by reducing effects of tidal advection on dissolved oxygen time series. *Limnology and Oceanography: Methods* 13(12): 731-745.

Benjamini, Y., and Y. Hochberg. 1995. Controlling the False Discovery Rate: A Practical and Powerful Approach to Multiple Testing. *Journal of the Royal Statistical Society: Series B (Methodological)* 57(1): 289–300.

Borges, A. V., W. Champenois, N. Gypens, B. Delille, and J. Harlay. 2016. Massive marine methane emissions from near-shore shallow coastal areas. *Scientific Reports* 6(1): 27908.

Burrows, M. T., D. S. Schoeman, L. B. Buckley, P. Moore, E. S. Poloczanska, K. M. Brander, C. Brown, J. F. Bruno, C. M. Duarte, B. S. Halpern, J. Holding, C. V. Kappel, W. Kiessling, M. I. O'Connor, J. M. Pandolfi, C. Parmesan, F. B. Schwing, W. J. Sydeman, and A. J. Richardson. 2011. The Pace of Shifting Climate in Marine and Terrestrial Ecosystems. *Science* 334(6056): 652–655.

Caffrey, J. M. 2004. Factors Controlling Net Ecosystem Metabolism in U. S. Estuaries. *Estuaries* 27(1): 90–101.

Cai, W. J., X. Hu, W. J. Huang, M. C. Murrell, J. C. Lehrter, S. E. Lohrenz, W. C. Chou, W. Zhai, J. T. Hollibaugh, Y. Wang, P. Zhao, X. Guo, K. Gundersen, M. Dai, G. C. Gong. 2011. Acidification of subsurface coastal waters enhanced by eutrophication. *Nature Geoscience* 4(11): 766-770.

Cairns, J. 1971. Thermal Pollution: A Cause for Concern. *Journal (Water Pollution Control Federation)* 43(1): 55-66.

Caissie, D. 2006. The thermal regime of rivers: a review. *Freshwater Biology* 51(8): 1389–1406.

Carslaw, D. C., and K. Ropkins. 2012. openair --- an R package for air quality data analysis. *Environmental Modelling & Software* 27-28: 52-61.

Chan, F., J. A. Barth, K. J. Kroeker, J. Lubchenco, and B. A. Menge. 2019. The dynamics and impact of ocean acidification and hypoxia. *Oceanography* 32(3): 62-71.

Collins, M., M. Sutherland, L. Bouwer, S.-M. Cheong, H. J. D. Combes, M. K. Roxy, I. Losada, K. McInnes, B. Ratter, E. Rivera-Arriaga, R. D. Susanto, D. Swingedouw, L. Tibig, P. Bakker, C. M. Eakin, K. Emanuel, M. Grose, M. Hemer, L. Jackson, A. Kääb, J. Kajtar, T. Knutson, C. Laufkötter, I. Noy, M. Payne, R. Ranasinghe, G. Sgubin, M.-L. Timmermans, A. Abdulla, M. H. González, and C. Turley. 2019. *IPCC Special Report on the Ocean and Cryosphere in a Changing Climate*: Extremes, Abrupt Changes and Managing Risks 6: 589-655.

Ding, H., A. J. Elmore. 2015. Spatio-temporal patterns in water surface temperature from Landsat time series data in the Chesapeake Bay, U.S.A. *Remote Sensing of Environment* 168: 335-345.

Doney, S. C., V. J. Fabry, R. A. Feely, and J. A. Kleypas. 2009. Ocean Acidification: The Other CO_2 Problem. *Annual Review of Marine Science* 1(1): 169–192.

Doney, S. C., M. Ruckelshaus, J. Emmett Duffy, J. P. Barry, F. Chan, C. A. English, H. M. Galindo, J. M. Grebmeier, A. B. Hollowed, N. Knowlton, J. Polovina, N. N. Rabalais, W. J. Sydeman, and L. D. Talley. 2012. Climate Change Impacts on Marine Ecosystems. *Annual Review of Marine Science* 4(1): 11–37.

Doney, S. C., D. S. Busch, S. R. Cooley, and K. J. Kroeker. 2020. The Impacts of Ocean Acidification on Marine Ecosystems and Reliant Human Communities. *Annual Review of Environment and Resources* 45(1): 83–112.

Duarte, C. M., I. E. Hendriks, T. S. Moore, Y. S. Olsen, A. Steckbauer, L. Ramajo, J. Carstensen, J. A. Trotter, and M. McCulloch. 2013. Is Ocean Acidification an Open-Ocean Syndrome? Understanding Anthropogenic Impacts on Seawater pH. *Estuaries and Coasts* 36(2): 221–236.

Easterling, D. R. 2000. Climate Extremes: Observations, Modeling, and Impacts. *Science* 289(5487): 2068–2074.

Forbes, A. M. G. 1988. Fourier transform filtering: A cautionary note. *Journal of Geophysical Research: Oceans* 93(C6): 6958-6962.

Frölicher, T. L., E. M. Fischer, and N. Gruber. 2018. Marine heatwaves under global warming. *Nature* 560(7718): 360–364.

Garrabou, J., R. Coma, N. Bensoussan, M. Bally, P. Chevaldonné, M. Cigliano, D. Diaz, J. G. Harmelin, M. C. Gambi, D. K. Kersting, J. B. Ledoux, C. Lejeusne, C. Linares, C. Marschal, T. Pérez, M. Ribes, J. C. Romano, E. Serrano, N. Teixido, O. Torrents, M. Zabala, F. Zuberer, and C. Cerrano. 2009. Mass mortality in Northwestern Mediterranean

rocky benthic communities: effects of the 2003 heat wave. *Global Change Biology* 15(5): 1090–1103.

Gobler, C. J., and H. Baumann. 2016. Hypoxia and acidification in ocean ecosystems: coupled dynamics and effects on marine life. *Biology Letters* 12(5): 20150976.

Gruber, N. 2011. Warming up, turning sour, losing breath: ocean biogeochemistry under global change. *Philosophical Transactions of the Royal Society A: Mathematical, Physical and Engineering Sciences* 369(1943): 1980–1996.

Hirsch, R. M., J. R. Slack, and R. A. Smith. 1982. Techniques of trend analysis for monthly water quality data. *Water Resources Research* 18(1): 107–121.

Hobday, A. J., L. V. Alexander, S. E. Perkins, D. A. Smale, S. C. Straub, E. C. J. Oliver, J. A. Benthuysen, M. T. Burrows, M. G. Donat, M. Feng, N. J. Holbrook, P. J. Moore, H. A. Scannell, A. Sen Gupta, and T. Wernberg. 2016. A hierarchical approach to defining marine heatwaves. *Progress in Oceanography* 141: 227–238.

Hobday, A., E. Oliver, A. Sen Gupta, J. Benthuysen, M. Burrows, M. Donat, N. Holbrook, P. Moore, M. Thomsen, T. Wernberg, and D. Smale. 2018. Categorizing and Naming Marine Heatwaves. *Oceanography* 31(2): 162-173.

Hoegh-Guldberg, O., R. Cai, E.S. Poloczanska, P.G. Brewer, S. Sundby, K. Hilmi, V.J. Fabry, and S. Jung., 2014. The Ocean: Climate Change 2014: Impacts, Adaptation, and Vulnerability. *Part B: Regional Aspects. Contribution of Working Group II to the Fifth Assessment Report of the Intergovernmental Panel on Climate Change*. 1655-1731.

Jenuch, A., J. Kreyling, and C. Beierkuhnlein. 2007. A New Generation of Climate-Change Experiments: Events, Not Trends. *Frontiers in Ecology and the Environment* 5(7): 365-374.

Kaushal, S. S., G. E. Likens, N. A. Jaworski, M. L. Pace, A. M. Sides, D. Seekell, K. T. Belt, D. H. Secor, and R. L. Wingate. 2010. Rising stream and river temperatures in the United States. *Frontiers in Ecology and the Environment* 8(9): 461–466.

Kaushal, S. S., G. E. Likens, R. M. Utz, M. L. Pace, M. Grese, and M. Yepsen. 2013. Increased river alkalinization in the Eastern U.S. *Environmental Science & Technology* 47(18): 10302-10311

Kendrick, G. A., R. J. Nowicki, Y. S. Olsen, S. Strydom, M. W. Fraser, E. A. Sinclair, J. Statton, R. K. Hovey, J. A. Thomson, D. A. Burkholder, K. M. McMahon, K. Kilminster, Y. Hetzel, J. W. Fourqurean, M. R. Heithaus, and R. J. Orth. 2019. A Systematic Review of How Multiple Stressors from an Extreme Event Drove Ecosystem-Wide Loss of Resilience in an Iconic Seagrass Community. *Frontiers in Marine Science* 6: 455.

Lau, N. C., and M. J. Nath. 2012. A Model Study of Heat Waves over North America: Meteorological Aspects and Projections for the Twenty-First Century. *Journal of Climate* 25(14): 4761–4784.

Lima, F. P., and D. S. Wethey. 2012. Three decades of high-resolution coastal sea surface temperatures reveal more than warming. *Nature Communications* 3(1): 704.

Llansó, R. J. 1992. Effects of hypoxia on estuarine benthos: the lower Rappahannock River (Chesapeake Bay), a case study. *Estuarine, Coastal and Shelf Science* 35(5): 491-515.

Madeira, D., L. Narciso, H. N. Cabral, and C. Vinagre. 2012. Thermal tolerance and potential impacts of climate change on coastal and estuarine organisms. *Journal of Sea Research* 70: 32–41.

Major, R. L., Mighell, J.L., 1967. Influence of rocky reach dam and the temperature of the okanogan river on the upstream migration of sockeye salmon. *Fisheries Bulletin*, 66: 131-147.

Marbà, N., and C. M. Duarte. 2009. Mediterranean warming triggers seagrass (Posidonia oceanica) shoot mortality. *Global Change Biology* 16(8): 2366–2375.

Marotta, H., L. Pinho, C. Gudasz, D. Bastviken, L. J. Tranvik, and A. Enrich-Prast. 2014. Greenhouse gas production in low-latitude lake sediments responds strongly to warming. *Nature Climate Change* 4(6): 467–470.

NOAA National Centers for Environmental Information. 2016. Meteorological versus astronomical seasons. https://www.ncei.noaa.gov/news/meteorological-versus-astronomical-seasons

NOAA National Estuarine Research Reserve System (NERRS). 2020. System-wide Monitoring Program. Data accessed from the NOAA NERRS Centralized Data Management Office website: http://www.nerrsdata.org

Oliver, E. C. J., M. G. Donat, M. T. Burrows, P. J. Moore, D. A. Smale, L. V. Alexander, J. A. Benthuysen, M. Feng, A. Sen Gupta, A. J. Hobday, N. J. Holbrook, S. E. Perkins-Kirkpatrick, H. A. Scannell, S. C. Straub, and T. Wernberg. 2018. Longer and more frequent marine heatwaves over the past century. *Nature Communications* 9(1): 1-12.

Oliver, E. C. J., J. A. Benthuysen, S. Darmaraki, M. G. Donat, A. J. Hobday, N. J. Holbrook, R. W. Schlegel, A. Sen Gupta. 2021. Marine heatwaves. *Annual Review of Marine Science* 13: 313-342.

O'Reilly, C. M., S. Sharma, D. K. Gray, S. E. Hampton, J. S. Read, R. J. Rowley, P. Schneider, J. D. Lenters, P. B. McIntyre, B. M. Kraemer, G. A. Weyhenmeyer, D. Straile, B. Dong, R. Adrian, M. G. Allan, O. Anneville, L. Arvola, J. Austin, J. L. Bailey, J. S. Baron, J. D. Brookes, E. Eyto, M. T. Dokulil, D. P. Hamilton, K. Havens, A. L. Hetherington, S. N. Higgins, S. Hook, L. R. Izmest'eva, K. D. Joehnk, K. Kangur, P. Kasprzak, M. Kumagai, E. Kuusisto, G. Leshkevich, D. M. Livingstone, S. MacIntyre, L. May, J. M. Melack, D. C. Mueller-Navarra, M. Naumenko, P. Noges, T. Noges, R. P. North, P. Plisnier, A. Rigosi, A. Rimmer, M. Rogora, L. G. Rudstam, J. A. Rusak, N. Salmaso, N. R. Samal, D. E. Schindler, S. G. Schladow, M. Schmid, S. R. Schmidt, E. Silow, M. E. Soylu, K. Teubner, P. Verburg, A. Voutilainen, A. Watkinson, C. E. Williamson, and G. Zhang.

2015. Rapid and highly variable warming of lake surface waters around the globe. *Geophysical Research Letters* 42(24): 10773-10781

Osland, M. J., N. Enwright, R. H. Day, and T. W. Doyle. 2013. Winter climate change and coastal wetland foundation species: salt marshes vs. mangrove forests in the southeastern United States. *Global Change Biology* 19(5): 1482–1494.

Perkins, S. E., and L. V. Alexander. 2013. On the Measurement of Heat Waves. *Journal of Climate* 26(13): 4500–4517.

Piao, S., P. Ciais, P. Friedlingstein, P. Peylin, M. Reichstein, S. Luyssaert, H. Margolis, J. Fang, A. Barr, A. Chen, A. Grelle, D. Y. Hollinger, T. Laurila, A. Lindroth, A. D. Richardson, and T. Vesala. 2008. Net carbon dioxide losses of northern ecosystems in response to autumn warming. *Nature* 451(7174): 49–52.

Piatt, J. F., J. K. Parrish, H. M. Renner, S. K. Schoen, T. T. Jones, M. L. Arimitsu, K. J. Kuletz, B. Bodenstein, M. García-Reyes, R. S. Duerr, R. M. Corcoran, R. S. A. Kaler, G. J. McChesney, R. T. Golightly, H. A. Coletti, R. M. Suryan, H. K. Burgess, J. Lindsey, K. Lindquist, P. M. Warzybok, J. Jahncke, J. Roletto, and W. J. Sydeman. 2020. Extreme mortality and reproductive failure of common murres resulting from the northeast Pacific marine heatwave of 2014-2016. *PloS one* 15(1): e0226087.

R Core Team. 2020. R: A language and environment for statistical computing. R Foundation for Statistical Computing, Vienna, Austria. https://www.R-project.org/

Sanger, D. M., M. D. Arendt, Y. Chen, E. L. Wenner, A. F. Holland, D. Edwards, J. Caffrey. 2002. A Synthesis of Water Quality Data: National Estuarine Research Reserve System-wide Monitoring Program (1995-2000). *National Estuarine Research Reserve Technical Report Series 3*. South Carolina Department of Natural Resources, Marine Resources Division Contribution No. 500. 135 p.

Scanes, E., P. R. Scanes, and P. M. Ross. 2020. Climate change rapidly warms and acidifies Australian estuaries. *Nature Communications* 11(1): 1-11.

Schär, C., P. L. Vidale, D. Lüthi, C. Frei, C. Häberli, M. A. Liniger, and C. Appenzeller. 2004. The role of increasing temperature variability in European summer heatwaves. *Nature* 427(6972): 332–336.

Schlegel, R. W., and A. J. Smit. 2018. heatwaveR: A central algorithm for the detection of heatwaves and cold-spells. *Journal of Open Source Software* 3(27): 821

Schlegel, R. W., E. C. J. Oliver, A. J. Hobday, and A. J. Smit. 2019. Detecting Marine Heatwaves with Sub-Optimal Data. *Frontiers in Marine Science* 6: 737.

Stenseth, N. C., and A. Mysterud. 2002. Climate, changing phenology, and other life history traits: Nonlinearity and match-mismatch to the environment. *Proceedings of the National Academy of Sciences* 99(21): 13379–13381.

Thomson, R. E., W. J. Emery. 2014. Digital Filters. In *Data analysis methods in physical oceanography*, Third ed. 593-637. Waltham, MA: Elsevier B.V.. doi: 10.1016/B978-0-12-387782-6.00006-5

Tomaso, D. J., and R. G. Najjar. 2015. Long-term variations in the dissolved oxygen budget of an urbanized tidal river: The upper Delaware Estuary. *Journal of Geophysical Research: Biogeosciences* 120(6): 1027–1045.

Walters, R. A., and C. Heston. 1982. Removing tidal-period variations from time-series data using low-pass digital filters. *Journal of Physical Oceanography* 12(1): 112-115.

Webb, B. W., and F. Nobilis. 1995. Long term water temperature trends in Austrian rivers. *Hydrological Sciences Journal* 40(1): 83–96.

Wenner, E. L., A. F. Holland, M. D. Arendt, Y. Chen, D. Edwards, C. Miller, M. Meece, J. Caffrey. 2001. A synthesis of water quality data from the National Estuarine Research Reserve System-wide monitoring program. *Final Report to The Cooperative Institute for Coastal and Estuarine Environmental Technology* NOAA Grant No.: NA97OR0209SC. South Carolina Department of Natural Resources, Marine Resources Division, Contribution No. 459.

Wernberg, T., S. Bennett, R. C. Babcock, T. de Bettignies, K. Cure, M. Depczynski, F. Dufois, J. Fromont, C. J. Fulton, R. K. Hovey, E. S. Harvey, T. H. Holmes, G. A. Kendrick, B. Radford, J. Santana-Garcon, B. J. Saunders, D. A. Smale, M. S. Thomsen, C. A. Tuckett, F. Tuya, M. A. Vanderklift, and S. Wilson. 2016. Climate-driven regime shift of a temperate marine ecosystem. *Science* 353(6295): 169–172.

Whitney, M. M., and P. Vlahos. 2021. Reducing Hypoxia in an Urban Estuary Despite Climate Warming. *Environmental Science & Technology* 55(2): 941–951.

Wilhelm, S., and R. Adrian. 2008. Impact of summer warming on the thermal characteristics of a polymictic lake and consequences for oxygen, nutrients and phytoplankton. *Freshwater Biology* 53(2): 226-237.

Table 3.1 NERRS reserve and station descriptions. Total number of estuarine heatwave (EHW) events, low dissolved oxygen (DO) and low pH events, mean salinity, mean depth and mean tidal range reflect the time period 1996-2019. Habitat type was characterized by Wenner et al. 2001 and Sanger et al. 2002.

Estuary	Region	Reserve Code	Station ID	Total EHW	Total Low DO	Total Low pH	Habitat Type	Mean Salinity (± SD, g kg^{-1})	Mean Depth (m)	Mean Tidal Range (m)
Wells, ME	Northeast	WEL	IN	48	55	46	SAV	30.8 ± 1.9	4.08	1.82
Great Bay, NH		GRB	GB	45	43	37	SAV	23.6 ± 5.6	5.51	1.40
Hudson River, NY		HUD	SK	38	40	31	Upland	0.2 ± 0.0	1.04	0.01
			TS	43	40	44	Marsh	0.1 ± 0.0	1.55	0.80
Narragansett Bay, RI		NAR	PC	44	30	41	Open Water	28.5 ± 1.9	2.80	0.38
Delaware, DE	Mid-Atlantic	DEL	BL	57	60	59	Marsh	2.0 ± 2.1	1.67	0.87
			SL	60	60	47	Marsh	10.8 ± 6.9	1.71	0.82
Chesapeake Bay, VA		CBV	TC	55	51	47	Marsh	10.6 ± 4.5	1.61	0.29
North Carolina, NC	Southeast	NOC	EC	46	49	52	Marsh	22.1 ± 6.7	1.13	0.76
			RC	55	43	44	Marsh	30.1 ± 4.3	1.55	0.88
ACE Basin, SC		ACE	SP	62	61	55	Marsh	29.0 ± 4.5	2.47	1.20
Jobos Bay, PR		JOB	09	56	61	52	Mangrove	36.5 ± 2.7	1.03	0.02
Apalachicola, FL	Gulf of Mexico	APA	EB	60	51	51	Open Water	11.0 ± 8.5	2.16	0.12
			ES	61	47	55	Open Water	9.7 ± 7.9	2.16	0.12
Padilla Bay, WA	West	PDB	BY	63	43	45	SAV	29.0 ± 1.1	3.36	0.84
Elkhorn Slough, CA		ELK	AP	46	54	52	Marsh	31.5 ± 4.6	0.68	0.06
			SM	61	58	57	Marsh	31.8 ± 2.7	1.79	0.71

Table 3.2 Results of Mann-Kendall and Sen's slope (MK-SS) analysis related to atmospheric and estuarine heatwaves (AHW and EHW respectively), low DO and low pH events. Total tests run indicates the number of MK-SS analyses for each test (AHW = 5 variables*5 regions + 5 variables*4 seasons + 5 variables*(1)time = 50 total tests run; additionally EHW, low DO and low pH included 5 variables*5 salinity classes = 75 total tests run). Only statistically significant tests are presented.

Test	Total Tests Run	Test Type	Variable	Category	Slope	MK p-value	10% FDR
AHW	50	-	-	-	-	-	-
EHW	75	Time	Avg. Onset Rate		-0.01	0.001	0.020
Low DO	75	Time	Avg. Onset Rate		-0.01	0.003	0.020
			Avg. Decline Rate		-0.02	0.003	0.060
			Avg. Duration		-0.12	0.003	0.040
			Avg. Cumulative Intensity		-0.20	0.031	0.100
			Frequency		-0.05	0.008	0.080
		Season	Frequency	Summer	-0.03	< 0.001	0.005
			Avg. Duration		-0.14	0.005	0.010
			Avg. Decline Rate		-0.02	0.012	0.015
			Avg. Cumulative Intensity	Fall	-0.20	0.016	0.020
		Region	Avg. Cumulative Intensity	NE	-0.37	0.001	0.008
			Avg. Duration		-0.20	0.004	0.012
			Avg. Onset Rate	NE	-0.01	0.012	0.024
				Mid-Atlantic	-0.01	0.005	0.016
			Avg. Decline Rate	NE	-0.02	0.011	0.020
				Mid-Atlantic	-0.04	< 0.001	0.004
Low pH	75	Time	Frequency		-0.10	< 0.001	0.020
			Avg. Duration		-0.13	0.040	0.060
			Avg. Cumulative Intensity		-0.07	0.006	0.040
		Season	Frequency	Winter	-0.02	0.002	0.015
				Spring	-0.03	0.008	0.025
				Summer	-0.03	< 0.001	0.005
				Fall	-0.02	0.012	0.030
			Avg. Onset Rate		-0.004	0.016	0.035
			Avg. Duration	Spring	-0.29	0.004	0.020
			Avg. Cumulative Intensity		-0.12	0.001	0.010
		Salinity	Frequency	Tidal Fresh	-0.08	0.009	0.020
				Seawater	-0.10	0.003	0.004
			Avg. Decline Rate		-0.004	0.007	0.016
			Avg. Duration		-0.27	0.027	0.028
			Avg. Cumulative Intensity		-0.10	0.003	0.008
				Polyhaline	-0.11	0.011	0.024
				Mesohaline	-0.08	0.006	0.012
		Region	Frequency	West	-0.20	0.002	0.004
				NE	-0.10	0.004	0.008
				Mid-Atlantic	-0.10	0.026	0.032
				SE	-0.09	0.030	0.044
			Avg. Cumulative Intensity	West	-0.06	0.024	0.028
				NE	-0.10	0.014	0.024
				SE	-0.07	0.027	0.036
			Avg. Decline Rate	West	-0.004	0.007	0.016
				NE	-0.002	0.014	0.020
				SE	-0.01	0.007	0.012
			Avg. Onset Rate	NE	-0.002	0.027	0.040

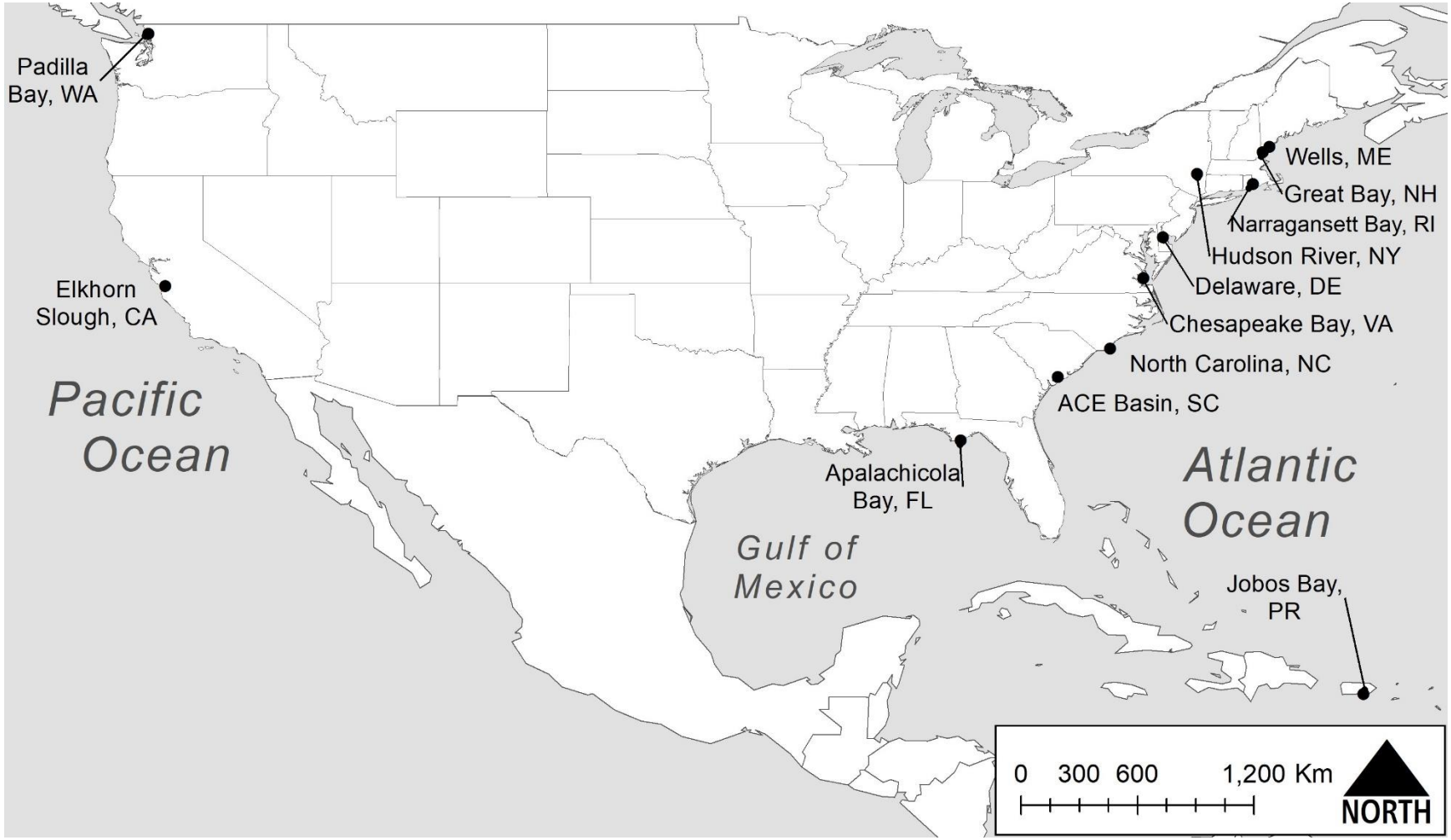

Figure 3.1 NERRS Reserve locations used for this analysis included all continuous water quality stations with records from 1996-2019.

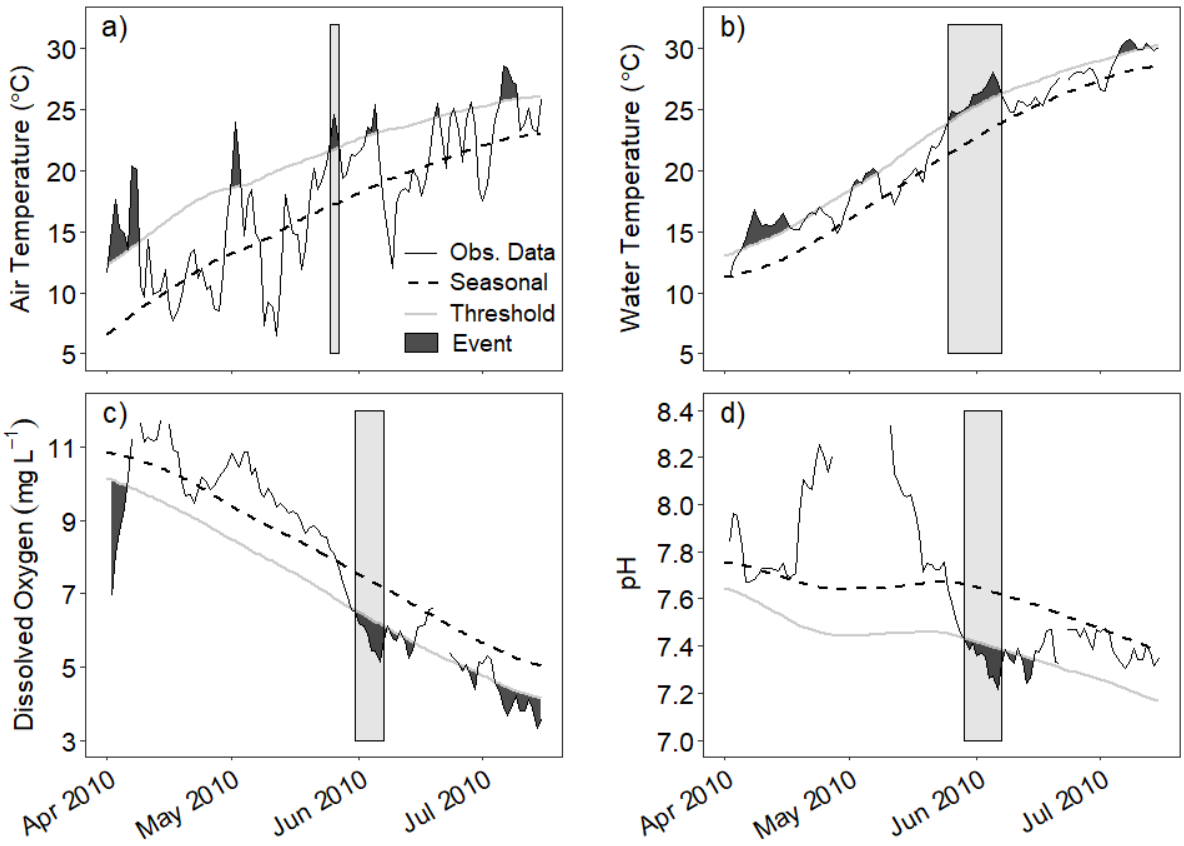

Figure 3.2 Example of atmospheric heatwaves (a), estuarine heatwaves (b), low dissolved oxygen (c), and low pH (d) events. The shaded bars in each figure are an example of a time when an estuarine heatwave co-occurred with an atmospheric heatwave, which co-occurred with a low DO and low pH event. Extreme events in the four variables are highlighted in dark grey. Seasonal refers to the predicted seasonal average value, while threshold refers to the position of the 90%-tile; both are based on a 24-year reference period for the water quality variables and a 18-year reference period for air temperature. Data come from Hudson River, NY – Tivoli South Bay (HUDTS) NERR.

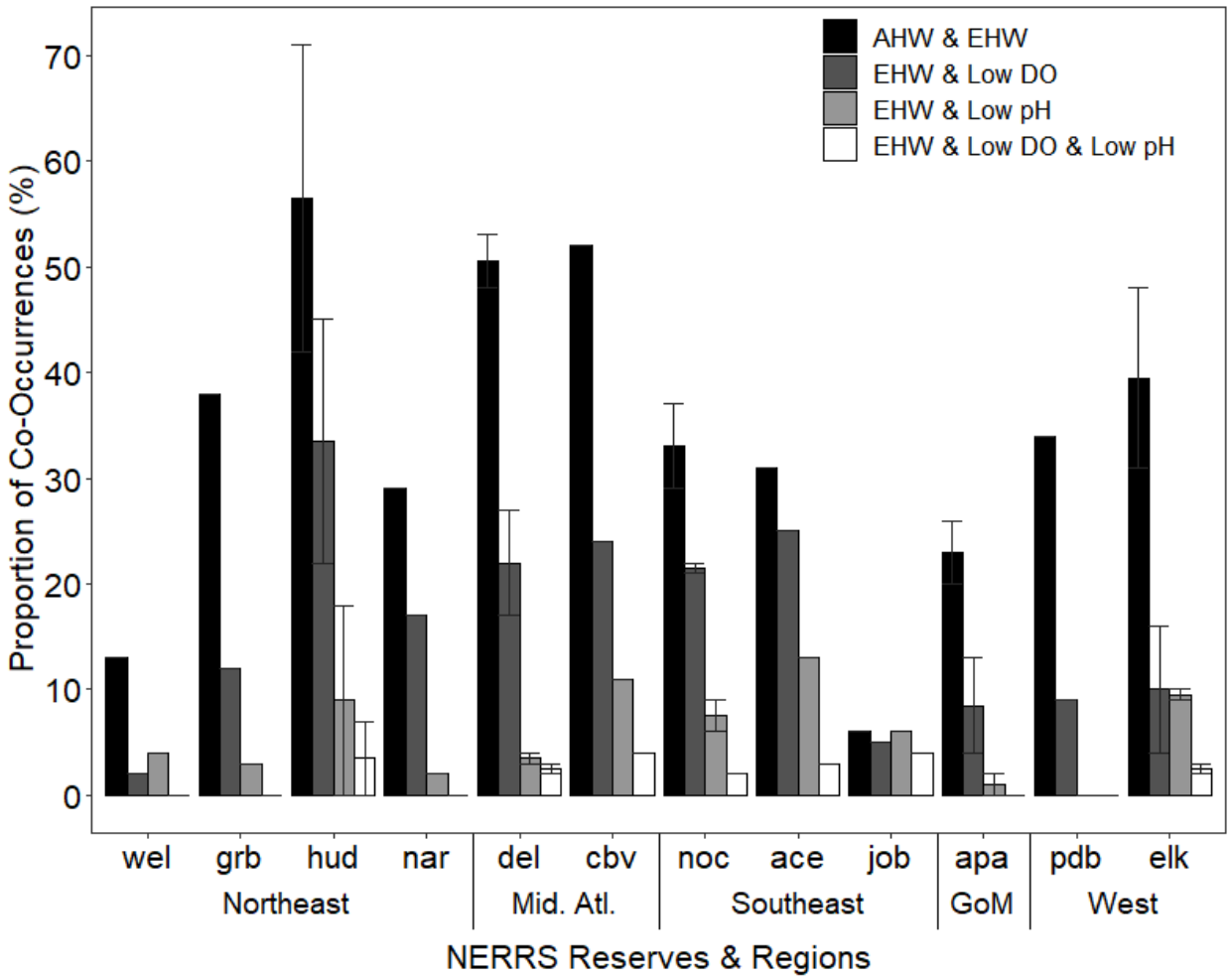

Figure 3.3 Proportion of co-occurrences between atmospheric & estuarine heatwaves (AHW and EHW, respectively), EHW & low DO events, EHW & low pH events, and EHW, low DO & low pH events. Error bars represent the range between multiple stations within a reserve.

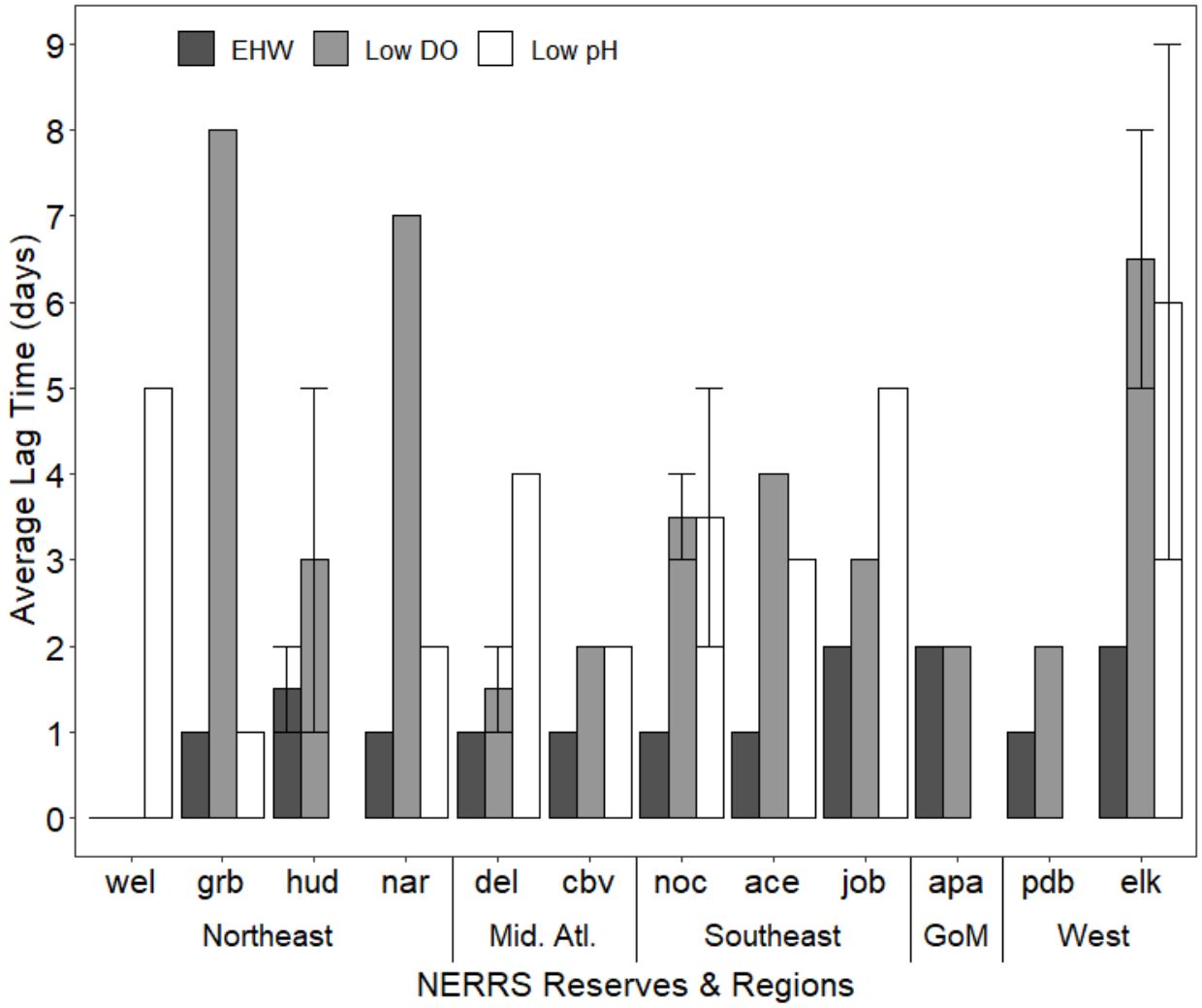

Figure 3.4 Average lag time between atmospheric-estuarine heatwave (EHW) events (dark grey), EHW-low DO events (light grey), and EHW-low pH events (white). Error bars represent the range between multiple stations within a reserve.

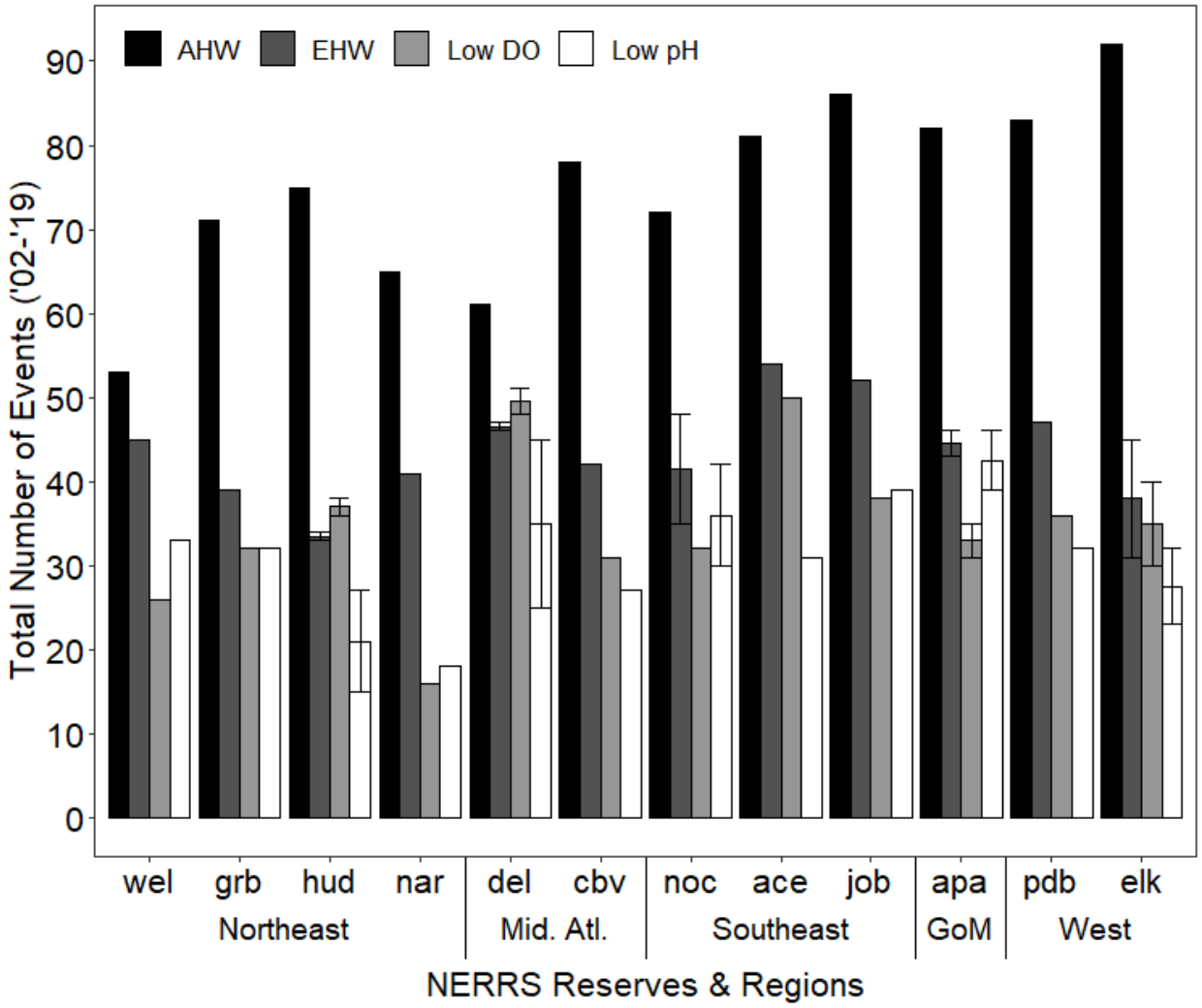

Figure 3.5 Total number of extreme events between 2002-2019 across NERRS reserves and U.S. regions. Error bars represent the range between multiple stations within a reserve.

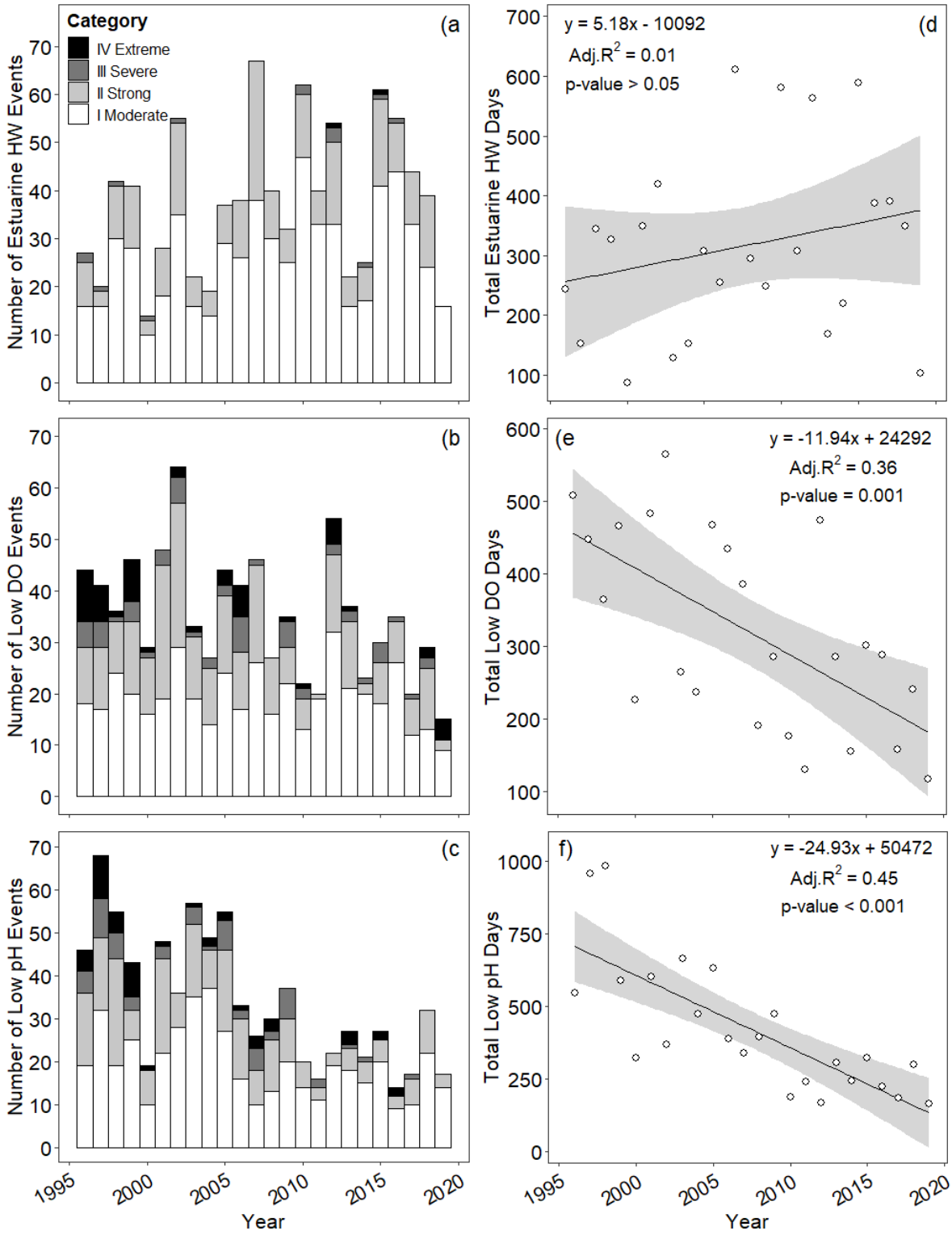

Figure 3.6 Severity classification of the annual total number of estuarine heatwaves (a), low DO events (b), and low pH events (c) throughout the 17 NERRS stations used in this analysis. Linear regression of total number of estuarine heatwave days (d), low DO days (e), and low pH days (f) amongst the 17 NERRS stations considered.

Chapter 4: Sediment heatwaves increase in frequency in a Virginia seagrass meadow

Abstract

Coastal marine heatwaves have destructive and lasting impacts on foundational species and have increased in frequency, duration, and magnitude in recent decades. While several studies have considered how anomalous atmospheric conditions can promote marine heatwave (MHW) conditions, the impact of MHWs on sediments has not been considered. This study examined the prevalence of MHW propagation into surficial sediments within a shallow, subtidal seagrass meadow in Virginia, USA. Sediment temperature was measured at hourly intervals at a depth of 5 cm between June 2020-October 2022 at the meadow edge and central interior. The observed sediment temperature, along with a 29-year record of water temperature and water level was used to develop a sediment temperature model for each location which was used to identify sediment heatwaves that may thermally stress belowground seagrass. Sediment heatwave (SHW) frequency significantly increased at the meadow center and meadow edge, coinciding with a 172% increase in the annual number of SHW days, from 11 to 30 days year^{-1} between 1994-2022. Sediment heatwaves at both meadow locations co-occurred with a MHW 79-81% of the time, with nearly all SHWs having a zero day lag. The top 10% most extreme MHWs and SHWs occurred between November and April. Sediment heatwaves co-occurred with an anomalously long duration MHW in June 2015 that is associated with a 90% decline in seagrass from this system, suggesting that SHWs may have contributed to the observed seagrass loss. These results provide the first assessment of SHWs in any aquatic ecosystem.

Introduction

Extreme high temperature events are expected to continue increasing in frequency, magnitude, and duration in the atmosphere and the global ocean (Meehl and Tebaldi 2004; Wuebbles et al. 2017; Frölicher et al. 2018; Oliver et al. 2018). In the marine environment, these discrete heatwaves disproportionately stress marine organisms and vegetated coastal ecosystems relative to longer-term increases in mean water temperature. Vegetated coastal ecosystems including, but not limited to, seagrass meadows, represent 5-8% of Earth's land surface, yet collectively store 20-30% of all soil carbon, often referred to as "blue" carbon for its location in oceanic sediments (hereafter, BC; Fourqurean et al. 2012; Nahlik and Fennessy 2016). While also being a major global carbon sink (Duarte et al. 2005; Fourqurean et al. 2012), vegetated coastal ecosystems provide other ecosystem services, including sediment stabilization, coastal erosion protection, nutrient and pathogen filtration, and fisheries maintenance (Hansen and Reidenbach 2012; McGlathery et al. 2012; Lamb et al. 2017; Unsworth et al. 2018). However, marine heatwaves (MHW) have been implicated in seagrass mass mortality events (Collier and Waycott 2014; Berger et al. 2020; Aoki et al. 2021), conversion of a seagrass meadow from autotrophy to heterotrophy (Berger et al. 2020), and BC loss from seagrass meadow sediments (Arias-Ortiz et al. 2018; Aoki et al. 2021).

Marine heatwaves are generated by anomalous horizontal advective heat fluxes from currents and tides, vertical diffusive heat fluxes across the air-water interface, and larger-scale climate phenomena (Schlegel et al. 2017a; Holbrook et al. 2019). These extreme water temperature events are associated with atmospheric subsidence and high-pressure blocking, which enhances vertical heat fluxes by reducing cloud cover, wind speed, and relative humidity which increases surface air temperature (Holbrook et al. 2019). Furthermore, reduced windspeed

decreases oceanic upwelling intensity, thermocline depth, and turbulence, thereby promoting water column stability (Holbrook et al. 2019). Additionally, offshore MHW can be advected horizontally to coastal regions via anomalous ocean circulation patterns, which can be exacerbated by local circulation and geomorphic features (Schlegel et al. 2017a; Schlegel et al. 2017b).

In a recent survey, Macreadie et al. (2019) identified fundamental questions to advance BC science, including better characterization of disturbance events in sediments that impact long-term BC storage. While heatwaves are known to occur in the atmosphere (AHW) and the pelagic environment of vegetated coastal marine ecosystems, there has been no study of heatwaves in coastal marine sediments. This is due to a lack of long-term sediment temperature monitoring, difficulty in predicting when and where heatwaves will occur, and perception that sediment temperature is less variable than atmospheric and water temperature. Nonetheless, MHW events have doubled in duration in recent decades (Frölicher et al. 2018) and are increasing in frequency (Oliver et al. 2018), threatening above and below-ground BC storage, ecosystem resilience, and ecosystem services. Therefore, developing a deeper understanding of MHW transfer into vegetated coastal sediments is critical.

In June 2015, the restored *Zostera marina* seagrass meadow in South Bay, VA, experienced a 14-day MHW event that is associated with a 90% reduction in seagrass shoot density (Berger et al. 2020) and a 20% loss of buried BC (Aoki et al. 2021). The mass mortality of *Z. marina* was spatially heterogenous, with the central meadow region experiencing the greatest loss. In contrast, the meadow's edge was undisturbed due in part to lower thermal stress provided by greater oceanic exchange from a nearby inlet (Berger et al. *in review*). However, it remains unclear if the decline in seagrass occurred in part due to high sediment temperatures. To

investigate sediment temperature in the seagrass meadow, I established a 2.5-year long continuous time series of this variable at 5 cm depth within the central and northern edge regions of the South Bay *Z. marina* meadow. This record was used to model sediment temperature in relation to water temperature, water level, day of year, and hour. Using the long-term modeled sediment temperature, sediment heatwaves (SHWs) were retroactively determined within the meadow. This study addressed: 1) do heatwaves occur in vegetated coastal sediments? 2) if so, are there spatial differences in vegetated coastal sediment heatwave characteristics? and 3) specifically, did the MHW in June 2015 produce a concurrent sediment heatwave in South Bay? As heatwaves are known to occur in coastal oceans, it was hypothesized that MHW would be transferred into shallow coastal sediments. However, whether and how frequently sediment temperatures exceed the 90th percentile for 5 consecutive days is unknown with the possibility that sediments buffer temperature extremes such that exceedances of the threshold are typically short-lived. As the water temperature at the edge of the South Bay seagrass meadow is cooler due to greater oceanic exchange with an inlet, it was hypothesized that the central region of the meadow would experience a greater frequency, duration, and intensity of sediment heatwaves relative to the edge. Lastly, due to the observed spatial heterogeneity in seagrass loss following the June 2015 MHW event, it was hypothesized that the central meadow region had a concurrent sediment heatwave while the edge did not.

Methods

Study Site

The region between the Virginia mainland of the Delmarva peninsula and Virginia's 14 coastal barrier islands makes up the Virginia Coast Reserve (VCR). Since 1987, the VCR has been one of 28 National Science Foundation Long-Term Ecological Research sites. West of

Wreck Island is the shallow lagoon - South Bay, with a mean depth of ≤ 1.5 m and tidal range = 1.2 m (Hansen and Reidenbach 2013; Safak et al. 2015). South Bay is bordered by oceanic inlets to the north and south of Wreck Island and by Man and Boy Channel to the west. *Z. marina* was locally extinct from the VCR system for ~70 years however, restoration efforts beginning in 1999 have led to a 20.3 km^2 continuous *Z. marina* meadow in South Bay (Orth et al. 2020). In June 2015, a 14-day MHW preceded a 90% reduction in *Z. marina* shoot density and a 20% reduction in stored BC within the central region of the South Bay meadow, which took 2-4 years to recover (Berger et al. 2020; Aoki et al. 2021).

Data Collection

Continuous monitoring of sediment temperature at a depth of 5 cm occurred between June 2020 and October 2022 at the central (37.2638 °N, -75.8153 °W) and northern edge (37.2773 °N, -75.8092 °W) of the South Bay seagrass meadow (~1.4 km apart). A depth of 5 cm was chosen from a visual inspection of where *Z. marina* rhizomes were most abundant. Sediment temperature was measured at one-hour intervals using Onset HOBO pendant temperature data loggers with a factory temperature accuracy of ± 0.53 °C (accuracy < ± 0.53 °C between 0-40 °C). Within each location (i.e., central and edge), two data loggers were buried approximately 26 m apart in areas where seagrass shoot density was undisturbed and areas where seagrass shoot density was experimentally removed and allowed to recover (see Chapter 5 for more information on the experimental seagrass disturbance). Linear regression slopes and R^2 of 0.99 confirmed no significant difference in sediment temperature between disturbed and undisturbed seagrass sites within each meadow location. Therefore, sediment temperatures were averaged at each meadow location. Concurrent water temperature was measured within each location at a fixed height of 20 cm above the sediment surface to compare *in-situ* water temperature with *in-situ* sediment

temperature. Water and sediment thermistors were replaced at monthly intervals between April-November and were deployed for the entirety of the winter months (December-March). Overall, sensor malfunction or loss resulted in 1.9% and 3.9% of the sediment temperature data being missing from the central and edge locations, respectively, while ≤ 0.7% of the water temperature data was missing from both locations.

Continuous meteorological and water temperature monitoring has been ongoing within the VCR since 1989 and 1994, respectively. Gap-filled daily mean atmospheric temperature collected from the VCR Oyster Meteorological Station (37.2909 °N, -75.9268 °W; Groleger et al. 2022), approximately 10 km west of South Bay, was used to determine long-term atmospheric temperature trends as well as characterize AHW for comparison with MHW. The National Oceanic and Atmospheric Administration's (NOAA) Wachapreague, VA tide station (station ID: 8631044; 37.6078 °N, -75.6858 °W) provides publicly-available, continuous hourly water temperature measurements. This NOAA monitoring station is approximately 38 km north of South Bay, and the water temperature record from this station was used to confirm the presence of the June 2015 MHW event (Aoki et al. 2021). Monitoring records from this station were accessed via the NOAA Tides & Currents webpage (tidesandcurrents.noaa.gov/stationhome.html?id=8631044). This station's water temperature time series was used to determine long-term water temperature trends and characterize MHWs in the VCR. Long-term monthly mean atmospheric and water temperature trend analyses were conducted using Seasonal-Kendall trend tests with Sen's slope estimates using the R package 'wql' (Jassby and Cloern 2017; Tassone et al. 2022a). Months with ≥ 10 missing days were removed prior to trend testing.

Model Development

The lack of long-term sediment temperature time series necessitated the development of sediment temperature models that used the continuous sediment temperature time series from each South Bay location as a dependent variable. Multiple-linear regression models of hourly sediment temperature for each South Bay meadow location were developed using Wachapreague water temperature and mean-centered water level (both spanning 1994-2022), day of the year (i.e., 1-365), and hour (i.e., 1-24) as covariates to account for diffusive, advective, seasonal, and diurnal temperature variability respectively. Gaps ≤ 5 hours were linearly interpolated prior to model development. Model building and validation used a 75:25 split-sample design, where 75% of the hourly observed sediment temperature (n = 15,168) was randomly sampled and used as the dependent variable during model building. The remaining 25% of the hourly observed sediment temperature (n = 5,056) was used to validate the model predictions. Model validation between the observed and predicted hourly sediment temperatures for each meadow location was assessed using linear regression.

A complementary statistical model was developed to gap-fill the observed water and sediment temperature time series prior to conducting wavelet transform analyses. Wavelet transforms were used to detect the power spectrum in the water and sediment temperature time series at the central and edge locations using the R package 'biwavelet' (Gouhier et al. 2021).

Extreme Event Detection

Aquatic and sediment heatwave detection was determined using the conventional MHW definition such that a heatwave event occurs when the daily mean temperature exceeds a local, seasonally-varying 90^{th} percentile threshold for ≥ 5 days and without a drop > 2 days below the threshold (Hobday et al. 2016). Atmospheric heatwaves used a similar definition as MHWs however, the threshold duration was ≥ 3 days, with no drop below the threshold during an event.

The difference in these definitions is related to the increased temperature variability in the atmosphere relative to the water and convention within the atmospheric and oceanographic fields (Perkins and Alexander 2013; Oliver et al. 2021; Tassone et al. 2022b). The severity of all heatwaves was classified based on Hobday et al. (2018), which described heatwave event severity based upon multiples of the difference between the local climatology and the 90th percentile threshold and the peak magnitude of the observed temperature. Heatwave event detection and classification were conducted using the R package 'heatwaveR' (Schlegel and Smit 2018). As heatwaves are rare events that can span monthly boundaries, long-term trends in heatwave metrics (i.e., frequency, duration, intensity) were conducted on annual time series using non-parametric Mann-Kendall tests with Sen's slope estimates ("Kendall" and "trend" R packages; McLeod 2011; Pohlert 2020; Tassone et al. 2022a). All statistical analyses were conducted in the R environment for statistical computing (R Core Team 2022) and are archived on GitHub (https://github.com/spencer-tassone/SedimentHeatwaves).

Results

Observed Sediment and Water Temperature

Sediment temperature at the central meadow and edge locations followed a northern hemisphere temperate seasonal cycle. The maximum summer (June-August of 2020-2022) sediment temperature of the central meadow (32.1 °C) was 0.6 °C greater than the edge location (31.6 °C; Figure 4.1a). Both locations experienced similar low winter (December-February of 2021-2022) temperatures of 1.4 °C and 1.5 °C for the central meadow and edge, respectively. Daily mean sediment temperature at the central meadow was up to 4.1 °C greater than the edge during spring and summer (Figure 4.1b). Conversely, the daily mean sediment temperature at the edge was up to 1.1 °C greater than the central meadow during fall and winter.

Sediment temperature seasonality closely followed water temperature seasonality at both locations (Figure 4.2a, b). The water temperature range was 2.6 °C and 2.3 °C greater than the sediment temperature at the central meadow and edge locations, respectively. Water temperature was generally warmer than sediment temperature during summer and cooler than the sediments during winter (Figure 4.2c, d). The temperature difference range between the water and sediment was 8.6 °C and 6.0 °C at the edge and central locations, respectively. The water and sediment temperature power spectrum at the edge location had a diurnal (24-hour) and semi-diurnal (12-hour) periodicity, while the central sites retained a diurnal signal (Figure 4.3). Additionally, statistically significant power spectrum regions around 10-days were observed, possibly indicating frontal passage.

Modeled Sediment Temperature

All covariates (i.e., water temperature, mean-centered water level, day of the year, and hour) for the long-term multiple linear regression were statistically significant at the edge location (p-value < 0.001; Table 4.2). Similarly, all covariates were statistically significant for the central site, except for the mean-centered water level (p-value > 0.05; Table 4.2). The slope of the linear regression between the observed and predicted hourly sediment temperature for the central meadow was 0.98 ± 0.01 (± SE) and 0.97 ± 0.01 for the edge ($R^2 \geq 0.97$; Figure 4.4). Wachapreague water temperature and/or water level were missing for 2006, 2007, and 2017, limiting modeled sediment temperature availability for those periods (Figure 4.5).

Heatwaves

Between 1994-2022 there was a total of 125 AHWs in the VCR (Figure 4.6a). There was an average (± SD) of 4 ± 2 events $year^{-1}$, with a mean duration of 4 days and a maximum duration of 9 days (Table 4.1). The mean intensity of the AHWs was 2.1 °C above the seasonally

adjusted 90th percentile threshold and was up to 15.7 °C above the threshold. The majority of AHWs occurred in summer (35%), with the other seasons sharing between 21-22% of the remaining AHWs (Figure 4.7). All of the top 10% most intense AHW occurred between November-March, with 67% (n = 8) occurring in winter and the remaining 33% occurring in fall (n = 2) and spring (n = 2). Atmospheric heatwave frequency had a positive linear increase over the study period however, this trend was not statistically significant (p-value > 0.05). Similarly, the annual total number of AHW days had a positive trend that was not statistically significant (Figure 4.6b). Cook's Distance (D_i) values for the annual total number of AHW days were > $4/n$ in 1998 and 2014, suggestive of influential outliers in the regression model (D_i = 0.17 and 0.15 respectively). Additionally, a long-term air temperature trend was present at a rate of 0.032 °C year^{-1} (p-value < 0.001).

There were 67 MHWs during the 29-year study period, averaging 3 ± 2 events year^{-1} (Figure 4.6c). The mean MHW duration was 8 days and ranged up to 26 days (Table 4.1). The mean MHW intensity was 1.3 °C above the seasonally adjusted 90th percentile threshold and was up to 6.5 °C above the threshold. The majority of MHWs occurred in summer (34 %), followed by winter (25%), spring (24%), and fall (16%; Figure 4.7). The top 10% most intense MHWs occurred during winter (n = 4) and spring (n = 3) between December-April. Heatwave frequency in the water column significantly increased over the study duration at a rate of 0.09 events year^{-1} (p-value = 0.024; Figure 4.6c). The annual total number of MHW days significantly increased by 0.67 days year^{-1} (p-value = 0.022; Figure 4.6d), representing a 172% increase in the annual total number of heatwave days between 1994 (11 days) and 2022 (30 days). D_i exceeded $4/n$ for the annual total number of MHW days in 1995, 2020, and 2021 (D_i = 0.19, 0.35, 0.15 respectively). The 14-day duration of the June 2015 MHW event was in the 94th percentile of all

Wachapreague MHW events between 1994-2022. Lastly, the long-term water temperature trend was 0.041 °C year^{-1} (p-value < 0.001).

Among the two SHW locations, there were 66 and 64 SHW at the central and edge locations, respectively (Figure 4.6e, g). Annual SHW frequency was, on average, greater at the central meadow location (3 ± 2 events year^{-1}) relative to the meadow edge (2 ± 2 events year^{-1}; Table 4.1). The mean and maximum duration of SHWs were equal among locations, averaging 8 days and ranging up to a maximum duration of 25 days (Table 4.1). Similarly, the mean SHW intensity relative to the 90th percentile threshold was equal among locations (mean = 1.2 °C) however, the maximum intensity relative to the 90th percentile threshold was marginally greater at the central meadow location (max = 5.8 °C) relative to the edge location (max = 5.7 °C). Both central and edge locations had the greatest proportion of sediment heatwaves occur in summer (35% and 36%, respectively), followed by spring (26% and 27%, respectively), winter (23% and 20%, respectively), and fall (both 17%; Figure 4.7). The top 10% most intense SHWs occurred between November-April. Sediment heatwave frequency at both locations significantly increased at a rate of 0.10 events year^{-1} (p-values ≤ 0.015; Figure 4.6e, g). The annual total number of SHW days significantly increased at an equal rate of 0.67 days year^{-1} for each location, representing an increase from an average of 11 SHW days in 1994 to 30 SHW days in 2022 (p-values ≤ 0.041; Figure 4.6f, h). Cook's distance was > $4/n$ at the central sites in 2020 (D_i = 0.45) and at the edge sites in 1995 (D_i = 0.14) and 2020 (D_i = 0.47).

Of the 67 MHW events, 33% started during an active AHW event. Of those 22 co-occurring AHW and MHW events, the MHW lagged the AHW on average by 1 ± 1 day, with a maximum lag of 4 days. Sediment heatwaves co-occurred with an active MHW 79% of the time at the edge and 81% of the time at the central meadow location. Furthermore, the average lag

time between MHWs and SHWs was zero days at both locations, and up to 1 day at the central meadow location. The 14-day MHW in June 2015 associated with the observed aboveground seagrass dieback co-occurred with a SHW at both locations (Figure 4.8). There was no lag between the June 2015 MHW and SHWs, with each persisting for 14 days (June 12, 2015 – June 25, 2015). Additionally, there were three atmospheric heat spikes (i.e., daily mean temperature > 90^{th} percentile threshold for a duration < 3 days) and a single 3-day AHW (June 21-23, 2015) that occurred during the MHW and SHWs (Figure 4.8).

Discussion

The hypothesis that MHWs would be incorporated into shallow coastal sediments was supported as 79-81% of the observed SHWs co-occurred with an active MHW. All but one of the SHWs that coincided with a MHW had a zero-day lag, suggesting that extreme water and sediment temperatures are in phase and strongly coupled. Furthermore, MHWs in the VCR and SHWs in South Bay have increased in frequency and annual total number of heatwave days between 1994-2022. While MHWs are anticipated to continue to proliferate in the VCR (Wiberg, *in review*), the low number of annual MHWs and SHWs at the beginning of the record (1994-1997) and high number of MHWs and SHWs at the end of the record (2019-2022) were influential in the positive trend in MHWs and SHWs over time. For the water column, the linear rate of MHW frequency increase (0.09 events $year^{-1}$) was 2x greater than the open ocean global average of 0.045 events $year^{-1}$ (Oliver et al. 2018). This increase in MHW frequency was accompanied by a 172% increase in the annual total MHW days from 11 in 1994 to 30 in 2022. The increase in the annual number of MHW days was less than the globally averaged open ocean (Oliver et al. 2018) yet in agreement with the coastal ocean region of the temperate north-Atlantic (Lima and Wethey 2012; Thoral et al. 2022). For the sediments, the linear rate of SHW

frequency increase at both locations was 0.1 events year^{-1}, which is marginally greater than the increasing rate of MHW frequency in the VCR. This greater rate of SHW frequency increase than MHW and ~20% non-synchronous SHW with MHW suggest an additional sediment heating mechanism or that MHWs at the NOAA Wachapreague tidal station differ somewhat from those in South Bay (~38 km southeast of the NOAA tidal station). The lack of long-term (> 20 years) continuous water temperature records from South Bay limits the ability to test for spatial differences in MHWs. Nonetheless, the annual rate of total SHW days at both locations matched MHWs, increasing from 11 to 30 days year^{-1} during the study period. Marine heatwaves are regularly transferred into the surficial sediments of this shallow, subtidal temperate lagoonal system, inducing SHWs.

The central meadow and edge locations had commensurate increasing rates of SHW frequency, annual total SHW days, the proportion of co-occurrence with MHWs, and SHW characteristics. These results did not support the hypothesis that SHW metrics would be greater at the central meadow relative to the edge due to greater oceanic exchange that reduces thermal stress at the edge. Evidence of greater oceanic exchange at the meadow edge was observed as the pelagic and sediment temperature power spectrums exhibited semi-diurnal (12-hour) and diurnal (24-hour) periods, while the central location solely exhibited diurnal periods. Additionally, pelagic and sediment temperatures during the summer were often greater at the central location relative to the edge, but during winter, when the most extreme MHWs and SHWs occurred, the meadow edge was typically warmer than the central meadow. The high proportion of MHW and SHW co-occurrence suggests that horizontal advective heat fluxes (transport of heat via tides and currents) within the South Bay lagoon drive SHWs in this system. The low co-occurrence of AHW and MHW in South Bay (33%) further supports that horizontal rather than vertical heat

flux (direct atmospheric heating of water and sediment) is the dominant driver of SHWs in this shallow coastal system. Coastal MHWs are driven, in part, by broad-scale processes such as anomalous oceanic and atmospheric circulation patterns, as well as local-scale influences such as circulation and bathymetric features (Schlegel et al. 2017a; Schlegel et al. 2017b). The VCR is a shallow system with a depth of < 0.25 m during some neap tides, therefore direct heating of the sediments from the atmosphere is possible. While attribution of MHWs was outside the scope of the present study, MHWs in South Bay can occur without an adjacent coastal ocean MHW (Aoki et al. 2021). Additionally, seagrass is known to alter circulation patterns in South Bay (Hansen and Reidenbach 2012) however, the presence of MHWs after seasonal seagrass senescence suggests additional local-scale features may promote localized MHW development.

Aboveground seagrass biomass loss from the central South Bay meadow region and the absence of seagrass disturbance from the meadow edge following the 14-day MHW in June 2015 indicated possible spatial variability in SHWs. This hypothesis was partially supported as a SHW at the central location started and ended on the same day as the June 2015 MHW. However, a concurrent SHW at the meadow edge also co-occurred with the June 2015 MHW. Differences in observed seagrass loss may be due, in part, to spatial differences in sediment organic matter (Oreska et al. 2017) and temperature that produce greater hydrogen sulfide (H_2S) production within the meadow interior (Berger et al. *in review*). High sediment temperatures are associated with increased H_2S production in marine sediments and increased sulfide isotope concentration in seagrass tissues (Berger et al. *in review*), which have sub-lethal and lethal impacts on *Z. marina* (Goodman et al. 1995; Pedersen et al. 2004; Höffle et al. 2011; Dooley et al. 2013). Furthermore, H_2S can become concentrated in marine sediments during organic matter decomposition (Dooley et al. 2013). The fraction of organic matter in South Bay seagrass

meadow sediments is up to 3x greater within the central meadow relative to the northern edge (Oreska et al. 2017). Additionally, while *Z. marina* become thermally stressed at 28.6 °C (Berger and Berg, *in review*), heatwave metrics (i.e., climatology, 90th percentile threshold) are localized in space. While the SHW in June 2015 at the central meadow location exceeded 28.6 °C for three days, the SHW at the meadow edge did not exceed the *Z. marina* thermal stress threshold. Lastly, while the intensity of the June 2015 MHW was moderate, the 14-day duration of the event was extreme, putting it in the 94th percentile of all MHWs observed during the study period. The duration of the MHW, increased H_2S production in the meadow interior, and presence of a co-occurring SHW that exceeded the *Z. marina* thermal stress threshold at the meadow interior but not the meadow edge likely contributed to differences in observed *Z. marina* loss following the June 2015 MHW.

Anomalously high sediment temperature events likely have ecosystem and species-level consequences. Optimal microbial temperatures during winter, when SHWs are most intense, are often 20 °C greater than ambient temperatures (Joint and Smale 2017) such that a SHW in winter likely increases ecosystem respiration rates while primary producers remain light-limited. Additionally, summer SHW may enhance sediment respiration rates above primary production if the primary producers become thermally stressed. The enhancement of winter and summer ecosystem respiration would likely reduce sediment BC stocks, potentially impacting the ability of seagrass to sequester carbon and reducing the valuation of seagrass in carbon markets (Oreska et al. 2020). At a species level, surficial sediments in subtidal seagrass meadows likely have limited capacity as thermal refugia for sessile and slow-moving organisms during MHWs, given the high proportion of MHW-SHW co-occurrence. This coupling could negatively impact ectothermic benthic marine organisms such as foraminifera which significantly contribute to

bioturbation and biogeochemical cycling (Deldicq et al. 2021). Nonetheless, some organisms, including blue crabs (*Callinectes sapidus*), may benefit from increasing SHWs, particularly in the winter, as elevated bottom water temperatures are predicted to increase overwinter survival (Glandon et al. 2019). Future studies should consider the vertical profile of SHWs to better understand the depth to which heatwaves propagate and how SHWs impact ecosystem-level metabolism, BC stores, biogeochemical processes, and organismal responses.

Sediment heatwaves at a depth of 5 cm regularly co-occur with MHW events in the shallow, subtidal vegetated coastal sediments of South Bay, VA. Furthermore, MHWs and SHWs significantly increased in frequency as did the annual total number of heatwave days during the 29 years between 1994-2022. While there were differences in pelagic and sediment temperature periodicity, there were no substantial differences in SHW metrics between the central and northern edge meadow locations. The June 2015 MHW associated with the 90% decline in aboveground seagrass density, 20% loss in BC stocks, and metabolic conversion of the meadow from autotrophy to heterotrophy (Berger et al. 2020, Aoki et al. 2021) coincided with SHWs at the central and edge meadow locations which may have contributed to observed patterns in seagrass loss. As these results provide the first documentation of SHW in any aquatic system, future studies should consider how SHWs impact key ecosystem and species-level processes, including biogeochemical cycling, ecosystem metabolism, and species abundance and reproduction.

References

Aoki, L. R., McGlathery, K. J., Wiberg, P. L., Oreska, M. P. J., Berger, A. C., Berg, P., & Orth, R. J. (2021). Seagrass Recovery Following Marine Heat Wave Influences Sediment Carbon Stocks. *Frontiers in Marine Science*, *7*, 576784. https://doi.org/10.3389/fmars.2020.576784

Arias-Ortiz, A., Serrano, O., Masqué, P., Lavery, P. S., Mueller, U., Kendrick, G. A., Rozaimi, M., Esteban, A., Fourqurean, J. W., Marbà, N., Mateo, M. A., Murray, K., Rule, M. J., & Duarte, C. M. (2018). A marine heatwave drives massive losses from the world's largest seagrass carbon stocks. *Nature Climate Change*, *8*(4), 338–344. https://doi.org/10.1038/s41558-018-0096-y

Berger, A. C., Berg, P., McGlathery, K. J., & Delgard, M. L. (2020). Long-term trends and resilience of seagrass metabolism: A decadal aquatic eddy covariance study. *Limnology and Oceanography*, *65*(7), 1423–1438. https://doi.org/10.1002/lno.11397

Berger, A. C., & Berg, P. (*In review*). Temperature threshold for seagrass (*Zostera marina*) production derived from in situ aquatic eddy covariance measurements.

Berger, A. C., Berg, P., McGlathery, K. J., Aoki, L. R., & Kerns, K. (*In review*). Impacts of ocean warming and marine heatwaves on seagrass measured by novel metrics.

Collier, C. J., & Waycott, M. (2014). Temperature extremes reduce seagrass growth and induce mortality. *Marine Pollution Bulletin, 83*(2), 483-490.

Deldicq, N., Langlet, D., Delaeter, C., Beaugrand, G., Seuront, L., & Bouchet, V. M. (2021). Effects of temperature on the behavior and metabolism of an intertidal foraminifera and consequences for benthic ecosystem functioning. *Scientific Reports, 11*(1), 4013.

Dooley, F. D., Wyllie-Echeverria, S., Roth, M. B., & Ward, P. D. (2013). Tolerance and response of *Zostera marina* seedlings to hydrogen sulfide. *Aquatic Botany, 105*, 7-10.

Duarte, C. M., Middelburg, J. J., & Caraco, N. (2005). Major role of marine vegetation on the oceanic carbon cycle. *Biogeosciences, 2*(1), 1-8.

Fourqurean, J. W., Duarte, C. M., Kennedy, H., Marbà, N., Holmer, M., Mateo, M. A., Apostolaki, E. T., Kendrick, G. A., Krause-Jensen, D., McGlathery, K. J., & Serrano, O. (2012). Seagrass ecosystems as a globally significant carbon stock. *Nature Geoscience*, *5*(7), 505–509. https://doi.org/10.1038/ngeo1477

Frölicher, T. L., E. M. Fischer, and N. Gruber. 2018. Marine heatwaves under global warming. *Nature* 560(7718): 360–364.

Glandon, H. L., Kilbourne, K. H., & Miller, T. J. (2019). Winter is (not) coming: Warming temperatures will affect the overwinter behavior and survival of blue crab. *PLoS One, 14*(7), e0219555.

Goodman, J. L., Moore, K. A., & Dennison, W. C. (1995). Photosynthetic responses of eelgrass (*Zostera marina* L.) to light and sediment sulfide in a shallow barrier island lagoon. *Aquatic Botany*, *50*(1), 37-47.

Gouhier, T. C., Grinsted, A., and Simko, V. (2021). R package {biwavelet}: Conduct univariate and bivariate wavelet analyses (Version 0.20.21). https://github.com/tgouhier/biwavelet

Groleger, N., Morreale, J., and Porter, J. H. (2022). Gap-filled Meteorological Data for the Virginia Coast Reserve LTER - 1989-2022. Virginia Coast Reserve Long-Term Ecological Research Project Data Publication knb-lter-vcr.337.2 doi:10.6073/pasta/4cf8f0db83783b71f7ee001d794e0016.

Hansen, J., & Reidenbach, M. (2012). Wave and tidally driven flows in eelgrass beds and their effect on sediment suspension. *Marine Ecology Progress Series*, *448*, 271–287. https://doi.org/10.3354/meps09225

Hansen, J. C. R., & Reidenbach, M. A. (2013). Seasonal Growth and Senescence of a *Zostera marina* Seagrass Meadow Alters Wave-Dominated Flow and Sediment Suspension Within a Coastal Bay. *Estuaries and Coasts*, *36*(6), 1099–1114. https://doi.org/10.1007/s12237-013-9620-5

Hobday, A. J., Alexander, L. V., Perkins, S. E., Smale, D. A., Straub, S. C., Oliver, E. C. J., Benthuysen, J. A., Burrows, M. T., Donat, M. G., Feng, M., Holbrook, N. J., Moore, P. J., Scannell, H. A., Sen Gupta, A., and Wernberg, T. (2016). A hierarchical approach to defining marine heatwaves. *Progress in Oceanography*, *141*, 227–238. https://doi.org/10.1016/j.pocean.2015.12.014

Hobday, A., Oliver, E., Sen Gupta, A., Benthuysen, J., Burrows, M., Donat, M., Holbrook, N., Moore, P., Thomsen, M., Wernberg, T., and Smale, D. (2018). Categorizing and Naming Marine Heatwaves. *Oceanography*, *31*(2). https://doi.org/10.5670/oceanog.2018.205

Höffle, H., Thomsen, M. S., & Holmer, M. (2011). High mortality of *Zostera marina* under high temperature regimes but minor effects of the invasive macroalgae *Gracilaria vermiculophylla*. *Estuarine, Coastal and Shelf Science*, *92*(1), 35-46.

Holbrook, N.J., Scannell, H.A., Sen Gupta, A., Benthuysen, J.A., Feng, M., Oliver, E.C., Alexander, L.V., Burrows, M.T., Donat, M.G., Hobday, A.J. and Moore, P.J., (2019). A global assessment of marine heatwaves and their drivers. *Nature Communications, 10*(1), 1-13. https://doi.org/10.1038/s41467-019-10206-z

Jassby, A. D., and Cloern, J. E. (2017). wq: Some tools for exploring water quality monitoring data. R package version 0.4.9 https://cran.r-project.org/package=wq

Joint, I., & Smale, D. A. (2017). Marine heatwaves and optimal temperatures for microbial assemblage activity. *FEMS Microbiology Ecology*, *93*(2), fiw243.

https://doi.org/10.1093/femsec/fiw243

Lamb, J. B., van de Water, J. A. J. M., Bourne, D. G., Altier, C., Hein, M. Y., Fiorenza, E. A., Abu, N., Jompa, J., & Harvell, C. D. (2017). Seagrass ecosystems reduce exposure to bacterial pathogens of humans, fishes, and invertebrates. *Science*, *355*(6326), 731–733. https://doi.org/10.1126/science.aal1956

Lima, F. P., & Wethey, D. S. (2012). Three decades of high-resolution coastal sea surface temperatures reveal more than warming. *Nature Communications*, *3*(1), 704. https://doi.org/10.1038/ncomms1713

Macreadie, P. I., Anton, A., Raven, J. A., Beaumont, N., Connolly, R. M., Friess, D. A., Kelleway, J. J., Kennedy, H., Kuwae, T., Lavery, P. S., Lovelock, C. E., Smale, D. A., Apostolaki, E. T., Atwood, T. B., Baldock, J., Bianchi, T. S., Chmura, G. L., Eyre, B. D., Fourqurean, J. W., … Duarte, C. M. (2019). The future of Blue Carbon science. *Nature Communications*, *10*(1), 3998. https://doi.org/10.1038/s41467-019-11693-w

McGlathery, K., Reynolds, L., Cole, L., Orth, R., Marion, S., & Schwarzschild, A. (2012). Recovery trajectories during state change from bare sediment to eelgrass dominance. *Marine Ecology Progress Series*, *448*, 209–221. https://doi.org/10.3354/meps09574

McLeod, A. I. 2011. Kendall: Kendall rank correlation and Mann-Kendall trend test. R package version 2.2. https://CRAN.R-project.org/package=Kendall

Meehl, G. A., & Tebaldi, C. (2004). More Intense, More Frequent, and Longer Lasting Heat Waves in the 21st Century. *Science*, *305*(5686), 994–997. https://doi.org/10.1126/science.1098704

Nahlik, A. M., & Fennessy, M. S. (2016). Carbon storage in US wetlands. *Nature Communications*, *7*(1), 1-9.

Oliver, E. C. J., Benthuysen, J. A., Darmaraki, S., Donat, M. G., Hobday, A. J., Holbrook, N. J., Schlegel, R. W., & Sen Gupta, A. (2021). Marine Heatwaves. *Annual Review of Marine Science*, *13*(1), 313–342. https://doi.org/10.1146/annurev-marine-032720-095144

Oliver, E. C. J., Donat, M. G., Burrows, M. T., Moore, P. J., Smale, D. A., Alexander, L. V., Benthuysen, J. A., Feng, M., Sen Gupta, A., Hobday, A. J., Holbrook, N. J., Perkins-Kirkpatrick, S. E., Scannell, H. A., Straub, S. C., & Wernberg, T. (2018). Longer and more frequent marine heatwaves over the past century. *Nature Communications*, *9*(1), 1324. https://doi.org/10.1038/s41467-018-03732-9

Oreska, M. P. J., McGlathery, K. J., Aoki, L. R., Berger, A. C., Berg, P., & Mullins, L. (2020). The greenhouse gas offset potential from seagrass restoration. *Scientific Reports*, *10*(1), 7325. https://doi.org/10.1038/s41598-020-64094-1

Oreska, M. P. J., McGlathery, K. J., & Porter, J. H. (2017). Seagrass blue carbon spatial patterns at the meadow-scale. *PLOS ONE*, *12*(4), e0176630. https://doi.org/10.1371/journal.pone.0176630

Orth, R. J., Lefcheck, J. S., McGlathery, K. S., Aoki, L., Luckenbach, M. W., Moore, K. A., Oreska, M. P. J., Snyder, R., Wilcox, D. J., & Lusk, B. (2020). Restoration of seagrass habitat leads to rapid recovery of coastal ecosystem services. *Science Advances*, *6*(41), eabc6434. https://doi.org/10.1126/sciadv.abc6434

Pedersen, O., Binzer, T., & Borum, J. (2004). Sulphide intrusion in eelgrass (*Zostera marina* L.). *Plant, Cell and Environment*, *27*(5), 595–602. https://doi.org/10.1111/j.1365-3040.2004.01173.x

Perkins, S. E., & Alexander, L. V. (2013). On the Measurement of Heat Waves. *Journal of Climate*, *26*(13), 4500–4517. https://doi.org/10.1175/JCLI-D-12-00383.1

Pohlert, T. 2020. trend: Non-Parametric Trend Tests and Change-Point Detection. R package version 1.1.4. https://CRAN.R-project.org/package=trend

R Core Team. 2022. R: A language and environment for statistical computing. R Foundation for Statistical Computing, Vienna, Austria. https://www.R-project.org/.

Safak, I., Wiberg, P. L., Richardson, D. L., & Kurum, M. O. (2015). Controls on residence time and exchange in a system of shallow coastal bays. *Continental Shelf Research*, *97*, 7–20. https://doi.org/10.1016/j.csr.2015.01.009

Schlegel, R. W., Oliver, E. C. J., Perkins-Kirkpatrick, S., Kruger, A., & Smit, A. J. (2017a). Predominant Atmospheric and Oceanic Patterns during Coastal Marine Heatwaves. *Frontiers in Marine Science*, *4*, 323. https://doi.org/10.3389/fmars.2017.00323

Schlegel, R. W., Oliver, E. C. J., Wernberg, T., & Smit, A. J. (2017b). Nearshore and offshore co-occurrence of marine heatwaves and cold-spells. *Progress in Oceanography*, *151*, 189–205. https://doi.org/10.1016/j.pocean.2017.01.004

Schlegel, R. W., & J. Smit, A. (2018). heatwaveR: A central algorithm for the detection of heatwaves and cold-spells. *Journal of Open Source Software*, *3*(27), 821. https://doi.org/10.21105/joss.00821

Tassone, S. J., Besterman, A. F., Buelo, C. D., Ha, D. T., Walter, J. A., & Pace, M. L. (2022a). Increasing heatwave frequency in streams and rivers of the United States. *Limnology and Oceanography Letters*, lol2.10284. https://doi.org/10.1002/lol2.10284

Tassone, S. J., Besterman, A. F., Buelo, C. D., Walter, J. A., & Pace, M. L. (2022b). Co-occurrence of Aquatic Heatwaves with Atmospheric Heatwaves, Low Dissolved Oxygen, and Low pH Events in Estuarine Ecosystems. *Estuaries and Coasts*, *45*(3), 707–720. https://doi.org/10.1007/s12237-021-01009-x

Thoral, F., Montie, S., Thomsen, M. S., Tait, L. W., Pinkerton, M. H., & Schiel, D. R. (2022). Unravelling seasonal trends in coastal marine heatwave metrics across global biogeographical realms. *Scientific Reports*, *12*(1), 7740. https://doi.org/10.1038/s41598-022-11908-z

Unsworth, R. K. F., Collier, C. J., Waycott, M., Mckenzie, L. J., & Cullen-Unsworth, L. C.

(2015). A framework for the resilience of seagrass ecosystems. *Marine Pollution Bulletin*, *100*(1), 34–46. https://doi.org/10.1016/j.marpolbul.2015.08.016

Wiberg, P. L. (*In review*). Temperature amplification and marine heatwave alteration in shallow coastal bays.

Wuebbles, D. J., Fahey, D. W., Hibbard, K. A., DeAngelo, B., Doherty, S., Hayhoe, K., Horton, R., Kossin, J. P., Taylor, P. C., Waple, A. M., & Yohe, C. P. (2017). *Executive summary. Climate Science Special Report: Fourth National Climate Assessment, Volume I*. U.S. Global Change Research Program. https://doi.org/10.7930/J0DJ5CTG

Table 4.1 Heatwave characteristics for the VCR atmosphere at Oyster, VA, water column of Wachapreague, VA, and the sediments at the northern edge and central South Bay meadow locations. Frequency results are the annual mean number of events ± standard deviation.

Variable	Atmosphere	Water	Edge	Central
Total Events	125	67	64	66
Frequency (events year $^{-1}$)	4 ± 2	3 ± 2	2 ± 2	3 ± 2
Mean Duration (days)	4	8	8	8
Max Duration (days)	9	26	25	25
Mean Intensity - Rel. Thres. (^{o}C)	2.1	1.3	1.2	1.2
Max Intensity - Rel. Thres. (^{o}C)	15.7	6.5	5.7	5.8

Table 4.2 Multiple linear regression model characteristics for South Bay sediment temperature. The long-term mean was removed from the Water Level variable prior to model development.

Location	Variable	Estimate ± SE	Variable p-val.	Adj. R^2	Model p-val.
Edge	Intercept	0.782 ± 0.034	< 0.001	0.974	< 0.001
	Water Temp. (°C)	0.879 ± 0.001	< 0.001		
	Water Level (m)	-0.744 ± 0.053	< 0.001		
	Day of Year	0.005 ± 0	< 0.001		
	Hour	0.01 ± 0.002	< 0.001		
Central	Intercept	0.513 ± 0.029	< 0.001	0.982	< 0.001
	Water Temp. (°C)	0.934 ± 0.001	< 0.001		
	Water Level (m)	0.022 ± 0.045	0.623		
	Day of Year	0.003 ± 0	< 0.001		
	Hour	0.02 ± 0.001	< 0.001		

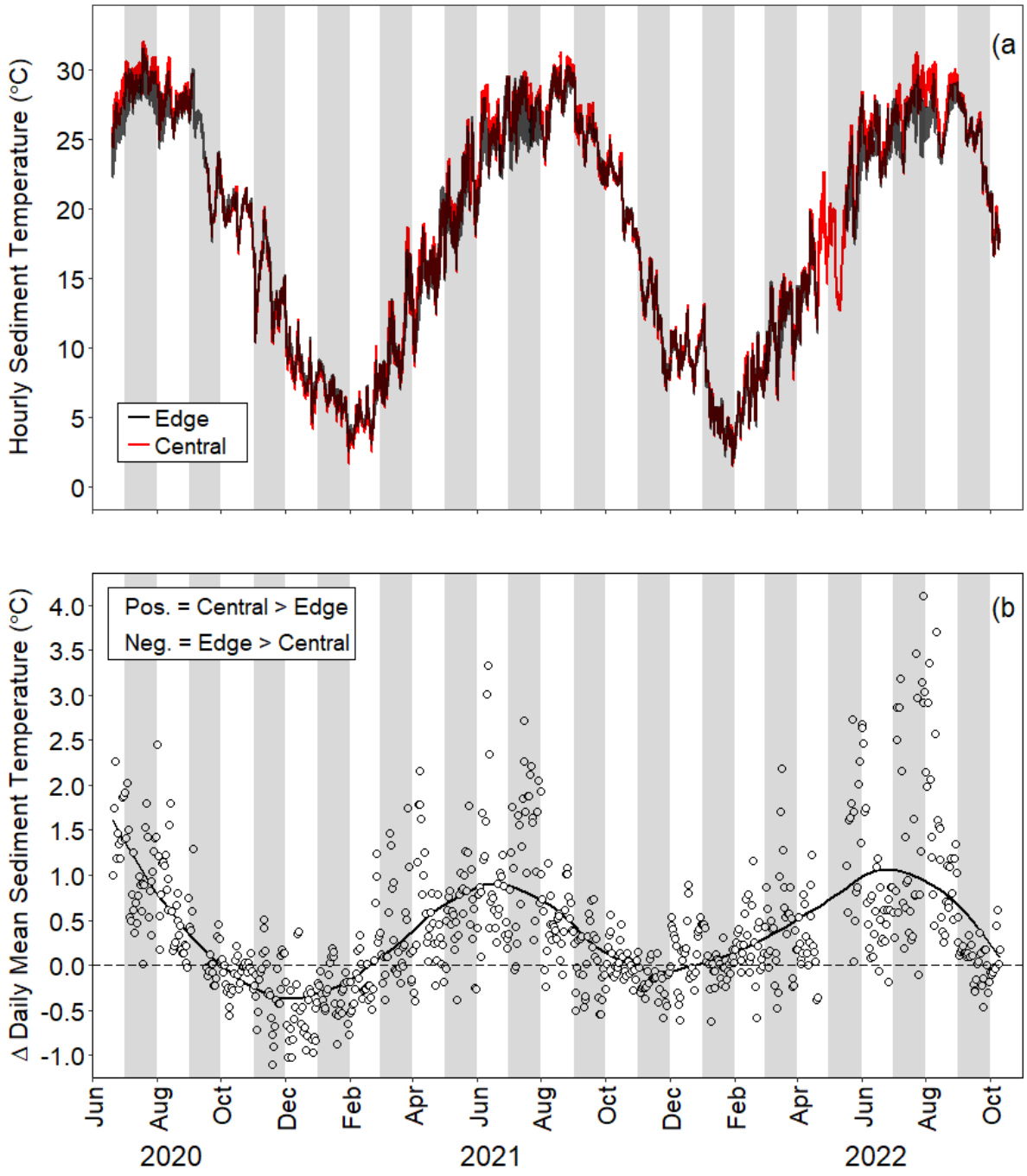

Figure 4.1 Hourly sediment temperature for the northern edge and central locations within the South Bay seagrass meadow (a). Daily mean difference in sediment temperature between the edge and central locations within South Bay (b). Positive values indicate that the central site was warmer than the edge, whereas negative values indicated that the edge was warmer than the central site. Dots represent the daily mean difference. The smoothing line is a locally weighted polynomial regression**.**

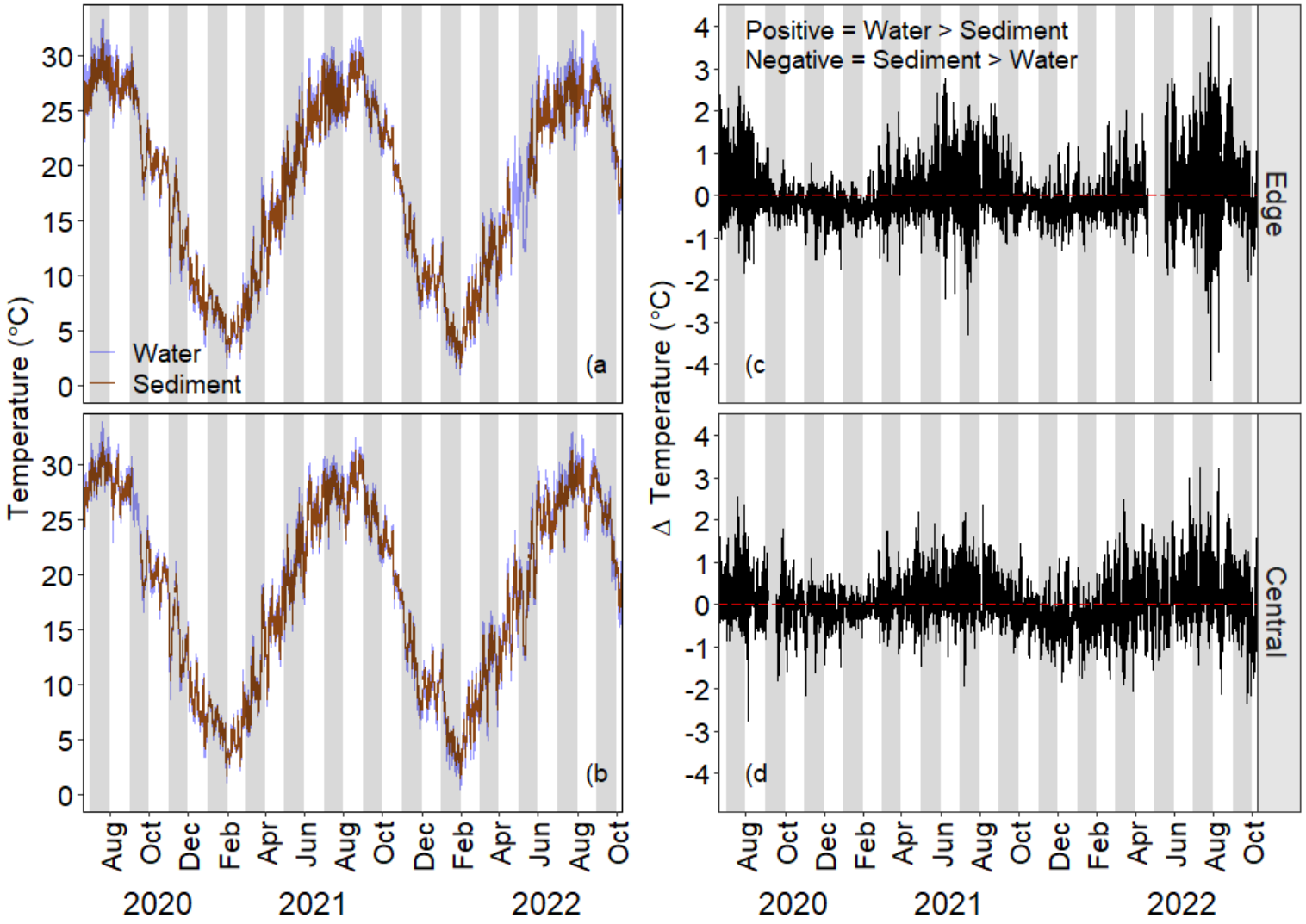

Figure 4.2 Observed hourly water (20 cm above sediment) and sediment (5 cm depth) temperature for the northern edge (a) and central (b) locations within the South Bay seagrass meadow. Hourly difference between water and sediment temperature for the northern edge (c) and central (d) locations. Positive values indicate that the water temperature was greater than the sediment temperature, whereas negative values indicate that the sediment temperature was greater than the water temperature.

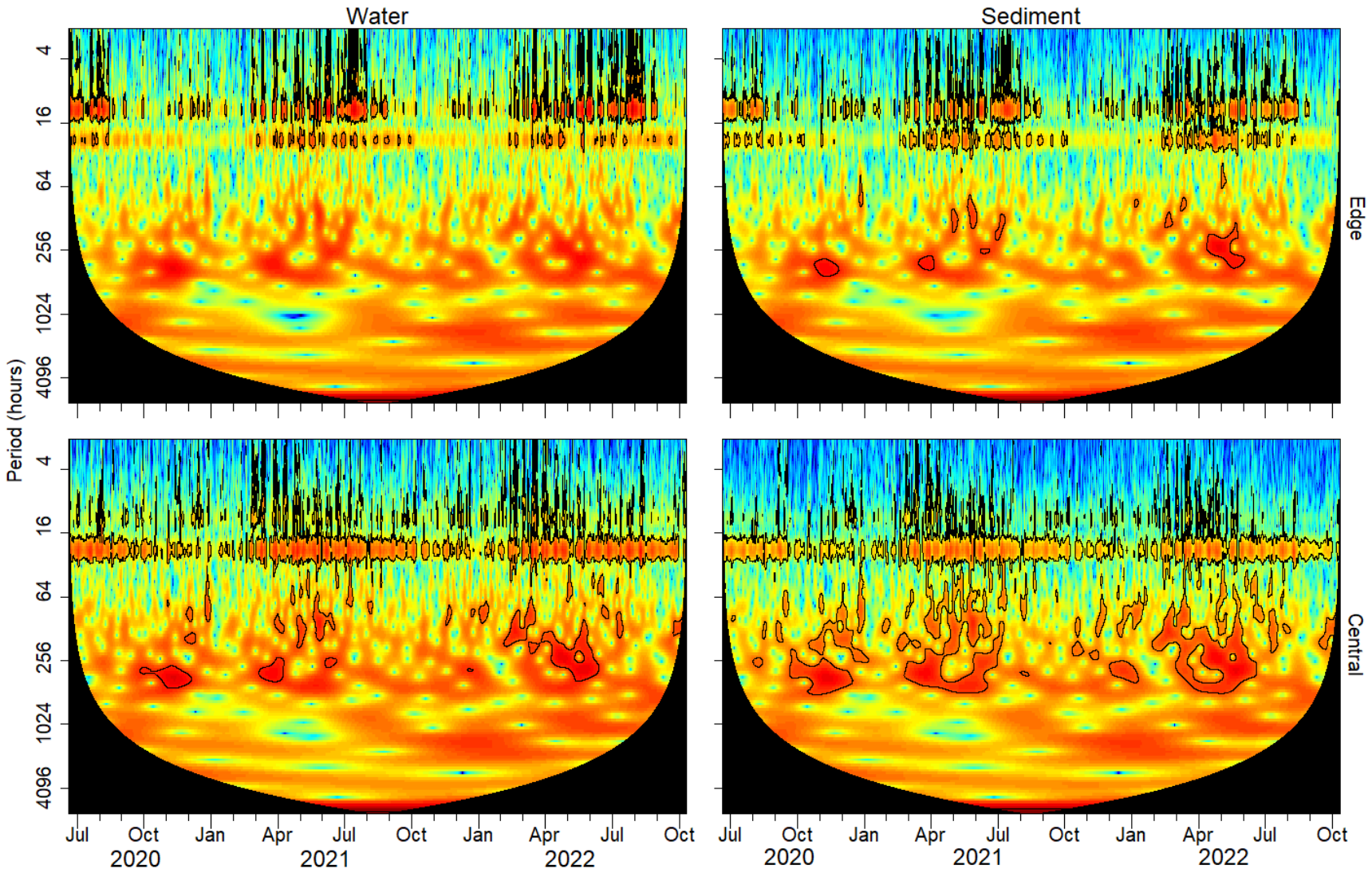

Figure 4.3 Wavelet spectrum of the observed hourly water and sediment temperature from the northern edge and central meadow South Bay locations. Colors represent spectral power, ranging from low (i.e., cool colors - blue) to high (i.e., warm colors - red). Statistically significant spectrums are encompassed within the solid black lines. Note the two horizontal bands around 12 and 24 hours for the northern edge site and the one band at 24 hours for the central site.

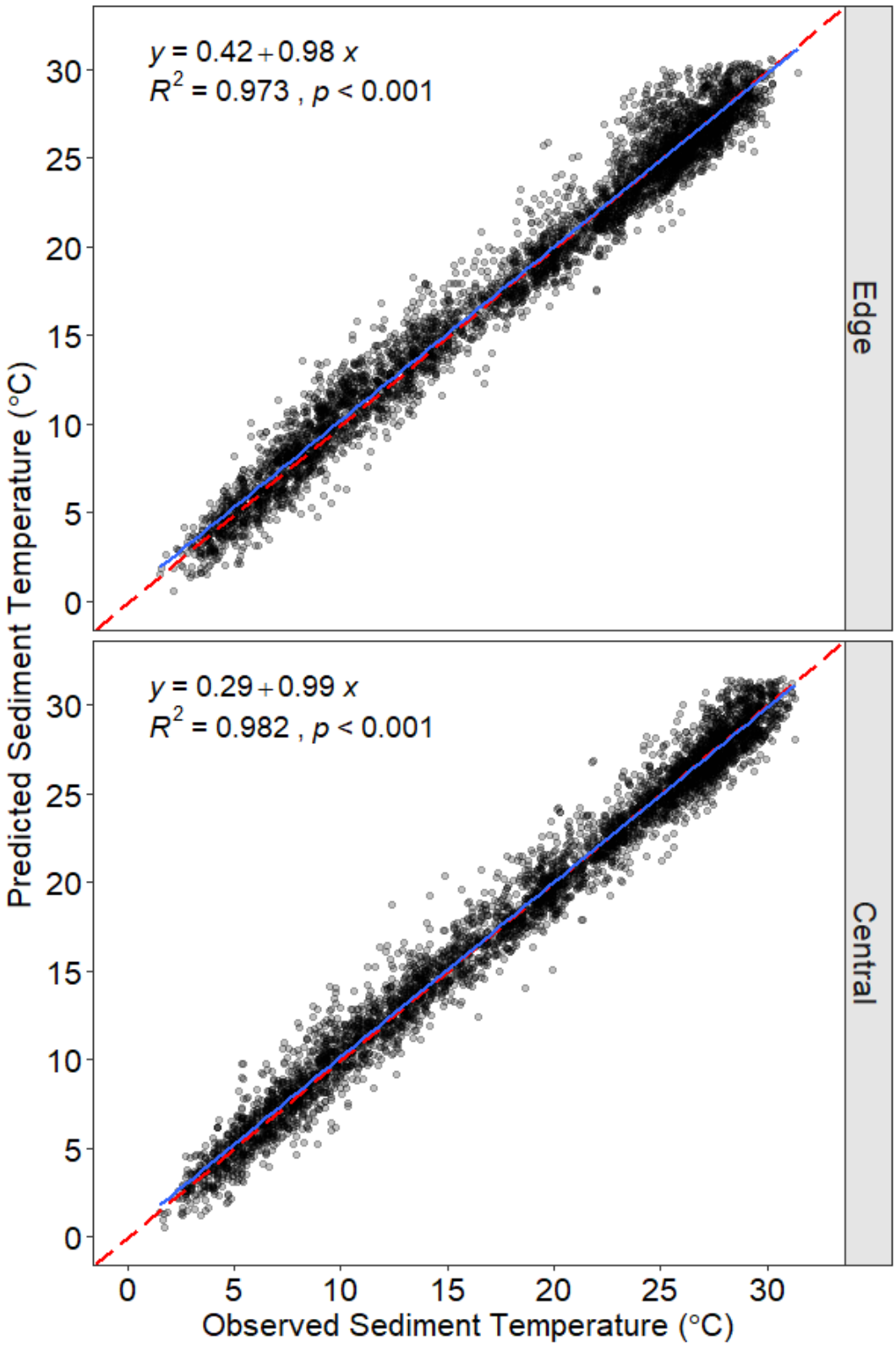

Figure 4.4 Sediment temperature model validation for the northern edge (top) and central meadow (bottom) locations of the South Bay seagrass meadow. The red dashed lines represent the 1:1 line, while the blue lines represent the line of best fit from linear regression.

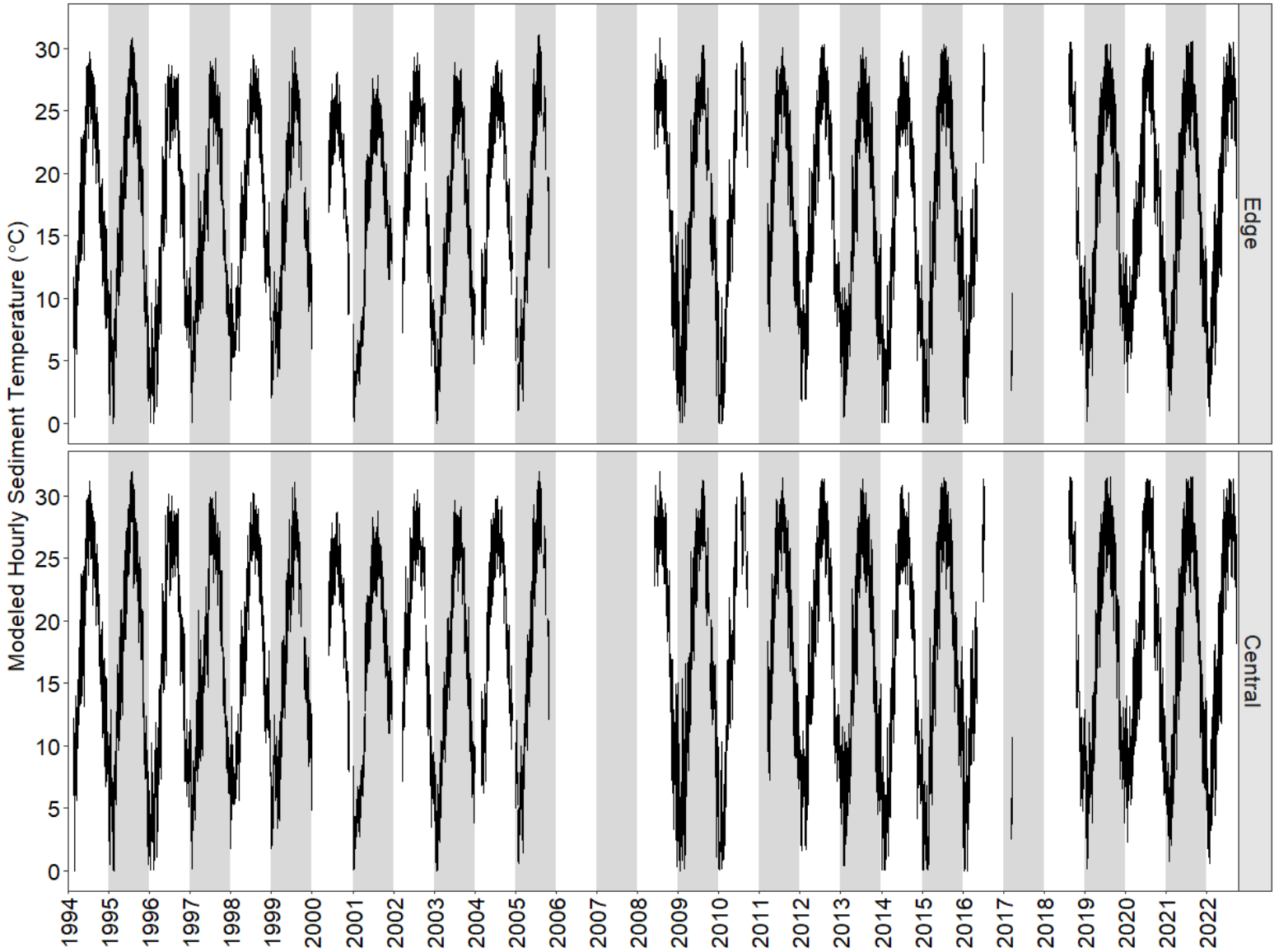

Figure 4.5 Modeled hourly sediment temperature (5 cm depth) for the northern edge (top) and central (bottom) South Bay meadow locations. Data gaps are due to missing Wachapreague water temperature and/or water level observations.

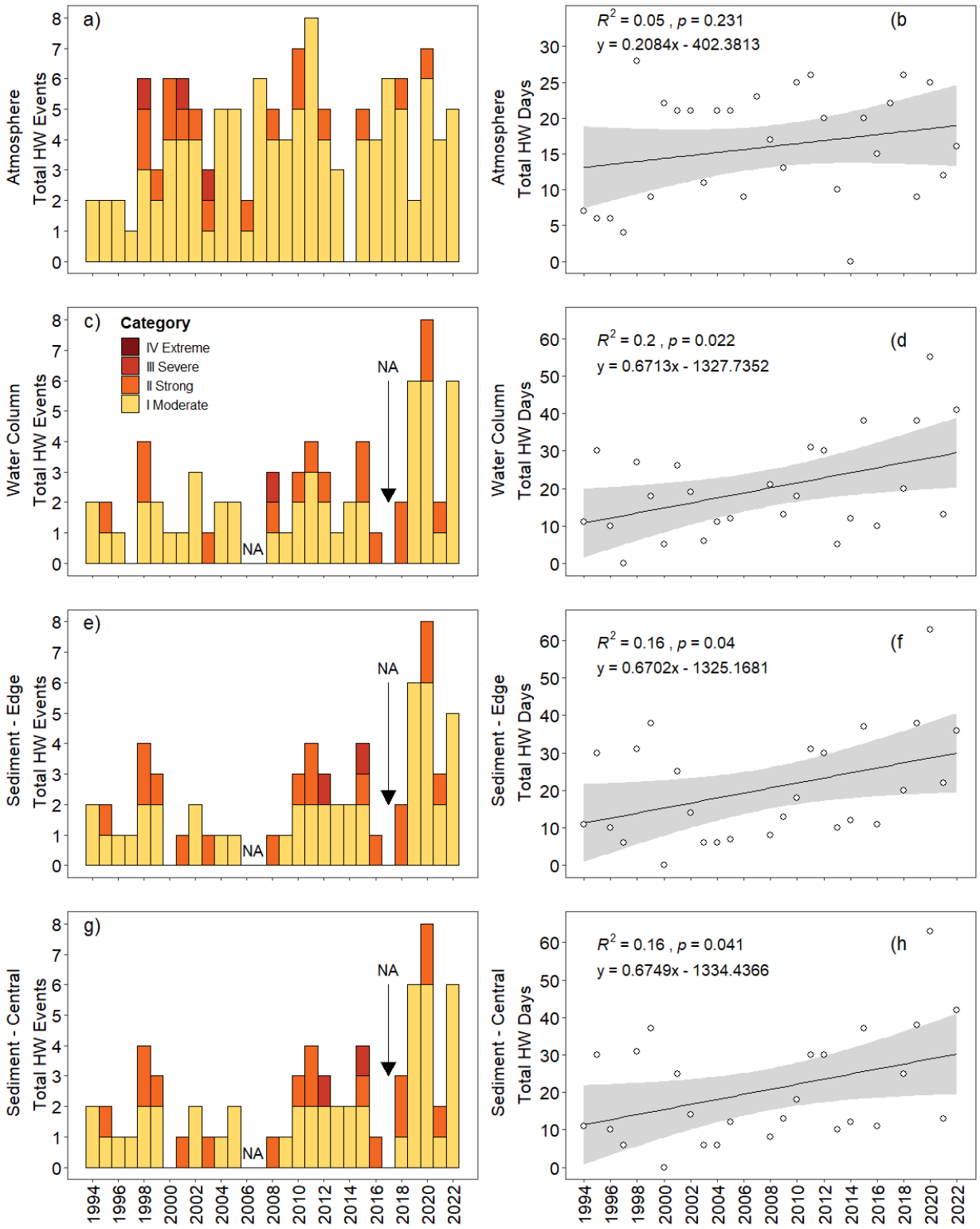

Figure 4.6 Annual heatwave frequency for VCR atmosphere (a), the South Bay water column (c), northern edge (e), and central meadow (g) sediments. Linear regression of the annual total number of heatwave days for the atmosphere (b) water column (d), northern edge (f), and central meadow sediments (h).

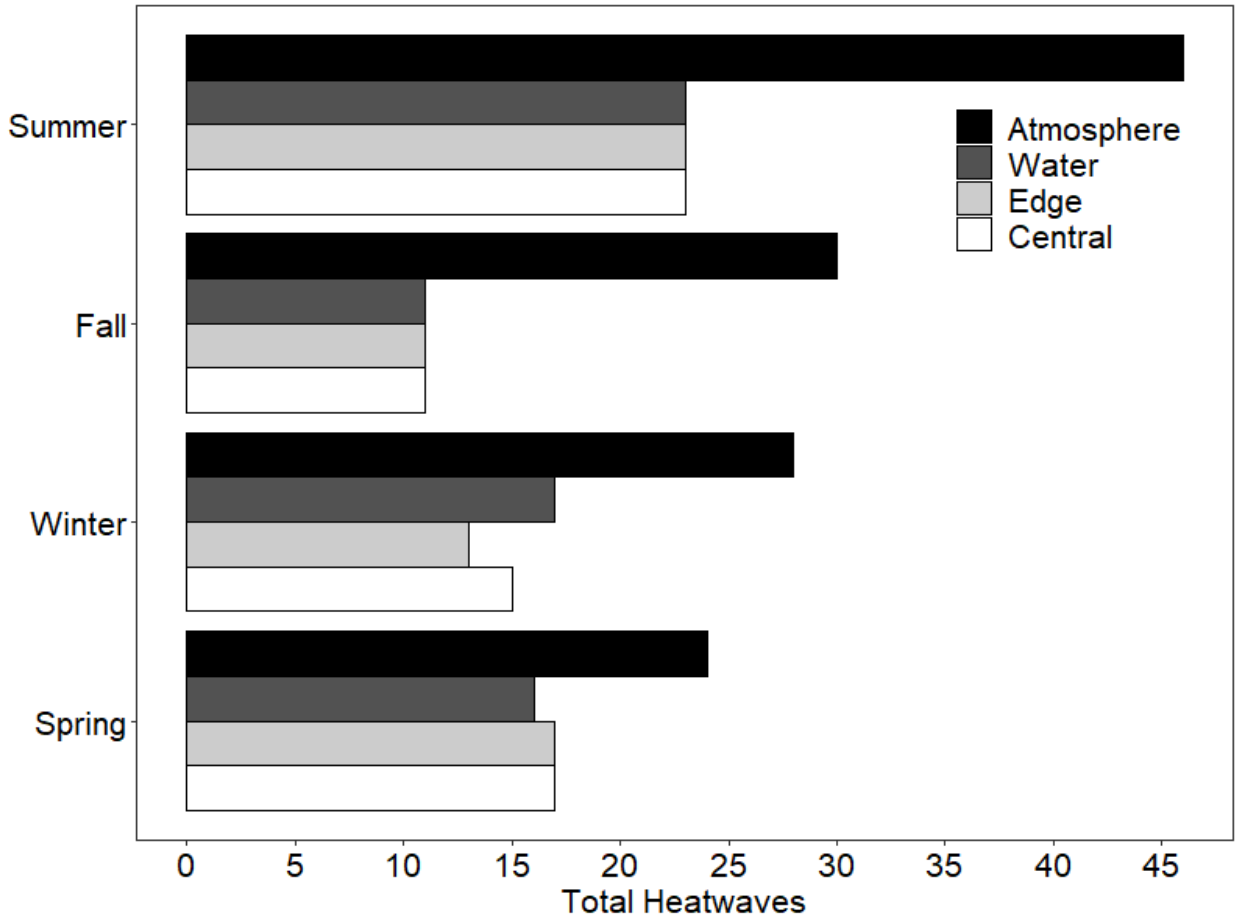

Figure 4.7 Total number of heatwaves between 1994-2022 per season for the VCR atmosphere, Wachapreague water column, and South Bay meadow sediments.

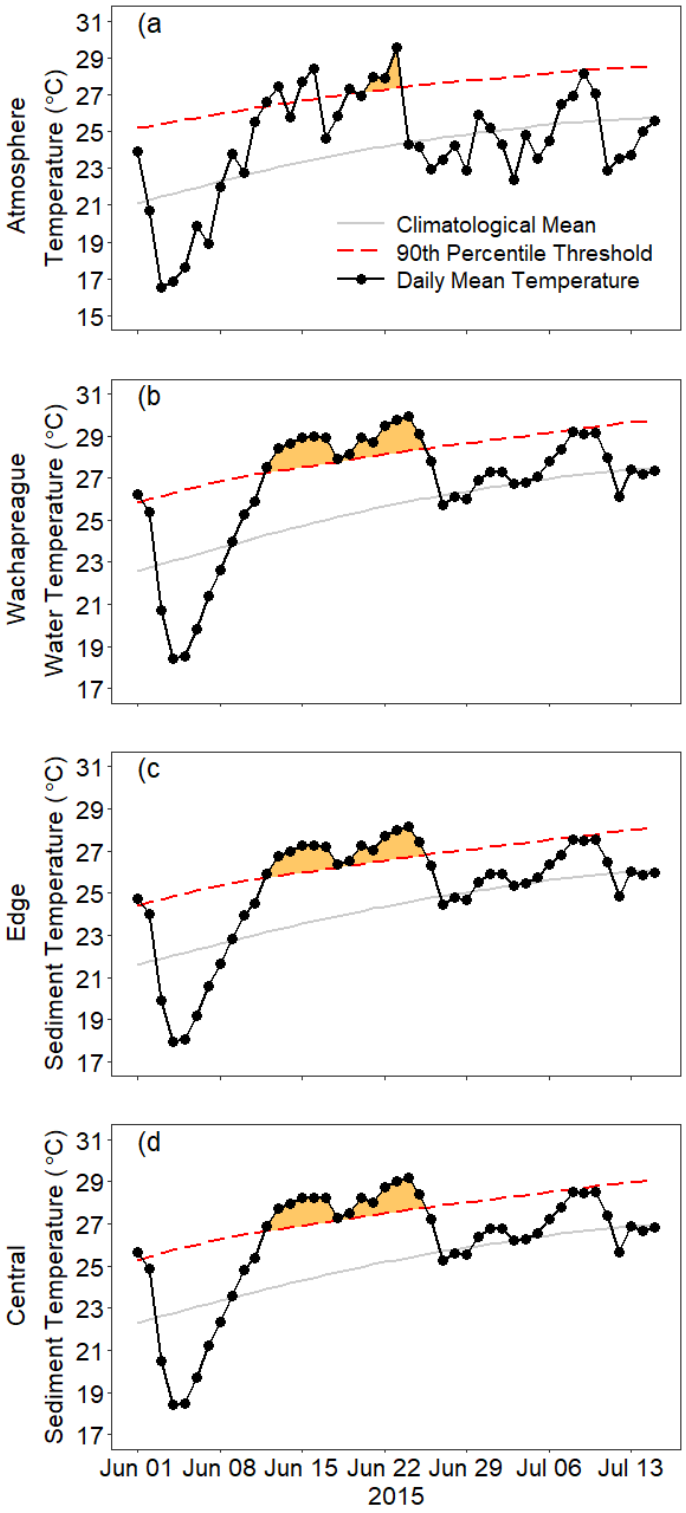

Figure 4.8 For June 2015, concurrent heatwaves in the atmosphere (a), water column (b), northern edge sediments (c), and central meadow (d) sediments. Atmosphere and water column are measured; sediments are modeled. Areas under the curve between the daily mean temperature and 90th percentile represent heatwave conditions with color denoting heatwave severity. All heatwaves represented were moderate in severity.

Chapter 5: Seagrass ecosystem recovery: experimental removal and synthesis of disturbance studies

Abstract

Global seagrass losses have spurred efforts to better understand the processes that support seagrass ecosystem stability. To understand intra-meadow stability, I experimentally removed aboveground seagrass biomass in 28.3 m^2 plots within the interior and along an edge of a restored seagrass meadow in South Bay, VA. I specifically asked 1) is recovery faster at sites with less thermal stress owing to greater exchange with cooler oceanic water at the meadow edge? 2) what is the shape of recovery? and 3) what are the recovery mechanisms? Linear recovery occurred within the meadow interior after 24 months, whereas recovery was incomplete at the meadow edge and projected to require 158 months. Differences in recovery times were likely due to storm-driven sediment erosion at the edge sites that damaged rhizomes and advected seeds. At both locations, recovery was facilitated by lateral clonal growth from the disturbance edge and seedling recruitment. Additionally, I synthesized results from prior seagrass disturbance-recovery studies summarizing spatial scales of experimental and observational research, rates of recovery, and factors related to recovery. The literature synthesis provided evidence that 47% of known seagrass species have been included in disturbance-recovery studies but that the majority of studies have occurred in monocultures of the genus *Zostera*. Experimental disturbances were most often conducted on relatively small spatial scales (median = 0.25 m^2), likely inflating the contribution of lateral clonal growth to recovery and limiting scalability by neglecting the impact of hydrodynamic factors on recovery rates that occurs within larger disturbance gaps. These limitations likely contribute to the positive, non-linear relationship between recovery time and disturbance area. The combined results indicate that seagrass meadows are resilient to disturbances large and small and that the seagrass meadow

state is stable across a broad set of conditions. Furthermore, meadow position influences disturbance susceptibility, and the geographic range and species diversity of seagrasses are under-represented in English language disturbance-recovery studies.

Introduction

Seagrass are a functional group of 72 species of highly productive submerged marine and estuarine flowering plants that form extensive meadows when hydrodynamic, underwater light, sediment, and water temperature conditions are favorable (Short et al. 2011). Vegetated coastal marine ecosystems, including seagrass, make up 5-8% of Earth's land surface, yet collectively store 20-30% of all soil carbon (Fourqurean et al. 2012; Nahlik and Fennessy 2016). However, seagrass meadows are among the globe's most threatened ecosystems as the annual median areal loss rate accelerated from < 1% to 7% during the 20th century (Waycott et al. 2009), representing an estimated global net loss of 19.1% (Dunic et al. 2021). Drivers of seagrass decline include physical (i.e., shell fishing, anchoring, coastal development), chemical (i.e., eutrophication, anoxia), disease (i.e., wasting disease), and climatological (i.e., storm, heatwave) processes (Berger et al. 2020; Dunic et al. 2021). These factors can rapidly reduce aboveground biomass, thereby decreasing ecosystem resilience and increasing the potential for a regime shift to unvegetated, turbid, and less productive bare sediments with reduced ecosystem services.

Global net seagrass losses have spurred restoration to reverse habitat loss and interest in how these systems respond to various disturbances. The coastal bays of Virginia, USA, are home to the largest successful seagrass restoration project, which began in 1999 and now spans ~36 km^2 of continuous meadow (Orth et al. 2020). However, in June 2015, a marine heatwave (MHW) in one of the coastal bays (South Bay) caused ~90% reductions in *Zostera marina* shoot density, 20% reductions in sediment carbon stores, and shifted the metabolism of the meadow to net heterotrophy (Berger et al. 2020; Aoki et al. 2021). Spatial patterns in *Z. marina* shoot density loss were not uniform, as the damage was confined to the meadow interior, while the meadow edge had no loss of shoot density or canopy cover. Annual aerial canopy cover imagery

and annual summer (June or July) shoot density counts from within the disturbance area suggested that seagrass recovered in ~2-4 years following the MHW disturbance (Aoki et al. 2021). The lack of MHW effects at the meadow edge suggests this area may be more resilient to MHWs than the meadow interior. Furthermore, the 2015 MHW disturbance raised questions about the pattern of recovery (i.e., linear or non-linear) and the recovery mechanisms (i.e., lateral clonal extension or new seedling recruitment).

In this study, I designed an experiment to evaluate aspects of a MHW disturbance by removing aboveground *Z. marina* from interior and edge sites of a seagrass meadow. I asked 1) is recovery faster at sites with greater oceanic exchange (i.e., meadow edge) that have lower thermal stress? 2) what is the shape of recovery? and 3) what are the recovery mechanisms? Based on earlier work of Berger (2021), showing greater interior meadow heat stress relative to the edge, and Aoki et al. (2021), showing greater interior meadow seagrass loss, faster recovery was hypothesized for the meadow edge due to lower thermal stress provided by greater oceanic exchange. Furthermore, the Virginia coastal bays had a rapid areal expansion of seagrass, which has been attributed to seeding recruitment (Orth et al. 2012), suggesting seedling recruitment rather than lateral clonal growth as the dominant recovery mechanism. Lastly, some have observed a non-linear (i.e., sigmoidal, exponential) recovery shape for *Zostera spp*. after disturbance (Short 1983; Preen 1995; Neckles et al. 2005; Vaudrey et al. 2010; Lundquist et al. 2018) while others have observed linear recovery (Frederiksen et al. 2004; Cardoso et al. 2010; Macreadie et al. 2014; Smith et al. 2016; Qin et al. 2016). Prior research that tracked shoot density in South Bay during restoration showed linear increases following an initial lag period (McGlathery et al. 2012). I hypothesized that the shape of shoot density recovery would be linear without a lag, given the established state of the meadow.

Prior experimental and observational studies have measured the aboveground recovery of seagrass following disturbance (Zieman 1976; Williams 1988; Rasheed 1999; Aoki et al. 2021). These studies of disturbance-recovery dynamics are geographically extensive, include mono- and mixed-species beds, and represent diverse disturbance types. Despite the breadth of seagrass disturbance-recovery studies, there has been little cross-system examination of the resulting patterns. Therefore, I synthesized studies of seagrass ecosystem disturbance and recovery to summarize spatial scales of experimental and observational research, rates of recovery and factors related to recovery to both provide greater context for the experiment presented in this paper and to assess possible generalities about seagrass recovery.

It is important to note that I consider recovery, as studied here, an attribute of ecosystem stability (Ives and Carpenter 2007). I distinguish this process from ecological resilience, defined by Holling (1973) as the tendency to remain in a specific state rather than transition to a different state. This view contrasts conceptually with what has been called 'engineering resilience' (Zampieri 2021), which is the ability of a system to resist disturbance and the rate at which it returns to equilibrium. Ecologists often use the term resilience in this context (Zampieri 2021), but theory related to stability is well developed and consistent with my interest in the return of seagrass to full shoot density as supported by local conditions. The study of stability helps identify mechanisms that maintain resilience but do not measure resilience, which instead requires methods that either anticipate (Scheffer et al. 2015) or directly assess movement among states (Scheffer et al. 1997; Wernberg et al. 2016). In this context, the experiment and comparative synthesis explore the stability landscape of seagrass and what maintains these systems rather than the mechanisms that 'break' the seagrass system and move it to an alternate state.

Methods

Study Site

Along the Virginia portion of the Delmarva peninsula are a series of 14 coastal barrier islands with a North-South orientation that parallel the mainland. Since 1987, the area from the edge of the mainland to the ocean edge of the barrier islands constitutes a protected region known as the Virginia Coast Reserve (VCR). The VCR is one of 28 National Science Foundation Long-Term Ecological Research (LTER) Network sites. West of the VCR barrier islands are lagoons where subtidal seagrass meadow restoration has been ongoing since 1999. South Bay contains one seagrass meadow located landward of Wreck Island that has been successfully restored and covers approximately 20.3 km^2 (Orth et al. 2020; Figure 5.1).

The physical structure of seagrass in South Bay alters the hydrodynamic environment and water quality conditions (Hansen and Reidenbach 2012; Hansen and Reidenbach 2013). The water residence time within South Bay varies between 12-80 hours, with longer residence times as distance from the northern oceanic inlet increases (Safak et al. 2015). Similarly, water temperature varies with distance from the northern oceanic inlet such that summer water temperature is, on average, 0.7 °C warmer in the meadow interior relative to the northern edge (Berger 2021).

Experimental Design

In June 2020, triplicate paired seagrass treatment and control plots were established at two locations (i.e., center of the meadow, northern edge of the meadow) approximately 1.4 km apart within South Bay (Figure 5.1). These locations were selected due to their observed differences in seagrass canopy cover and shoot density following the June 2015 MHW (Berger et al. 2020; Aoki et al. 2021). As the predominant flow direction in South Bay is N-S (Hansen and

Reidenbach 2013), control and treatment plots were placed E-W to maintain hydrodynamic similarity and minimize disturbance among plots. Central sites had a linear orientation, while northern edge sites had a triangular orientation due to depth differences, the presence of other ongoing research in the area, and the distance to the meadow edge (distance to meadow edge at northern sites was ~50 m). Control and treatment pairs were spaced 20 m apart edge-to-edge to minimize the treatment's potential impact on the control while maintaining similar depth, seagrass density, and hydrodynamic properties (e.g., flow velocity and direction). Each pair block was separated by 50 m edge-to-edge to further minimize any potential impact from flow disruption within the treatment plots and from working within each pair block. Within treatment plots, seagrass was manually removed by hand on June 5, 2020 (Commonwealth of Virginia Marine Resources Commission permit # 2020-0277).

Data Collection

Z. marina shoots were counted monthly *in situ* between June-October 2020, May-October 2021, and April-October 2022 using a 0.25 m^2 quadrat. Within each plot, shoots were counted at 0.5, 1.5, and 2.5 m from the edge of the plot at random orientations. Adverse weather prohibited sampling the central sites in September 2022. Water temperature was monitored at fixed positions 20 cm above the sediment surface at the center of each plot using Onset HOBO Pendant 64K temperature loggers. Water temperature was collected at 15-minute intervals between April-October and hourly intervals between November-March. To further characterize differences between the meadow interior and edge, benthic chlorophyll and surface water quality samples were collected. Benthic chlorophyll-a samples were collected with a 10 cm^3 syringe corer to a depth of 1 cm at 0.5, 1.5, and 2.5 m from the edge of each control and treatment plot. Samples were kept in the dark on ice and frozen immediately upon return to the laboratory.

Benthic chlorophyll-a samples were analyzed within 4 weeks of collection, by overnight extraction in 90% acetone and subsequent determination of absorption on extracts at 665 and 750 nm before and after acidification using a Shimadzu UVmini-1240 spectrophotometer (Lorenzen 1967; McGlathery et al. 2012). Surface water grab samples were collected from the center of each plot using dark 1-L Nalgene bottles and used to quantify turbidity, total suspended sediment (TSS) concentration, and pelagic chlorophyll-a. Turbidity was analyzed immediately upon return to the laboratory using a Hach 2100Q portable turbidimeter. TSS was determined by gravimetric filtration of surface water through pre-dried, pre-weighed 47 mm Whatman GF/C glass microfiber filters, which were then dried to a constant weight in a 60 °C oven. TSS concentration was derived as the difference in dry weight between the before and after sampling filter weights divided by the volume of water filtered. Pelagic chlorophyll-a samples were filtered through 47 mm Whatman GF/C glass microfiber filters (pore size = 1.2 μm), homogenized, extracted overnight in 90% acetone, and centrifuged before spectrophotometric analysis of the supernatant as described above. Water quality variables such as dissolved oxygen saturation and salinity were collected at each site during each visit using a YSI Pro Plus Multiparameter meter. Depth was measured at 15-minute intervals using Onset HOBO Water Level Data Logger between October-November 2021 within five of the six pair blocks (two in the central meadow and three at the northern edge). Lastly, seagrass bed elevation was measured once in October 2022 along an 18-meter N-S transect, centered on the middle of each plot, using an Emlid Reach RS2 RTK GNSS receiver with a vertical precision of 1.4 cm.

Literature Synthesis

A quantitative synthesis of measured values for various parameters was derived from primary research articles on seagrass disturbance and recovery. Papers were initially identified

on July 7, 2021 and updated on May 13, 2022, using the Web of Science (WoS) database. This synthesis only considered original primary research written in the English language. The most relevant articles on the topic were identified using the search terms “seagrass”, “recoloni*”. The latter search term stemmed from studies on seagrass recovery from disturbance which tended to use the word “recolonization” rather than “recovery”. Of the 142 articles identified using the search terms, 36 were relevant as determined from reading the abstract. All relevant research articles cited within the 36 originally identified manuscripts were further assessed, and 24 additional studies were identified, leading to a total of 60 primary research articles containing quantitative values relevant to the planned analysis (SI Table 5.1). Studies with multiple treatments (e.g., different locations or depths) were treated independently, bringing the total number of observed disturbance and recovery comparisons to 138. Studies that were historical updates to previously published works were included in this review; however, in the case of updates, the prior results were excluded in favor of the longer-term observations. Articles were examined to identify study type (i.e., experimental or observational), geographic location, disturbance type, disturbance shape, disturbance area, total aboveground loss, recovery time, recovery trajectory (i.e., linear or non-linear), recovery method (i.e., lateral clonal growth, seedling recruitment, or both) and total aboveground recovery. Recovery rates were derived by dividing recovery time by disturbance area. Recovery rates were only examined for those sites where the total aboveground loss was ≥ 80%, and recovery during the study period was ≥ 90%.

Statistical Analysis

The recovery of shoot density for treatments relative to controls was determined using Welch’s t-test for each monthly sampling at each location (i.e., central and edge). To correct for multiple comparisons, p-values were adjusted using a 5% false discovery rate (Benjamini and

Hochberg 1995). Statistical significance for shoot density among control sites at each meadow location was determined using a three-way ANOVA with pair block number (i.e., 1-3 for central and 4-6 for edge), meadow location, and collection date as the independent variables. Pairwise comparisons of the three-way ANOVA resulted in three statistically significant differences out of 108 tests therefore, samples were pooled among sites at each location prior to statistical analysis. Recovery rate and trajectory were determined based on the relative recovery of the central and northern edge treatment sites to their control sites. Relative recovery was derived for each month based on the mean shoot density of the treatment sites ($\bar{x}_{ShootDensity,Treatment}$) relative to the mean shoot density of control sites ($\bar{x}_{ShootDensity,Control}$) for each location.

$$Relative\ Recovery = \left(\frac{\bar{x}_{ShootDensity,Treatment}}{\bar{x}_{ShootDensity,Control}}\right) * 100\%$$

The recovery mechanism (i.e., clonal vs. seedling) was assessed by comparing intra-plot patterns of shoot density within the treatment plots among central and northern edge locations. Seedling recovery was inferred if shoot density counts were independent of distance from the plot edge. Clonal recovery was inferred if there was a statistically significant greater *Z. marina* density at the 0.5 m distance from the edge relative to the 1.5 and 2.5 m distances. Statistical significance for the recovery mechanism was determined using a three-way ANOVA with location, distance from the plot edge, and collection date as the independent variables. Estimated marginal means were used to determine when significant differences in shoot density occurred between edge distances. For water quality metrics, Welch's t-tests were used to determine if there were significant differences between meadow locations.

Results

Site Conditions

The northern edge sites were, on average, 20 cm deeper (mean = 1.5 m) than the central sites (mean = 1.3 m), with both sites having an equal tidal range of 1.2 m (Table 5.1). Salinity was euhaline (> 30 g kg^{-1}) and did not significantly differ between locations (p-value = 0.277). Water temperature at the central sites was, on average, significantly warmer (mean ± SD = 21.2 ± 7.2 °C) than edge sites (20.7 ± 6.9 °C; p-value ≤ 0.001) however, edge sites were typically warmer (up to 4.2 °C) than central sites during winter (Dec.-Feb.; Figure 5.2). During summer (June-Aug.), water temperature at the central sites followed a diurnal cycle, whereas the northern edge sites followed a semidiurnal and diurnal cycle. These differences produced water temperature gradients of up to 8.9 °C with the central sites warmer than the edge sites. Dissolved oxygen (DO) was super-saturated at both locations, with the edge sites having a significantly greater DO saturation (138.9 ± 42.1%) than the central sites (114.5 ± 18.1%; p-value ≤ 0.001). Turbidity, total suspended solids, and pelagic chlorophyll-a concentration were all significantly greater at the edge locations (p-values ≤ 0.001) than at the central locations (Table 5.1). Benthic chlorophyll-a was significantly greater and more variable at the central sites (39.2 ± 34.9 mg m^{-2}) relative to the edge sites (29.0 ± 18.4 mg m^{-2}; p-value ≤ 0.001). Overall, site conditions varied between the central and edge locations, reflecting the greater exposure of oceanic exchange and resuspended sediments at the edge.

Seagrass Recovery Experiment

Shoot density removal at the northern and central treatment plots was 84% and 93% effective, respectively. Treatment site shoot density remained low (≤ 76 shoots m^{-2}) throughout 2020, while control sites senesced after July (Figure 5.3). In 2021, shoot density recovery within treatment sites was significantly greater (p-values ≤ 0.009) at the central sites relative to the northern sites for June and July, with an estimated marginal mean difference of 61 and 56 shoots

m^{-2} for the two months, respectively. Additionally, in 2021 the peak relative recovery at the central and northern edge treatment sites occurred in July and were 54% and 43%, respectively (Figure 5.4). At the beginning of the second growing season (April 2022), treatment sites at the central and northern locations had similar shoot densities; however, central treatment sites reached and maintained control site shoot density by June 2022 (Figure 5.5). Conversely, in 2022 the northern treatment sites' mean shoot density was less than the peak 2021 mean shoot density, with the standard deviation among northern treatment sites increasing up to ± 107 shoots m^{-2}. Furthermore, the mean shoot density at the northern treatment sites declined after June 2022, while the northern control sites increased until July 2022.

The relative recovery of shoot density increased linearly at the central treatment sites. Densities were no longer significantly different from control sites after 24 months. In contrast, for the edge treatment sites, the linearly estimated 100% relative recovery time was 158 months (Figure 5.4). A possible cause for the difference between the two treatment locations was a change in bed elevation. By October 2022, the bed elevation within the northern treatment plots was depressed by 14-17 cm based on transects that extended 6 meters north and south of each plot edge (Figure 5.6). No significant depression was observed within the central treatment plots.

Shoot density varied within plots consistent with both lateral growth and seedling recruitment. In the first year following shoot removal (i.e., 2021), *Z. marina* shoots were distributed throughout the treatment plots at low densities, and shoot density was not significantly different (p-value > 0.05) among distances from the plot edge for both central and northern locations (Figure 5.7). In the second year following shoot removal, the 0.5-meter edge distance was significantly greater than the 2.5-meter edge distance at the central location in May (estimated mean difference = 109 shoots m^{-2}; p-value = 0.008) and August (p-value = 0.030).

Similarly, at the northern location, the 0.5-meter and 1.5-meter edge distances had significantly greater shoot densities than the 2.5-meter distance in June (estimated mean difference = 120 and 95 shoots m^{-2}, respectively; p-values ≤ 0.025). Additionally, in 2022 the mean shoot density nearest the plot edge (i.e., 0.5 meters) was greater by 35, and 33 shoots m^{-2} than the interior positions (i.e., 1.5 and 2.5 meters from the plot edge) for the central and northern locations respectively. In July 2022, following full recovery at the central treatment sites, I manually disturbed plot edges to visually confirm that *Z. marina* rhizomes were growing laterally across the treatment plot edge. This inspection was done once at the end of the experiment to avoid disturbing the active recovery of *Z. marina* plants.

Literature Synthesis

Seagrass disturbance and recovery studies have been conducted across all continents except Antarctica, including 16 countries that span the northern and southern hemispheres and the Atlantic, Pacific, and Indian Ocean basins (Figure 5.8). The most common category of seagrass disturbance (58%) cited among the 60 studies considered were physical disturbances, such as shellfishing, trawling, hull grounding, propeller/anchor scarring, explosions, grazing, ice scour, and land reclamation (SI Figure 5.1). Additional categories of seagrass disturbance included chemical (i.e., eutrophication, anoxia), light availability (i.e., dredging), climate (i.e., marine heatwaves, cyclone), disease (i.e., wasting disease), and natural mass mortality (i.e., breakdown of a mutualistic relationship with a bivalve). Of the 72 recognized seagrass species, 47% (n = 34) were included in this synthesis, with *Z. marina* and the *Zostera* genus receiving the greatest attention (Figure 4.9). Most studies (53%) provided evidence that recovery was linear over time, while 17% indicated non-linear recovery, and the remaining not indicated (SI Figure 5.2).

Of the 60-seagrass disturbance and recovery studies considered, 45% (n = 27) were experimental, and 55% (n = 33) were observational. Most experimental and observational studies were conducted within single-species meadows (52% and 61%, respectively; SI Figure 5.3). The disturbance scale among experimental and observational studies varied by nine orders of magnitude, ranging between 0.01 m^2 to 1,220 km^2, with median experimental and observational disturbance areas of 0.25 m^2 and 124,900 m^2, respectively (SI Figure 5.4). Log-transformed recovery rate had a significant positive linear relationship with log-transformed disturbance area (slope = 0.15 ± 0.03, R^2 = 0.24, p-value < 0.001; Figure 5.10). Recovery rates normalized to disturbance area ranged between 0.0001-228 months m^{-2} but were not significantly different among latitudinal regions (SI Figure 5.5). The dominant recovery mechanism cited for experimental and observational studies was lateral clonal growth (56% and 30%, respectively; Figure 5.11). While none of the experimental studies cited seedling recruitment as the lone recovery mechanism, two studies provided evidence of both seedling recruitment and lateral clonal growth as co-contributors to recovery. Conversely, four observational studies cited seedling recruitment as the lone recovery mechanism, while five indicated both seedling and clonal growth as contributors to recovery.

Discussion

Seagrass Recovery Experiment

Contrary to the initial hypothesis that seagrass recovery would be quicker at the meadow edge relative to the interior based on patterns of loss during the June 2015 MHW and observed water temperature differences, shoot density at the central treatment plots was complete after 24 months, whereas recovery was incomplete and estimated to take 158 months at the edge sites. Absent a major MHW, the recovery rate of the central treatment sites agreed with annual shoot

density counts and annual aerial photography of South Bay that indicated recovery occurred 2-4 years following the June 2015 MHW (Berger et al. 2020; Aoki et al. 2021). Differences in recovery times between locations were likely due to storm-driven sediment erosion at the northern edge treatment locations between the April and May 2022 sampling periods. While seagrass meadow edges attenuate wave energy and near-bottom currents, they are exposed to stronger hydrodynamic conditions than meadow interiors (Granata et al. 2001; Hansen and Reidenbach 2012). In April 2022, shoot density at the northern edge control sites (mean ± SD = 202 ± 30 shoots m^{-2}) likely exerted strong current flow reduction resulting in low bed shear stress that did not erode control sites. Conversely, shoot densities within the northern edge treatment sites were low (mean = 85 ± 23 shoots m^{-2}) and likely unable to reduce current flow resulting in high bed sheer stress, sediment erosion, and decreased bed elevation of the treatment sites (Hansen and Reidenbach 2013; Zhu et al. 2022). Additionally, reproductive seagrass shoots develop in South Bay between April-May. This high current flow event likely advected seedlings and damaged rhizomes during sediment erosion thereby reducing seedling recruitment and seagrass recovery. While the June 2015 MHW in South Bay suggested stability was greater at the northern edge relative to the meadow interior, this study suggests the northern edge may be less stable relative to the meadow interior in relation to a second factor - stronger hydrodynamic forces at the meadow edge. Alternatively, the northern edge of the meadow may be more stable than the meadow interior to heatwave disturbances due to less thermal stress (Berger et al. *in review*), but being positioned near the edge may decrease stability due to hydrodynamic disturbances. Nevertheless, spatial position within the seagrass meadow alters disturbance susceptibility and recovery rates.

The relative recovery of shoot density at both locations was linear and facilitated by lateral clonal growth from the treatment plot edges and seedling recruitment within the treatment plots. The linear recovery trajectory for shoot density supports prior annual observations from within South Bay that followed seagrass shoot density during meadow restoration efforts (McGlathery et al. 2012). However, unlike recovery following South Bay meadow restoration, there was no initial lag in shoot density. Rather, shoot density increased throughout the first post-disturbance growing season at both locations. This suggests that mature seagrass meadows possess greater stability than young or newly restored meadows, analogous to forested systems of varying stand age (Sohn et al. 2016). While lateral clonal growth rates into treatment plots were not measured and it is also uncertain if seedlings were randomly distributed within treatment sites, prior studies are consistent with both lateral growth and seedling recruitment contributing to recovery. Specifically, *Z. marina* lateral clonal growth rates range from 0-2.26 m yr^{-1} (Castorani and Baskett 2020 and referenced therein) indicating how lateral growth of about 1 m yr^{-1} could have led to recovery. *Z. marina* seedlings (80-90%) disperse within ≤ 7.1 m of their origin (Orth et al. 1994) indicating the potential for seed deposition to contribute to recovery of the 6-meter diameter plots. While uncertainty remains regarding the recovery process, these lateral growth rates and seedling dispersal distances suggest that treatment sites benefitted from close proximity to undisturbed areas that promoted rapid shoot density recovery. However, these biological recovery mechanisms were offset by sediment erosion at the edge sites during the second growing season, resulting in a net-zero gain in shoot density between the first and second growing seasons. Nonetheless, seedling recruitment and lateral clonal growth from undisturbed areas will be important for the lagged recovery of the edge treatment sites.

Literature Synthesis

Experimental disturbances have largely been conducted on small spatial scales of < 1 m^2. This has likely contributed to the prevalence of asexual reproduction being cited as the dominant recovery mechanism in seagrass meadows. Additionally, recovery rates of small experimental disturbance areas likely do not scale for larger disturbances. This is due to an inadequate representation of the physical forcings, such as hydrodynamics, that are positively related to disturbance area (Carr et al. 2016; El Allaoui et al. 2016). Differences in the physical forcings experienced among small-scale experiments and large-scale observational studies likely contribute to the positive, non-linear relationship between recovery time and disturbance area, suggesting that recovery rates become increasingly slow as disturbance area increases. Additionally, disturbance area thresholds exist at which natural recovery is no longer possible, as was observed in the VCR following a concurrent pandemic slime mold disease and hurricane that eliminated seagrass from the system for 70+ years (Orth et al. 2020). Nonetheless, experimental seagrass disturbances on larger spatial scales better characterize recovery to large disturbance events and how *in-situ* processes influence recovery rates. Experimental efforts should further consider not only the disturbance area, but the volume of sediment disturbed, the effects of increased disturbance frequency, and the impact of targeted restoration actions (e.g., seeding, sediment in-filling, transplants) on large disturbance areas. Studies of the kind proposed will necessitate long-term monitoring and considerable experimental effort but will provide a greater understanding of seagrass stability and ecosystem management as the frequency, intensity, and spatial extent of pulsed coastal disturbances increase as the climate warms (Webster et al. 2005; Horton et al. 2016; Oliver et al. 2018; Smale et al. 2019).

Seagrass disturbance-recovery studies have provided insights into recovery rates and mechanisms across all continents except Antarctica, where seagrass is not known to occur

(Waycott et al. 2009; McKenzie et al. 2020; Dunic et al. 2021). However, these studies have not been well distributed among the world's coastlines, with a limited representation of islands and oceanic regions such as the Indian Ocean, South Atlantic, and Eastern Pacific. Furthermore, only 16 of the 136 countries (12%) with seagrass meadows have conducted disturbance-recovery studies (McKenzie et al. 2020). This limited biogeographic representation is likely due to only considering English language publications and why less than half (47%) of known seagrass species have been represented in disturbance-recovery studies, thus limiting recovery generalities primarily to genera *Zostera*, *Halophila*, and *Halodule*. Increasing language translations of scientific publications will help prioritize disturbance-recovery studies in underrepresented regions and on species with low representation, which will provide a baseline measure of resilience, better inform the stability landscape of these keystone species, and may serve as a conservation tool for species or regions with extended recovery rates.

Seagrass Recovery and Resilience

The extensive studies of seagrass recovery indicate that these systems are resilient to disturbances large and small. In conceptual terms, this means the seagrass state is a strong attractor, and there is likely a broad and deep stability landscape that sustains seagrass states. My experimental results, coupled with prior long-term observations (Berger et al. 2020; Aoki et al. 2021), support this view and indicate that the seagrasses in the VCR can recover from MHWs and likely from storm-driven hydrodynamic disturbances. Lacking, however, are measures of seagrass resilience where shallow subtidal areas transition from seagrass to bare or vice versa and maintain those states (as opposed to recover). Such a state shift occurred in the VCR in the 1930s and was only reversed with concerted restoration efforts beginning in 1999 (Orth et al. 2012). Prior modelling research in the VCR identified bistable states between seagrass and bare

sediment at a depth of 1.6-1.8 m mean sea-level due to reduced underwater light availability driven by feedbacks between plant biomass and sediment resuspension (Carr et al. 2012a). However, at shallow depths, *Z. marina* is subject to high water temperatures (> 30 °C) in summer that exceed their thermal tolerance (28.6 °C), potentially limiting their distribution (Aoki et al. 2020; Berger 2021). Nonetheless, there remains a limited understanding of the stability landscape of shallow subtidal bare sediments that might otherwise support seagrass and how these habitats interact with seagrass habitats following state shifts (McGlathery et al. 2013).

The frequency of seagrass disturbance and recovery rate should be emphasized in future studies. If mechanisms that maintain seagrass state at locations are altered by an increased frequency and intensity of forcings like MHW and storms, then disturbance may result in slowing recovery rates - an indicator of declining resilience (Carr et al. 2012b; Scheffer et al. 2015). Long-term studies have the potential to reveal such changes. In the specific case of the VCR, *Z. marina* is near the southern limit of its distribution (Jarvis et al. 2012) and may become increasingly temperature-stressed as the local climate warms. The current seagrass state might give way to alternates like bare sediment or the establishment of warm-water grasses. Additionally, sea-level rise within the VCR is accelerating and is among the fastest on the North American coast (relative sea-level rise = 4.1 ± 0.2 mm yr^{-1}; Sallenger et al. 2012; Blum et al. 2020). Current rates of sediment accumulation in seagrass meadows (Greiner et al. 2016; Oreska et al. 2017) are sufficient to keep pace with sea-level rise (Aoki et al. 2020). However, as sea-level rise accelerates, the spatial resilience of *Z. marina* will likely change as intertidal bare sediments become subtidal and deeper areas become light-limited. Finally, spatial resilience also differs among meadow locations, as observed in this study for central vs edge.

Summary

The seagrass recovery experiment did not support the initial hypothesis that the meadow edge would recover faster than the meadow interior. This was likely due to storm-induced hydrodynamic stress at the meadow edge, which resulted in sediment erosion, suggesting that while the system is sensitive to heat stress, recovery from disturbance is responsive to hydrodynamic stress. The removal sites in the meadow interior recovered at a rate similar to that observed following the June 2015 MHW, such that there is no evidence of recovery slowing there. However, as the northern edge treatment sites are projected to take > 10 years to recover due in part to sediment erosion, future studies should consider how recovery at the meadow edge changes in response to management actions or natural events. Efforts to stabilize and remediate large-scale erosional damage via sediment in-filling and seeding have succeeded in the subtropics and could be applied in the VCR at the northern edge of the South Bay meadow (Uhrin et al. 2011). Continued monitoring of seagrass shoot density at a high temporal frequency (e.g., sub-annual) will be essential to determine 1) if a disturbance event has occurred such that management action(s) can be undertaken and 2) if/when the resilience of the meadow changes.

The area of the seagrass resilience experiment was > 2x larger than the largest experimental seagrass disturbance based on my review of prior studies. At this scale, recovery was mediated by lateral clonal growth and seedling recruitment rather than exclusively lateral clonal growth, as is the predominant reported recovery mechanism in seagrass disturbance experiments. Additionally, I observed that the rate of seagrass recovery was impacted by hydrodynamic factors, which are negligible within small disturbance gaps (El Allaoui et al. 2016). The experiment occurred in the temperate northern Atlantic Ocean and within a monoculture of *Z. marina,* which is the most well-studied disturbance-recovery seagrass species. Future seagrass recovery studies should be conducted in regions and on species with low

representation to better resolve how these foundational species recover in a future of likely increasing disturbance frequency and magnitude. Lastly, as carbon stored in seagrass meadows is now part of the carbon market trade (Oreska et al. 2020), disturbances to these ecosystems and how quickly they recover versus possibly undergoing a state change will be of increasing financial and carbon management interest. Revenue from this seagrass carbon trade should be invested back into these productive systems to defray the costs associated with continuous monitoring, research, and restoration efforts of these valuable ecosystems.

References

Aoki, L. R., McGlathery, K. J., Wiberg, P. L., & Al-Haj, A. (2020). Depth Affects Seagrass Restoration Success and Resilience to Marine Heat Wave Disturbance. *Estuaries and Coasts*, *43*(2), 316–328. https://doi.org/10.1007/s12237-019-00685-0

Aoki, L. R., McGlathery, K. J., Wiberg, P. L., Oreska, M. P. J., Berger, A. C., Berg, P., & Orth, R. J. (2021). Seagrass Recovery Following Marine Heat Wave Influences Sediment Carbon Stocks. *Frontiers in Marine Science*, *7*, 576784. https://doi.org/10.3389/fmars.2020.576784

Benjamini, Y., & Hochberg, Y. (1995). Controlling the False Discovery Rate: A Practical and Powerful Approach to Multiple Testing. *Journal of the Royal Statistical Society: Series B (Methodological)*, *57*(1), 289–300. https://doi.org/10.1111/j.2517-6161.1995.tb02031.x

Berger, A. C., Berg, P., McGlathery, K. J., & Delgard, M. L. (2020). Long-term trends and resilience of seagrass metabolism: A decadal aquatic eddy covariance study. *Limnology and Oceanography*, *65*(7), 1423–1438. https://doi.org/10.1002/lno.11397

Berger, A. C. (2021). Long-term aquatic eddy covariance measurements of seagrass metabolism and ecosystem response to warming oceans. Ph.D. Dissertation. University of Virginia

Blum, L. K., Christian, R. R., Cahoon, D. R., & Wiberg, P. L. (2021). Processes Influencing Marsh Elevation Change in Low- and High-Elevation Zones of a Temperate Salt Marsh. *Estuaries and Coasts*, *44*(3), 818–833. https://doi.org/10.1007/s12237-020-00796-z

Cardoso, P. G., Leston, S., Grilo, T. F., Bordalo, M. D., Crespo, D., Raffaelli, D., & Pardal, M. A. (2010). Implications of nutrient decline in the seagrass ecosystem success. *Marine Pollution Bulletin*, *60*(4), 601–608. https://doi.org/10.1016/j.marpolbul.2009.11.004

Carr, J. A., D'Odorico, P., McGlathery, K. J., & Wiberg, P. L. (2012a). Stability and resilience of seagrass meadows to seasonal and interannual dynamics and environmental stress: stability and resilience of seagrass. *Journal of Geophysical Research: Biogeosciences*, *117*(G1). https://doi.org/10.1029/2011JG001744

Carr, J., D'Odorico, P., McGlathery, K., & Wiberg, P. (2012b). Modeling the effects of climate change on eelgrass stability and resilience: Future scenarios and leading indicators of collapse. *Marine Ecology Progress Series*, *448*, 289–301. https://doi.org/10.3354/meps09556

Carr, J. A., D'Odorico, P., McGlathery, K. J., & Wiberg, P. L. (2016). Spatially explicit feedbacks between seagrass meadow structure, sediment and light: Habitat suitability for seagrass growth. *Advances in Water Resources*, *93*, 315–325. https://doi.org/10.1016/j.advwatres.2015.09.001

Castorani, M. C., & Baskett, M. L. (2020). Disturbance size and frequency mediate the

coexistence of benthic spatial competitors. *Ecology*, *101*(1), e02904.

Dunic, J. C., Brown, C. J., Connolly, R. M., Turschwell, M. P., & Côté, I. M. (2021). Long-term declines and recovery of meadow area across the world's seagrass bioregions. *Global Change Biology*, *27*(17), 4096–4109. https://doi.org/10.1111/gcb.15684

El Allaoui, N., Serra, T., Colomer, J., Soler, M., Casamitjana, X., & Oldham, C. (2016). Interactions between Fragmented Seagrass Canopies and the Local Hydrodynamics. *PLoS One*, *11*(5), e0156264. https://doi.org/10.1371/journal.pone.0156264

Fourqurean, J. W., Duarte, C. M., Kennedy, H., Marbà, N., Holmer, M., Mateo, M. A., ... & Serrano, O. (2012). Seagrass ecosystems as a globally significant carbon stock. *Nature geoscience*, *5*(7), 505-509.

Frederiksen, M., Krause-Jensen, D., Holmer, M., & Laursen, J. S. (2004). Long-term changes in area distribution of eelgrass (*Zostera marina*) in Danish coastal waters. *Aquatic Botany*, *78*(2), 167–181. https://doi.org/10.1016/j.aquabot.2003.10.002

Granata, T., Serra, T., Colomer, J., Casamitjana, X., Duarte, C., & Gacia, E. (2001). Flow and particle distributions in a nearshore seagrass meadow before and after a storm. *Marine Ecology Progress Series*, *218*, 95–106. https://doi.org/10.3354/meps218095

Greiner, J. T., Wilkinson, G. M., McGlathery, K. J., & Emery, K. A. (2016). Sources of sediment carbon sequestered in restored seagrass meadows. *Marine Ecology Progress Series*, *551*, 95-105.

Hansen, J., & Reidenbach, M. (2012). Wave and tidally driven flows in eelgrass beds and their effect on sediment suspension. *Marine Ecology Progress Series*, *448*, 271–287. https://doi.org/10.3354/meps09225

Hansen, J. C. R., & Reidenbach, M. A. (2013). Seasonal Growth and Senescence of a *Zostera marina* Seagrass Meadow Alters Wave-Dominated Flow and Sediment Suspension Within a Coastal Bay. *Estuaries and Coasts*, *36*(6), 1099–1114. https://doi.org/10.1007/s12237-013-9620-5

Holling, C. S. (1973). Resilience and stability of ecological systems. *Annual Review of Ecology and Systematics*, *4*(1), 1-23.

Horton, R. M., Mankin, J. S., Lesk, C., Coffel, E., & Raymond, C. (2016). A Review of Recent Advances in Research on Extreme Heat Events. *Current Climate Change Reports*, *2*(4), 242–259. https://doi.org/10.1007/s40641-016-0042-x

Ives, A. R., & Carpenter, S. R. (2007). Stability and Diversity of Ecosystems. *Science*, *317*(5834), 58–62. https://doi.org/10.1126/science.1133258

Jarvis, J., Moore, K., & Kenworthy, W. (2012). Characterization and ecological implication of

eelgrass life history strategies near the species' southern limit in the western North Atlantic. *Marine Ecology Progress Series*, *444*, 43–56. https://doi.org/10.3354/meps09428

Lundquist, C. J., Jones, T. C., Parkes, S. M., & Bulmer, R. H. (2018). Changes in benthic community structure and sediment characteristics after natural recolonisation of the seagrass *Zostera muelleri*. *Scientific Reports*, *8*(1), 13250. https://doi.org/10.1038/s41598-018-31398-2

Macreadie, P. I., York, P. H., & Sherman, C. D. H. (2014). Resilience of *Zostera muelleri* seagrass to small-scale disturbances: The relative importance of asexual versus sexual recovery. *Ecology and Evolution*, *4*(4), 450–461. https://doi.org/10.1002/ece3.933

McGlathery, K., Reynolds, L., Cole, L., Orth, R., Marion, S., & Schwarzschild, A. (2012). Recovery trajectories during state change from bare sediment to eelgrass dominance. *Marine Ecology Progress Series*, *448*, 209–221. https://doi.org/10.3354/meps09574

McGlathery, K., Reidenbach, M., D'Odorico, P., Fagherazzi, S., Pace, M., & Porter, J. (2013). Nonlinear Dynamics and Alternative Stable States in Shallow Coastal Systems. *Oceanography*, *26*(3), 220–231. https://doi.org/10.5670/oceanog.2013.66

McKenzie, L. J., Nordlund, L. M., Jones, B. L., Cullen-Unsworth, L. C., Roelfsema, C., & Unsworth, R. K. F. (2020). The global distribution of seagrass meadows. *Environmental Research Letters*, *15*(7), 074041. https://doi.org/10.1088/1748-9326/ab7d06

Nahlik, A. M., & Fennessy, M. S. (2016). Carbon storage in US wetlands. *Nature Communications*, *7*(1), 1-9.

Neckles, H., Short, F., Barker, S., & Kopp, B. (2005). Disturbance of eelgrass *Zostera marina* by commercial mussel *Mytilus edulis* harvesting in Maine: Dragging impacts and habitat recovery. *Marine Ecology Progress Series*, *285*, 57–73. https://doi.org/10.3354/meps285057

Oliver, E. C. J., Donat, M. G., Burrows, M. T., Moore, P. J., Smale, D. A., Alexander, L. V., Benthuysen, J. A., Feng, M., Sen Gupta, A., Hobday, A. J., Holbrook, N. J., Perkins-Kirkpatrick, S. E., Scannell, H. A., Straub, S. C., & Wernberg, T. (2018). Longer and more frequent marine heatwaves over the past century. *Nature Communications*, *9*(1), 1324. https://doi.org/10.1038/s41467-018-03732-9

Oreska, M. P. J., McGlathery, K. J., Aoki, L. R., Berger, A. C., Berg, P., & Mullins, L. (2020). The greenhouse gas offset potential from seagrass restoration. *Scientific Reports*, *10*(1), 7325. https://doi.org/10.1038/s41598-020-64094-1

Orth, R. J., Luckenbach, M., & Moore, K. A. (1994). Seed dispersal in a marine macrophyte: implications for colonization and restoration. *Ecology*, *75*(7), 1927-1939.

Orth, R., Moore, K., Marion, S., Wilcox, D., & Parrish, D. (2012). Seed addition facilitates eelgrass recovery in a coastal bay system. *Marine Ecology Progress Series*, *448*, 177–195. https://doi.org/10.3354/meps09522

Orth, R. J., Lefcheck, J. S., McGlathery, K. S., Aoki, L., Luckenbach, M. W., Moore, K. A., Oreska, M. P. J., Snyder, R., Wilcox, D. J., & Lusk, B. (2020). Restoration of seagrass habitat leads to rapid recovery of coastal ecosystem services. *Science Advances*, *6*(41), eabc6434. https://doi.org/10.1126/sciadv.abc6434

Preen, A. (1995). Impacts of dugong foraging on seagrass habitats: observational and experimental evidence for cultivation grazing. *Marine Ecology Progress Series*, *124*, 201–213. https://doi.org/10.3354/meps124201

Qin, L.-Z., Li, W.-T., Zhang, X., Zhang, P., & Qiao, W. (2016). Recovery of the eelgrass *Zostera marina* following intense Manila clam *Ruditapes philippinarum* harvesting disturbance in China: The role and fate of seedlings. *Aquatic Botany*, *130*, 27–36. https://doi.org/10.1016/j.aquabot.2016.01.002

Rasheed, M. A. (1999). Recovery of experimentally created gaps within a tropical *Zostera capricorni* (Aschers.) seagrass meadow, Queensland Australia. *Journal of Experimental Marine Biology and Ecology*, *235*(2), 183–200. https://doi.org/10.1016/S0022-0981(98)00158-0

Safak, I., Wiberg, P. L., Richardson, D. L., & Kurum, M. O. (2015). Controls on residence time and exchange in a system of shallow coastal bays. *Continental Shelf Research*, *97*, 7–20. https://doi.org/10.1016/j.csr.2015.01.009

Sallenger, A. H., Doran, K. S., & Howd, P. A. (2012). Hotspot of accelerated sea-level rise on the Atlantic coast of North America. *Nature Climate Change*, *2*(12), 884–888. https://doi.org/10.1038/nclimate1597

Scheffer, M., Rinaldi, S., Gragnani, A., Mur, L. R. & van Nes, E. H. (1997). On the Dominance of Filamentous Cyanobacteria in Shallow, Turbid Lakes. *Ecology*, *78*(1), 272-282.

Scheffer, M., Carpenter, S. R., Dakos, V., & van Nes, E. H. (2015). Generic Indicators of Ecological Resilience: Inferring the Chance of a Critical Transition. *Annual Review of Ecology, Evolution, and Systematics*, *46*(1), 145–167. https://doi.org/10.1146/annurev-ecolsys-112414-054242

Short, F. T. (1983). The response of interstitial ammonium in eelgrass (*Zostera marina* L.) beds to environmental perturbations. *Journal of Experimental Marine Biology and Ecology*, *68*(2), 195–208. https://doi.org/10.1016/0022-0981(83)90159-4

Short, F. T., Polidoro, B., Livingstone, S. R., Carpenter, K. E., Bandeira, S., Bujang, J. S., Calumpong, H. P., Carruthers, T. J. B., Coles, R. G., Dennison, W. C., Erftemeijer, P. L. A., Fortes, M. D., Freeman, A. S., Jagtap, T. G., Kamal, A. H. M., Kendrick, G. A.,

Judson Kenworthy, W., La Nafie, Y. A., Nasution, I. M., … Zieman, J. C. (2011). Extinction risk assessment of the world's seagrass species. *Biological Conservation, 144*(7), 1961–1971. https://doi.org/10.1016/j.biocon.2011.04.010

Smale, D. A., Wernberg, T., Oliver, E. C. J., Thomsen, M., Harvey, B. P., Straub, S. C., Burrows, M. T., Alexander, L. V., Benthuysen, J. A., Donat, M. G., Feng, M., Hobday, A. J., Holbrook, N. J., Perkins-Kirkpatrick, S. E., Scannell, H. A., Sen Gupta, A., Payne, B. L., & Moore, P. J. (2019). Marine heatwaves threaten global biodiversity and the provision of ecosystem services. *Nature Climate Change*, *9*(4), 306–312. https://doi.org/10.1038/s41558-019-0412-1

Smith, T., York, P., Macreadie, P., Keough, M., Ross, D., & Sherman, C. (2016). Recovery pathways from small-scale disturbance in a temperate Australian seagrass. *Marine Ecology Progress Series*, *542*, 97–108. https://doi.org/10.3354/meps11531

Sohn, J. A., Saha, S., & Bauhus, J. (2016). Potential of forest thinning to mitigate drought stress: A meta-analysis. *Forest Ecology and Management*, *380*, 261–273. https://doi.org/10.1016/j.foreco.2016.07.046

Uhrin, A. V., Kenworthy, W. J., & Fonseca, M. S. (2011). Understanding uncertainty in seagrass injury recovery: An information-theoretic approach. *Ecological Applications*, *21*(4), 1365–1379. https://doi.org/10.1890/10-0761.1

Vaudrey, J. M. P., Kremer, J. N., Branco, B. F., & Short, F. T. (2010). Eelgrass recovery after nutrient enrichment reversal. *Aquatic Botany*, *93*(4), 237–243. https://doi.org/10.1016/j.aquabot.2010.08.005

Waycott, M., Duarte, C. M., Carruthers, T. J. B., Orth, R. J., Dennison, W. C., Olyarnik, S., Calladine, A., Fourqurean, J. W., Heck, K. L., Hughes, A. R., Kendrick, G. A., Kenworthy, W. J., Short, F. T., & Williams, S. L. (2009). Accelerating loss of seagrasses across the globe threatens coastal ecosystems. *Proceedings of the National Academy of Sciences*, *106*(30), 12377–12381. https://doi.org/10.1073/pnas.0905620106

Webster, P. J., Holland, G. J., Curry, J. A., & Chang, H.-R. (2005). Changes in Tropical Cyclone Number, Duration, and Intensity in a Warming Environment. *Science*, *309*(5742), 1844–1846. https://doi.org/10.1126/science.1116448

Wernberg, T., Bennett, S., Babcock, R. C., de Bettignies, T., Cure, K., Depczynski, M., Dufois, F., Fromont, J., Fulton, C. J., Hovey, R. K., Harvey, E. S., Holmes, T. H., Kendrick, G. A., Radford, B., Santana-Garcon, J., Saunders, B. J., Smale, D. A., Thomsen, M. S., Tuckett, C. A., … Wilson, S. (2016). Climate-driven regime shift of a temperate marine ecosystem. *Science*, *353*(6295), 169–172. https://doi.org/10.1126/science.aad8745

Williams, S. (1988). Disturbance and recovery of a deep-water Caribbean seagrass bed. *Marine Ecology Progress Series*, *42*, 63–71. https://doi.org/10.3354/meps042063

Zampieri, M. (2021). Reconciling the ecological and engineering definitions of resilience. *Ecosphere*, *12*(2). https://doi.org/10.1002/ecs2.3375

Zhu, Q., Wiberg, P. L., & McGlathery, K. J. (2022). Seasonal growth and senescence of seagrass alters sediment accumulation rates and carbon burial in a coastal lagoon. *Limnology and Oceanography*, *67*(9), 1931–1942. https://doi.org/10.1002/lno.12178

Zieman, J. C. (1976). The ecological effects of physical damage from motor boats on turtle grass beds in Southern Florida. *Aquatic Botany*, *2*, 127–139. https://doi.org/10.1016/0304-3770(76)90015-2

Table 5.1 Mean (± SD) site conditions for South Bay, VA, during monthly sampling between 2020-2022 at the central and northern edge locations. Statistical significance (p-value) determined by Welch's t-test.

Variable	Central	Edge	p-value
Salinity (g kg^{-1})	31.8 ± 0.9	31.6 ± 0.8	0.277
Depth (m) [1]	1.3 ± 1.2	1.5 ± 1.2	< 0.001
Water Temperature (^{o}C) [2]	21.2 ± 7.2	20.7 ± 6.9	< 0.001
Dissolved Oxygen saturation (%)	114.5 ± 18.1	138.9 ± 42.1	< 0.001
Turbidity (NTU)	5.7 ± 2.2	12.4 ± 7.7	< 0.001
Total Suspended Solids (mg L^{-1})	40.4 ± 10.9	60.6 ± 52.6	< 0.001
Pelagic Chlorophyll-a (µg L^{-1})	2.4 ± 1.5	3.9 ± 3.2	< 0.001
Benthic Chlorophyll-a (mg m^{-2})	39.2 ± 34.9	29 ± 18.4	< 0.001

[1] Mean depth ± mean tidal range for Oct. 14, 2020 – Nov. 10, 2020;

[2] Water temp. from continuous ≤ 1-hour measurements at 20 cm above sediment surface between Jun. 2020 - Oct. 2022

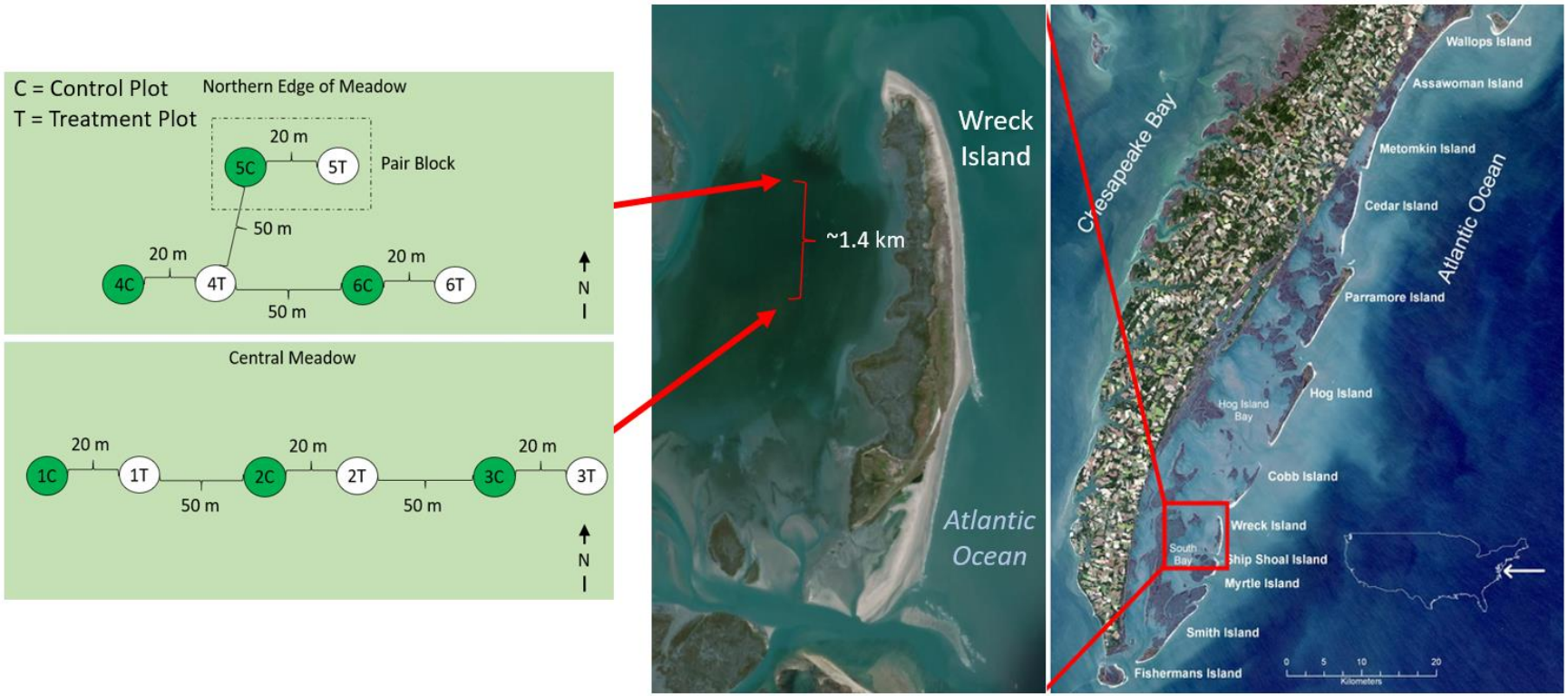

Figure 5.1 Location of the seagrass recovery experiment along with site location and plot layout. Each plot was circular with a 3-meter radius. Paired plots consisted of control (no seagrass removal) and treatment (aboveground seagrass removal), which were spaced 20 meters edge-to-edge, with plot pairs spaced 50 meters edge-to-edge. Differences in layout design were due to water depth, ongoing research in the area, and distance to meadow edge.

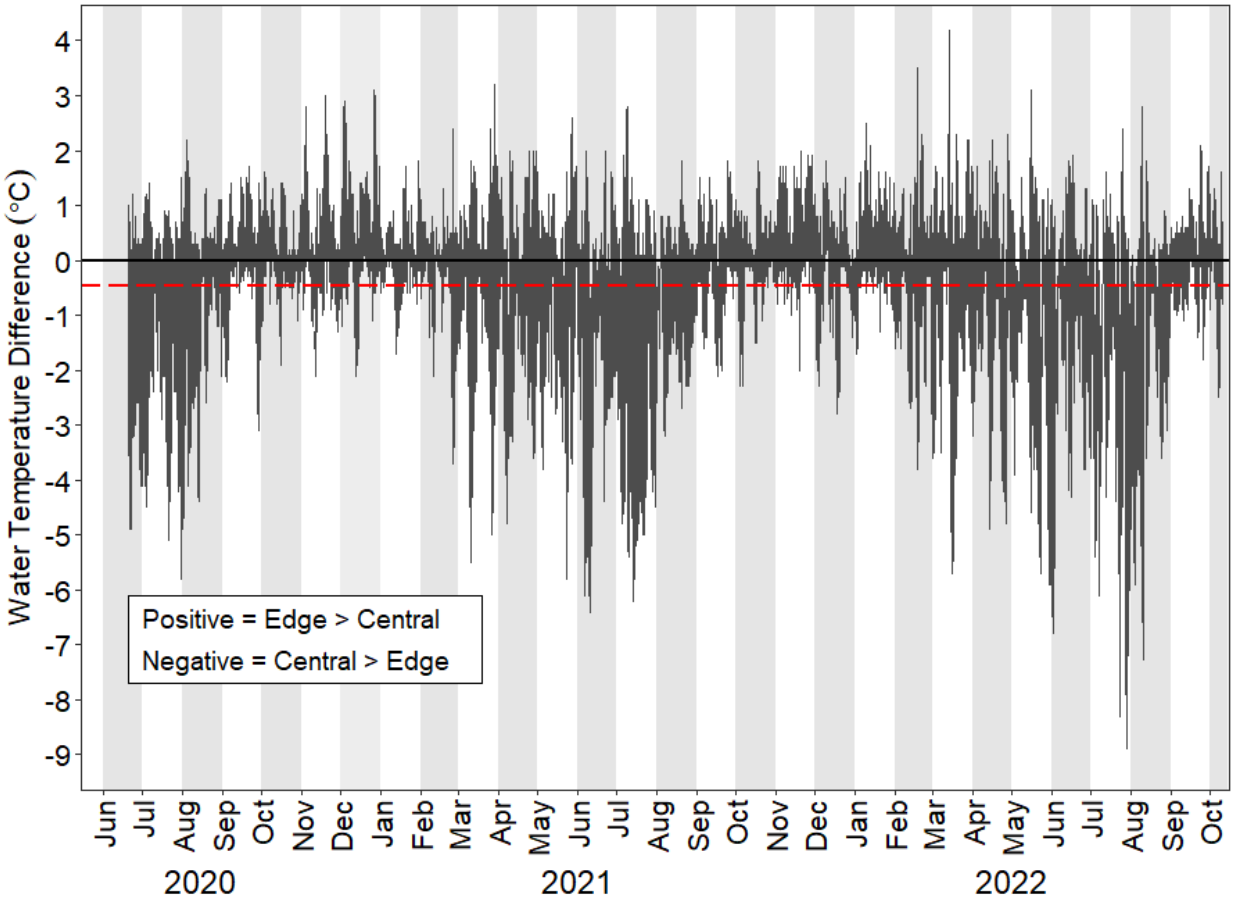

Figure 5.2 High frequency (≤ 1 hour) water temperature difference between central and northern edge meadow locations within South Bay, VA. Water temperature was collected at 15-minute intervals between spring and fall (April-November) and hourly in the winter (December-March). The red dashed line indicates the overall mean difference. Note strong differences in summer with higher temperatures at the central location.

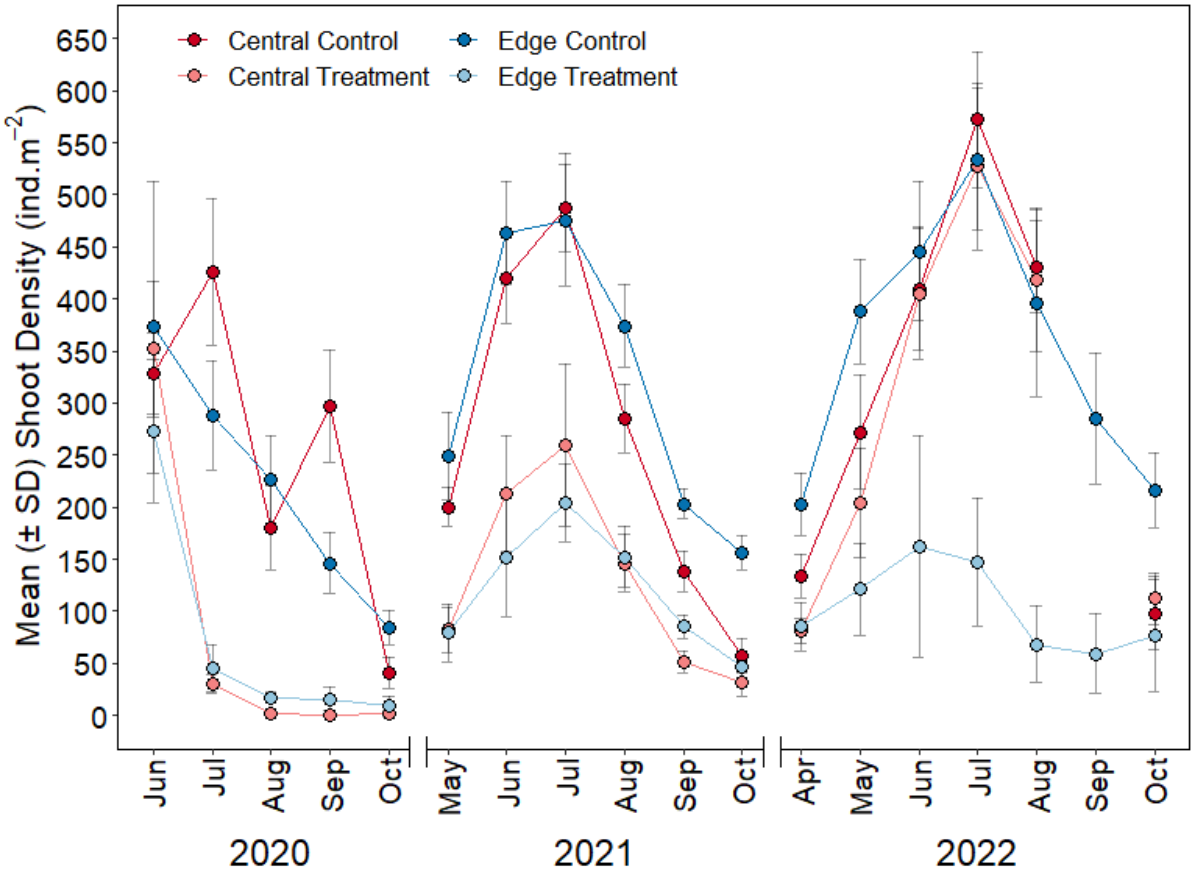

Figure 5.3 Mean (± SD) shoot density for control and treatment groups among the central (red) and northern edge (blue) locations of the South Bay, VA, seagrass meadow. Removal of seagrass from the treatment plots occurred on June 5, 2022 after the first sampling.

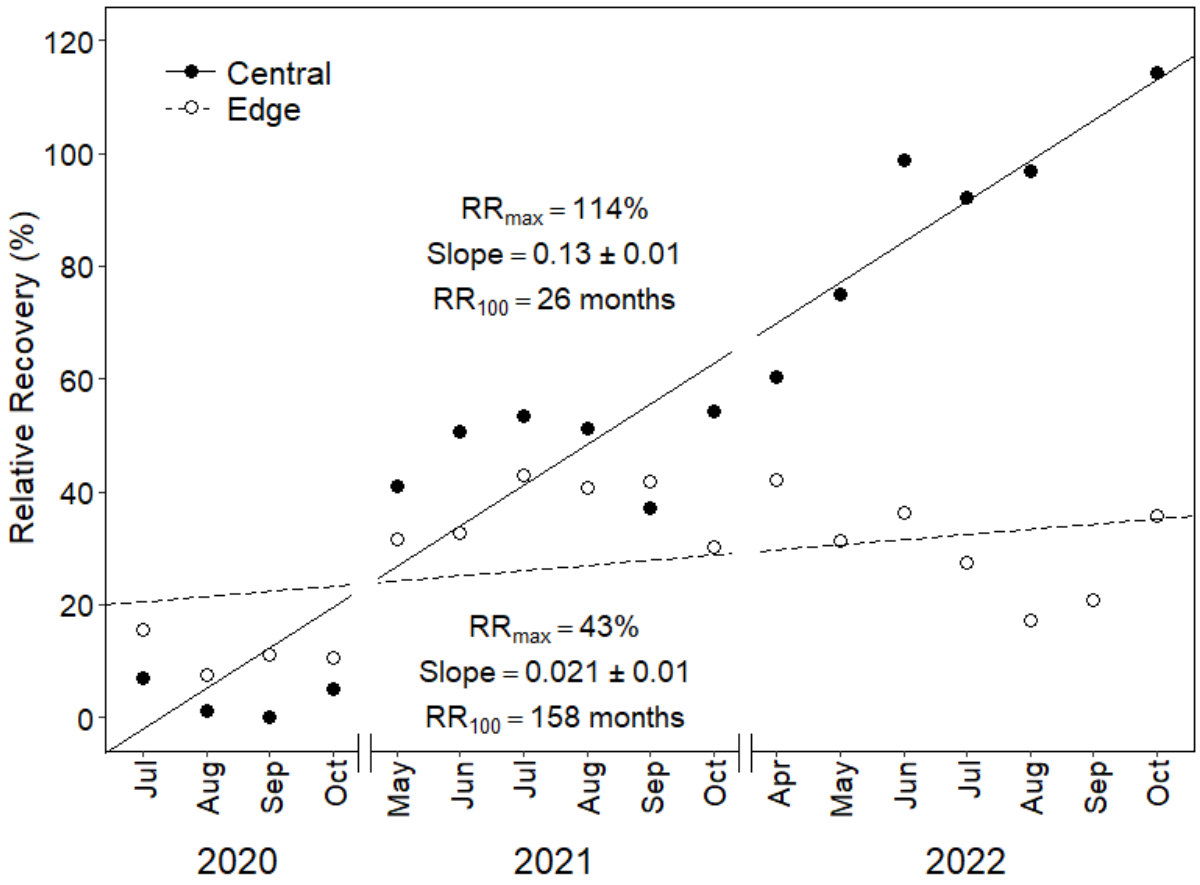

Figure 5.4 Relative recovery (RR) of the treatment groups for the central (solid dots) and northern edge (open points) locations. The solid line represents the linear recovery trend for the central sites, while the dashed line represents the linear recovery trend for the edge sites.

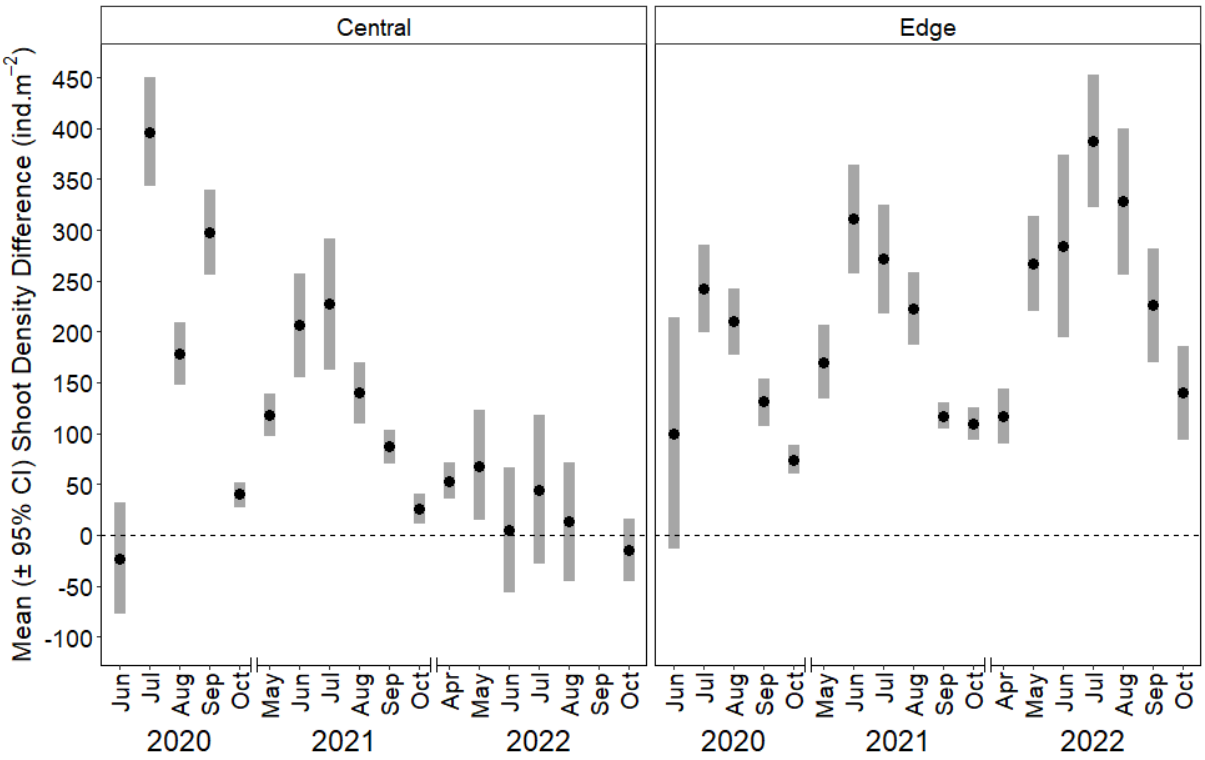

Figure 5.5 Mean (± 95% confidence interval) shoot density difference between control and treatment groups for the central (left) and northern edge (right) locations. The first sample in June 2020 was taken before removal occurred.

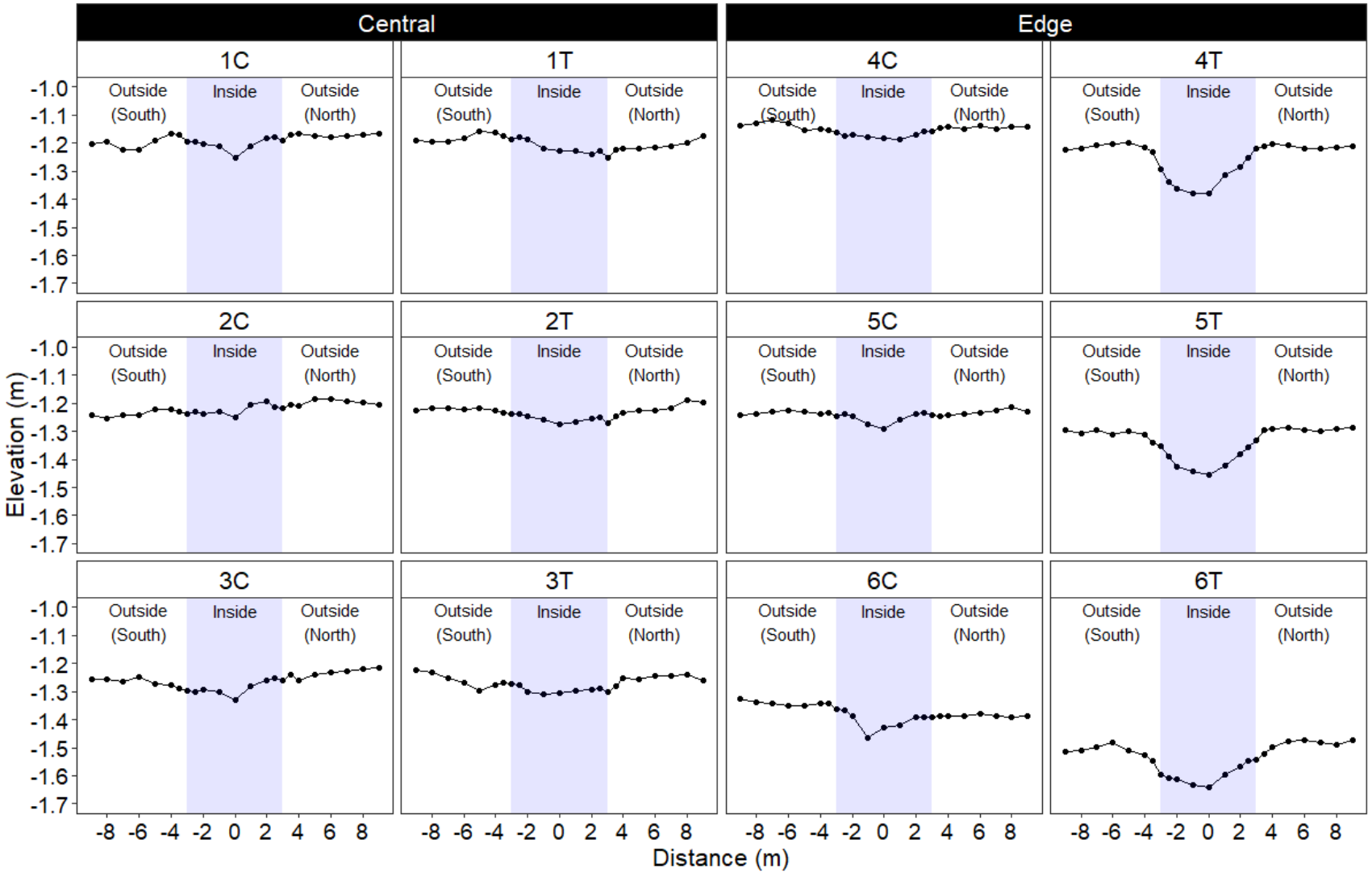

Figure 5.6 Bed elevation of control and treatment groups between sites relative to NAVD88 vertical datum. Sites 1-3 are from central South Bay, and sites 4-6 are from the northern edge. The C indicates control groups, and T represents treatment groups where seagrass was removed. Measurements were collected along a N-S transect, with the shaded areas representing data from within the plots and non-shaded areas representing areas outside the plots. Note the depressions in the northern edge treatment sites.

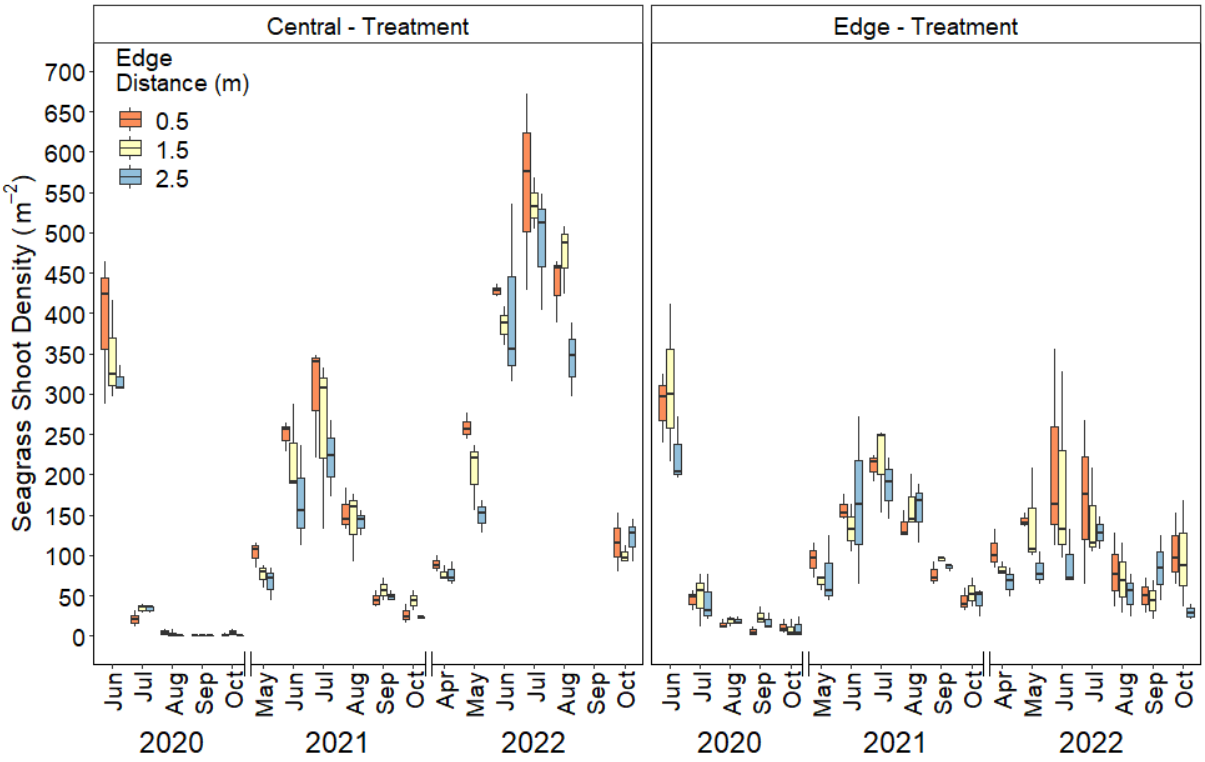

Figure 5.7 Seagrass shoot density boxplots as a function of distance from treatment plot edge for the central (left) and northern edge (right) meadow locations.

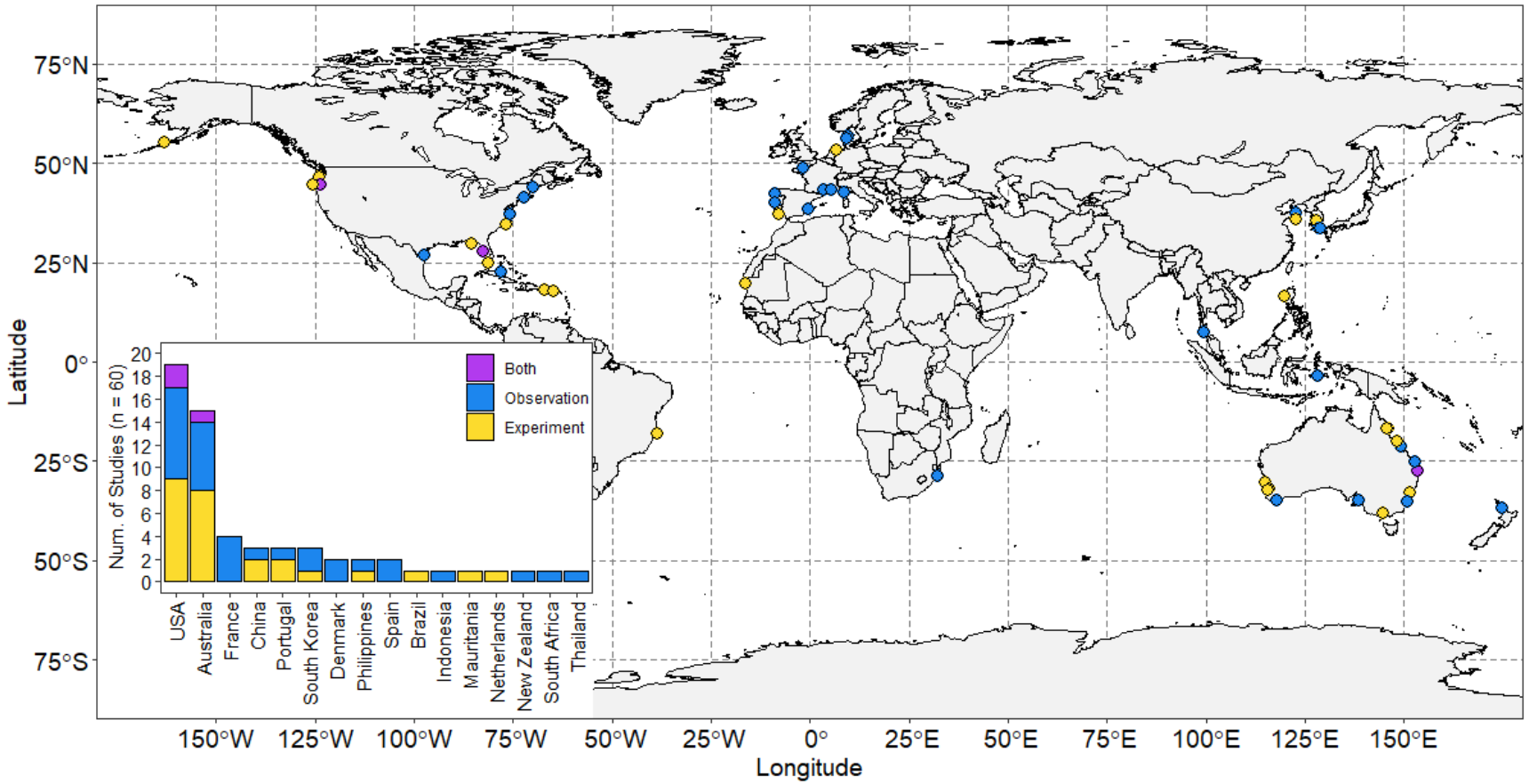

Figure 5.8 Seagrass disturbance and recovery study locations and distribution (inset) among countries.

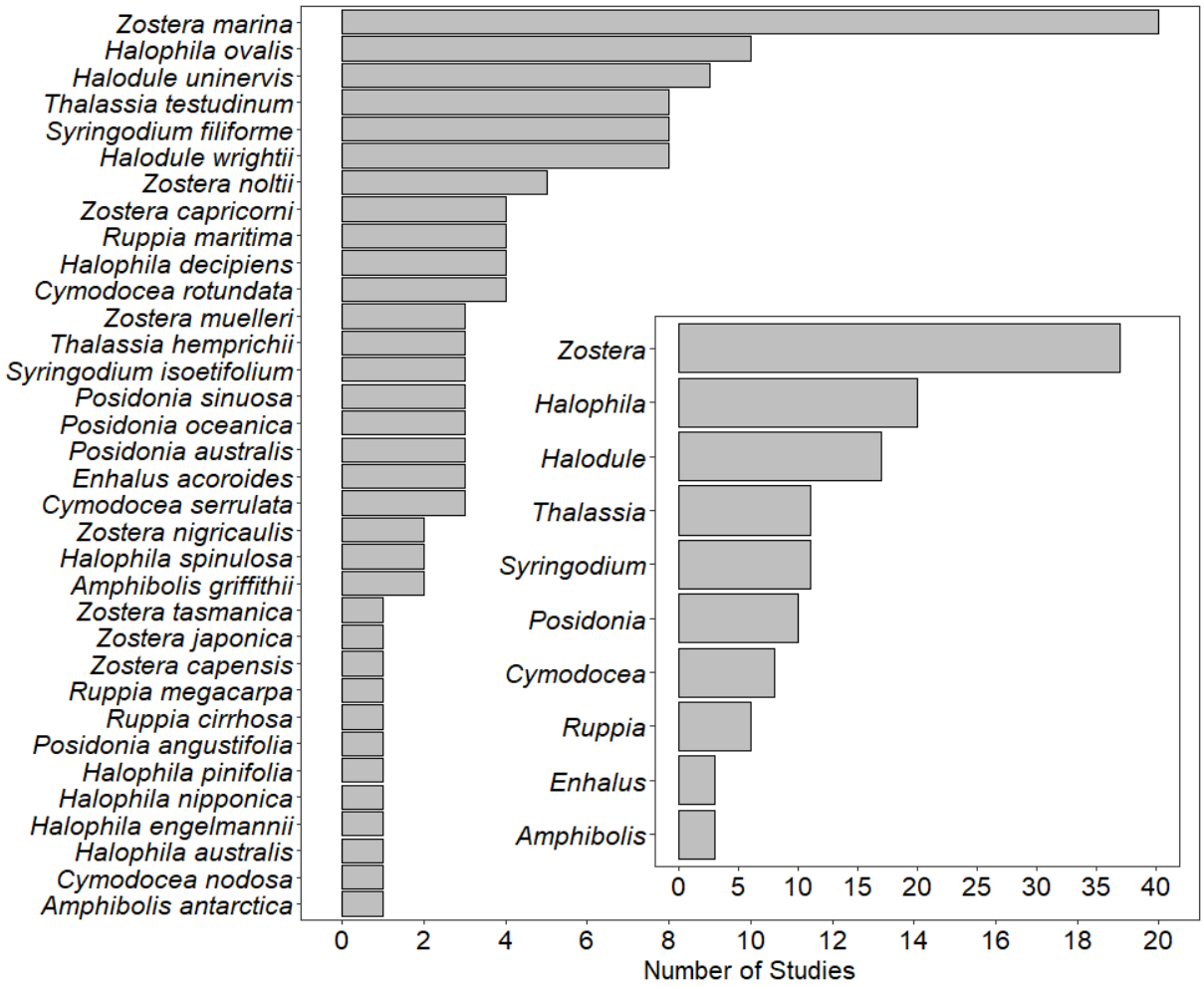

Figure 5.9 Total number of studies where seagrass species were present within the study meadow. The inset figure represents the same information with respect to seagrass genus.

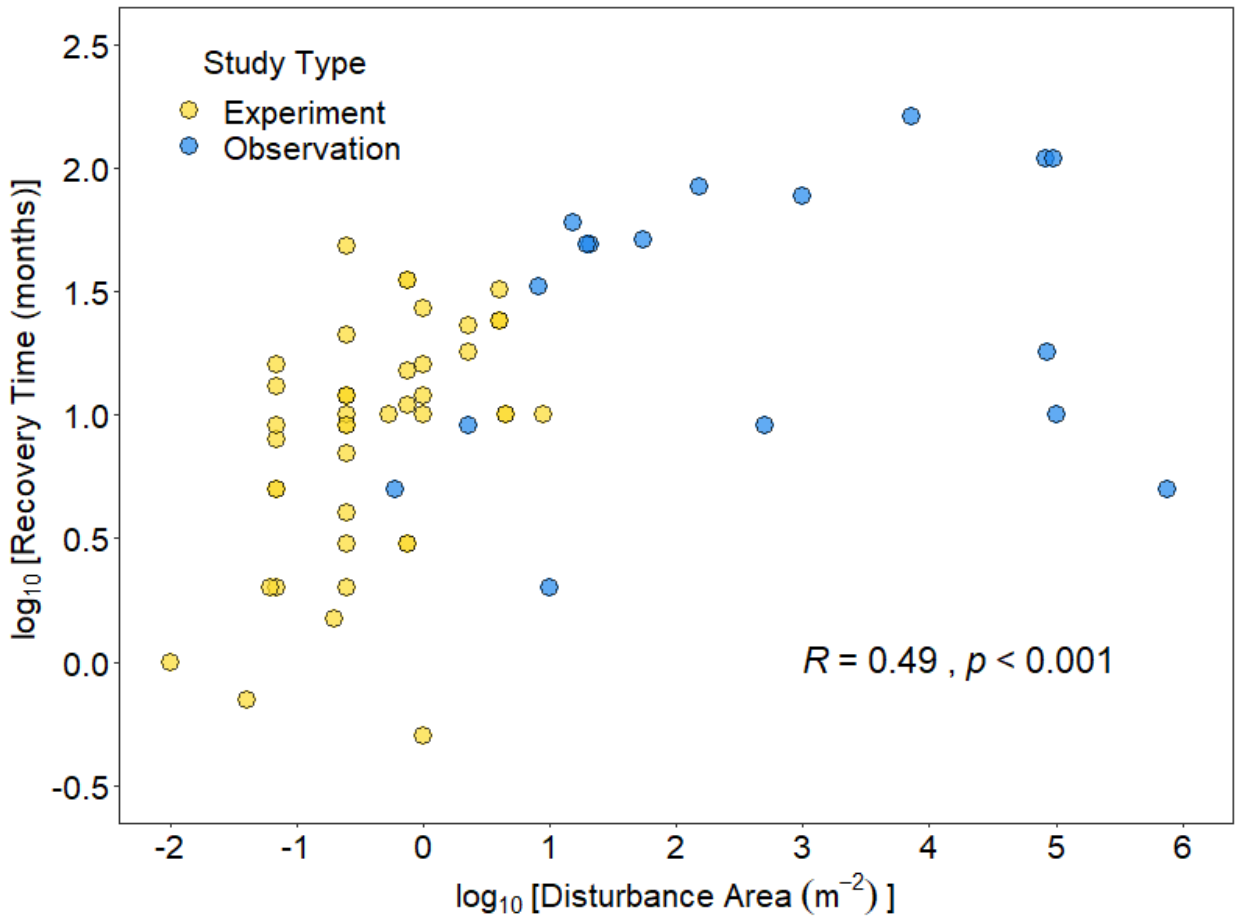

Figure 5.10 Correlation of log transformed recovery time as a function of log transformed disturbance area.

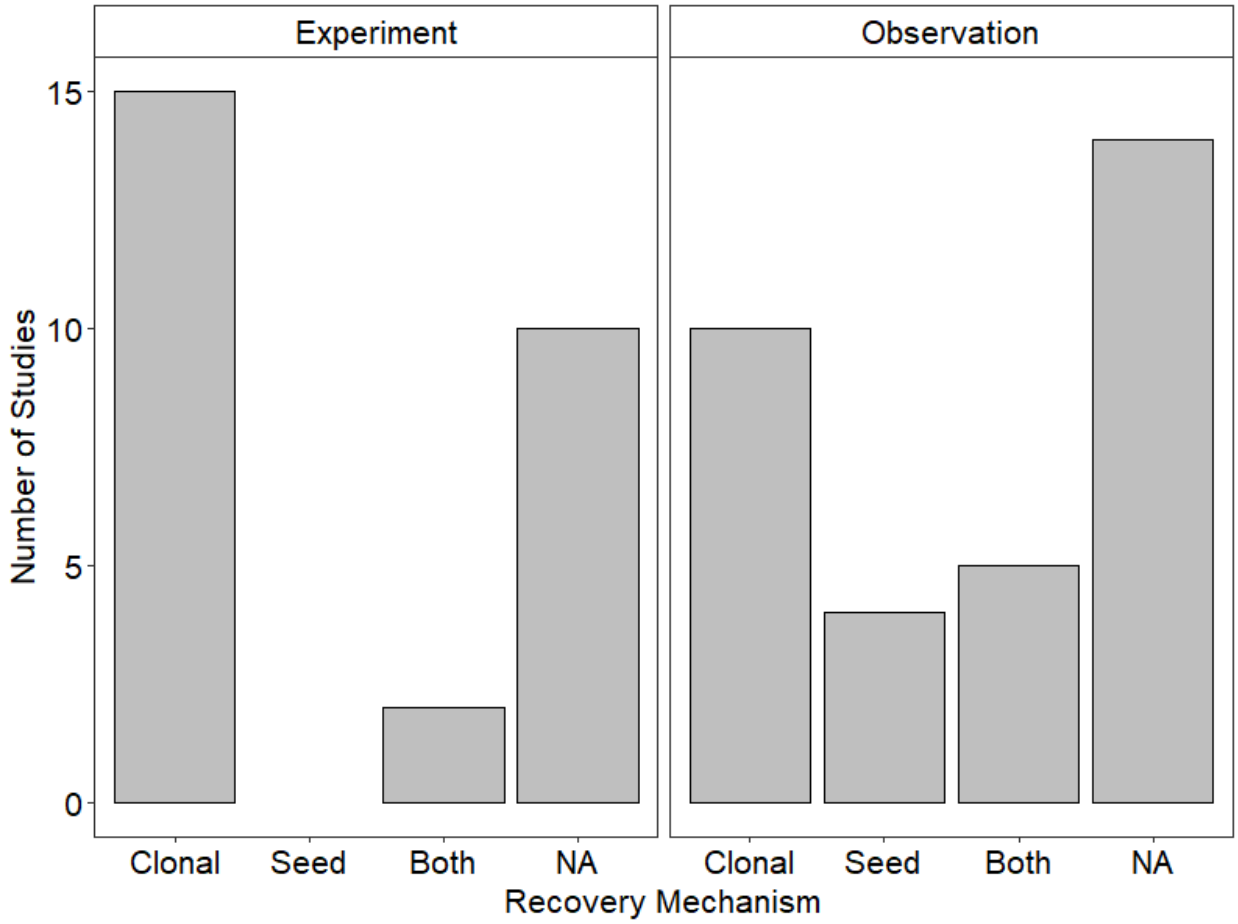

Figure 5.11 Recovery mechanism for experimental (left) and observational (right) studies of seagrass recovery. "NA" indicates recovery mechanism was not considered or not reported.

Chapter 6: Conclusions

Similar to heatwave trends in the atmosphere and global ocean, riverine heatwaves have increased in frequency across a broad geographic range in recent decades (Chapter 2). Given projected increases in atmospheric temperature (Meehl et al. 2007; Wuebbles et al. 2017) and low discharge conditions (Milly et al. 2005, van Vliet 2013), it is likely that the increasing trend in riverine heatwaves will continue. As such, inland water temperature monitoring will be essential to identify and prioritize restoration of waterways that are exceeding water temperature standards and provide protection for those currently meeting standards (Palmer et al. 2009). Additionally, the most extreme riverine heatwaves occurred during winter (Nov.-Feb.) suggesting that ecosystem respiration, a temperature dependent process that consumes dissolved oxygen and produces CO_2, may increase during a riverine heatwave while primary production remains light limited, at least in the case of turbid, temperate rivers. Future studies should consider if ecosystem metabolism (i.e., primary production and respiration) is affected by riverine heatwaves. Furthermore, many physiological processes are temperature dependent, as such increasing riverine heatwaves may reduce cold water habitat and increase the successful establishment of invasive species (Salis et al. 2023). Future studies should consider how watershed land cover change impacts downstream water temperature, as well as how riverine heatwaves impact species distribution. Nonetheless, destructive impacts on ecosystems resulting from heatwaves in the atmosphere and global ocean are under investigation with new results emerging (Breshears et al. 2021; Smale et al. 2019). Similar investigations of the effects of heatwaves on rivers and streams are warranted.

Unlike heatwaves in the atmosphere, global ocean, and rivers, trends in heatwave metrics have remained unchanged across a broad set of estuaries (Chapter 3). This is also in contrast to a

similar study of heatwaves in a single estuary, Chesapeake Bay, which had a significant increase in heatwave frequency, annual heatwave days, and annual cumulative intensity (Mazzini and Pianca 2022). Differences in estuarine heatwave trend results may be attributed to the greater number of Chesapeake Bay sites used in Mazzini and Pianca (2022), longer time series, the type of low-pass filter used to remove tidal and diurnal fluctuations from the time series, water temperature logger depth, and/or the type of regression analysis used. Nonetheless, annualized average heatwave metrics for Chesapeake Bay were similar among studies. Regardless of how estuarine heatwave trends are changing, heatwaves regularly occur in estuaries and there remains limited understanding of their impacts relative to marine systems. As many organisms use habitat across the river-estuary-coastal ocean continuum and are sensitive to seasonal extremes in these different locations, future studies should consider the community-level impacts of heatwaves within these valuable ecosystems, as well as how heatwaves propagate horizontally between rivers, estuaries, and the coastal ocean. These studies will aid resource managers working to restore aquatic ecosystems and conserve fisheries, along with improve understanding of cross-system heatwaves that will help to make their future predictability possible.

Similar to how atmospheric conditions can promote marine heatwaves (Schlegel et al. 2017; Oliver et al. 2018; Cook et al. 2022), a sediment heatwave can be induced by boundary layer conditions with the overlying water column (Chapter 4). The June 2015 MHW associated with a 90% die-off of seagrass, 20% loss of sediment carbon, and meadow metabolic conversion to net heterotrophy (Berger et al. 2020; Aoki et al. 2021) had a co-occurring sediment heatwave at a depth where seagrass rhizomes are most abundant. The occurrence of heatwaves within vegetated sediments represents a novel disturbance to aquatic ecosystems that likely reduces available thermal refugia for benthic organisms (Zhou et al. 2023) and threatens seagrass blue

carbon sequestration potential. Future studies should consider how deep heatwaves penetrate into seagrass sediments, along with the community and ecosystem-level impacts of sediment heatwaves. While this study provided evidence of sediment heatwaves at a depth of 5 cm, it remains unclear how deep heatwaves penetrate into sediments. The impact of sediment heatwaves on organic carbon remineralization and hydrogen sulfide (H_2S) production are important topics for further work. At the community level, the composition and abundance of benthic macroinvertebrate will likely become narrowed as community diversity and abundance shifts toward heat-tolerant organisms as sediment heatwave frequency continues increasing. Given the frequent co-occurrence of sediment and marine heatwaves, as well as both increasing in frequency, it is likely that the destructive and lasting effects associated with marine heatwaves has been and will continue to occur in South Bays' sedimentary ecosystem. The coupling of water and sediment heatwaves indicates water temperature can be used as a proxy for sediment heatwaves facilitating research campaigns on sediment processes when water column conditions signal an event underway.

While MHWs can disturb seagrass meadows, recovery from these disturbances is driven by hydrodynamic conditions (Chapter 5). This result is apparent across large disturbance gaps whereas small gaps have a negligible impact on hydrodynamic conditions (El Allaoui et al. 2016). Nevertheless, seagrass meadow ecosystems are resilient to disturbances large and small, suggestive of a broad and deep stability landscape that sustains seagrass state once established. However, there remains a limited understanding of the stability landscape of shallow subtidal bare sediments that might otherwise support seagrass and how these habitats interact with seagrass habitats following state shifts (McGlathery et al. 2013). A better understanding of the

stability landscape of shallow subtidal bare sediments would aid resource managers seeking to restore seagrass ecosystems and the valuable services they provide.

The future impact of heatwaves on species and ecosystems will depend in part on how heatwaves are defined. Many review papers have considered heatwave definitions and the data used to identify them in the atmosphere and in aquatic settings (Perkins and Alexander 2013; Smith et al. 2013; Oliver et al. 2021). This dissertation utilized long-term, daily mean temperatures and seasonally varying climatological 90th percentile thresholds from a fixed baseline period to define heatwaves in the atmosphere, rivers, estuaries, and coastal sediments, consistent with similar studies of the coastal and open ocean. Other heatwave definitions may be useful depending on research objectives such as using a flat absolute temperature threshold when studying specific species. Additionally, a seasonally varying threshold from a moving baseline may be useful when considering future heatwave variability as temperature trends are assigned to the moving climatology rather than to the temperature anomaly (Oliver et al. 2021). As the study of heatwaves in aquatic ecosystems advances, careful consideration of study objectives should be considered when selecting a heatwave definition.

This dissertation advanced the study of heatwave disturbances in aquatic ecosystems by conducting novel heatwave analyses for rivers, estuaries, and coastal sediments. Furthermore, by monitoring the recovery of the most extensive experimental seagrass disturbance to date and synthesizing related studies on seagrass recovery, this dissertation has also contributed to understanding coastal ecosystem stability. Chapter 2 established that riverine heatwaves have increased in frequency throughout the U.S. and that the annual mean number of heatwave days doubled between 1996-2021. These increases were driven, in part, by rising atmospheric temperature and were associated with low discharge conditions. Chapter 3 examined heatwaves

in estuaries and provided evidence that estuarine heatwaves regularly co-occur with atmospheric heatwaves, and at times with deleterious water quality conditions such as extreme low dissolved oxygen, and acidic pH events. Chapter 4 assessed heatwaves in a new medium, vegetated coastal sediments; and confirmed that similar to atmospheric conditions inducing marine heatwaves, that heatwaves in the water column can induce surficial sediment heatwaves. Chapter 5 offered support for seagrass meadow resilience to heatwave-like disturbances but exposed how recovery may be sensitive to hydrodynamic stress depending on disturbance area and position within a meadow. Additionally, chapter 5 demonstrated that 47% of known seagrass species have been included in English language disturbance-recovery studies, that the majority of studies have occurred in monocultures of the genus *Zostera* indicating a need for research on other species and seagrass habitats. Experimental disturbances of seagrass are often conducted on small spatial scales that likely emphasize lateral clonal growth leading to recovery. My larger scale experiment along with natural disturbances investigated in prior research indicate the significance of hydrodynamic factors on recovery rates. Collectively, the results of this dissertation demonstrate how climate change is manifesting in aquatic ecosystems and how one aquatic ecosystem, seagrass meadows, recovers following disturbance.

References

Aoki, L. R., McGlathery, K. J., Wiberg, P. L., Oreska, M. P. J., Berger, A. C., Berg, P., & Orth, R. J. (2021). Seagrass Recovery Following Marine Heat Wave Influences Sediment Carbon Stocks. *Frontiers in Marine Science*, *7*, 576784. https://doi.org/10.3389/fmars.2020.576784

Berger, A. C., Berg, P., McGlathery, K. J., & Delgard, M. L. (2020). Long-term trends and resilience of seagrass metabolism: A decadal aquatic eddy covariance study. *Limnology and Oceanography*, *65*(7), 1423–1438. https://doi.org/10.1002/lno.11397

Breshears, D. D., Fontaine, J. B., Ruthrof, K. X., Field, J. P., Feng, X., Burger, J. R., ... & Hardy, G. E. S. J. (2021). Underappreciated plant vulnerabilities to heat waves. *New Phytologist*, *231*(1), 32-39.

Cook, F., Smith, R. O., Roughan, M., Cullen, N. J., Shears, N., & Bowen, M. (2022). Marine heatwaves in shallow coastal ecosystems are coupled with the atmosphere: Insights from half a century of daily in situ temperature records. *Frontiers in Climate*, 207.

El Allaoui, N., Serra, T., Colomer, J., Soler, M., Casamitjana, X., & Oldham, C. (2016). Interactions between Fragmented Seagrass Canopies and the Local Hydrodynamics. *PLoS One*, *11*(5), e0156264. https://doi.org/10.1371/journal.pone.0156264

Mazzini, P. L., & Pianca, C. (2022). Marine heatwaves in the Chesapeake Bay. *Frontiers in Marine Science*, 8, 1968.

McGlathery, K., Reidenbach, M., D'Odorico, P., Fagherazzi, S., Pace, M., & Porter, J. (2013). Nonlinear Dynamics and Alternative Stable States in Shallow Coastal Systems. *Oceanography*, *26*(3), 220–231. https://doi.org/10.5670/oceanog.2013.66

Meehl, G.A., T.F. Stocker, W.D. Collins, P. Friedlingstein, A.T. Gaye, J.M. Gregory, A. Kitoh, R. Knutti, J.M. Murphy, A. Noda, S.C.B. Raper, I.G. Watterson, A.J. Weaver and Z.-C. Zhao, (2007) Global Climate Projections. In: Climate Change 2007: The Physical Science Basis. Contribution of Working Group I to the Fourth Assessment Report of the Intergovernmental Panel on Climate Change [Solomon, S., D. Qin, M. Manning, Z. Chen, M. Marquis, K.B. Averyt, M. Tignor and H.L. Miller (eds.)]. Cambridge University Press, Cambridge, United Kingdom and New York, NY, USA.

Milly, P. C. D., Dunne, K. A., and Vecchia, A. V. (2005). Global pattern of trends in streamflow and water availability in a changing climate. *Nature, 438*(7066), 347–350. https://doi.org/10.1038/nature04312

Oliver, E. C. J., Donat, M. G., Burrows, M. T., Moore, P. J., Smale, D. A., Alexander, L. V., Benthuysen, J. A., Feng, M., Sen Gupta, A., Hobday, A. J., Holbrook, N. J., Perkins-Kirkpatrick, S. E., Scannell, H. A., Straub, S. C., & Wernberg, T. (2018). Longer and more frequent marine heatwaves over the past century. *Nature Communications*, *9*(1),

1324. https://doi.org/10.1038/s41467-018-03732-9

Oliver, E. C., Benthuysen, J. A., Darmaraki, S., Donat, M. G., Hobday, A. J., Holbrook, N. J., ... & Sen Gupta, A. (2021). Marine heatwaves. *Annual Review of Marine Science, 13*, 313-342.

Palmer, M. A., Lettenmaier, D. P., Poff, N. L., Postel, S. L., Richter, B., and Warner, R. (2009). Climate Change and River Ecosystems: Protection and Adaptation Options. *Environmental Management, 44*(6), 1053–1068. https://doi.org/10.1007/s00267-009-9329-1

Perkins, S. E., & Alexander, L. V. (2013). On the measurement of heat waves. *Journal of Climate*, *26*(13), 4500-4517.

Salis, R. K., Brennan, G. L., and Hansson, L. A. (2023). Successful invasions to freshwater systems double with climate warming. *Limnology and Oceanography*. https://doi.org/10.1002/lno.12323

Schlegel, R. W., Oliver, E. C., Perkins-Kirkpatrick, S., Kruger, A., & Smit, A. J. (2017). Predominant atmospheric and oceanic patterns during coastal marine heatwaves. *Frontiers in Marine Science, 4*, 323.

Smale, D. A., Wernberg, T., Oliver, E. C. J., Thomsen, M., Harvey, B. P., Straub, S. C., Burrows, M. T., Alexander, L. V., Benthuysen, J. A., Donat, M. G., Feng, M., Hobday, A. J., Holbrook, N. J., Perkins-Kirkpatrick, S. E., Scannell, H. A., Sen Gupta, A., Payne, B. L., & Moore, P. J. (2019). Marine heatwaves threaten global biodiversity and the provision of ecosystem services. *Nature Climate Change*, *9*(4), 306–312. https://doi.org/10.1038/s41558-019-0412-1

Smith, T. T., Zaitchik, B. F., & Gohlke, J. M. (2013). Heat waves in the United States: definitions, patterns and trends. *Climatic Change, 118*, 811-825.

van Vliet, M. T. H., Franssen, W. H. P., Yearsley, J. R., Ludwig, F., Haddeland, I., Lettenmaier, D. P., and Kabat, P. (2013). Global river discharge and water temperature under climate change. *Global Environmental Change*, *23*(2), 450–464. https://doi.org/10.1016/j.gloenvcha.2012.11.002

Wuebbles, D. J., Fahey, D. W., Hibbard, K. A., DeAngelo, B., Doherty, S., Hayhoe, K., Horton, R., Kossin, J. P., Taylor, P. C., Waple, A. M., and Yohe, C. P. (2017). *Executive summary. Climate Science Special Report: Fourth National Climate Assessment, Volume I.* U.S. Global Change Research Program. https://doi.org/10.7930/J0DJ5CTG

Zhou, Z., Steiner, N., Fivash, G. S., Cozzoli, F., Blok, D. B., van Ijzerloo, L., van Dalen, J., Ysebaert, T., Walles, B., Bouma, T. J. (2023). Temporal dynamics of heatwaves are key drivers of sediment mixing by bioturbators. *Limnology and Oceanography*. https://doi.org/10.1002/lno.12332

Appendix 1: Supplemental Information to Chapter 2

Dams are listed in the National Inventory of Dams (NID) if 1) their failure would cause loss of human life, economic loss, environmental damage, or disruption of lifeline facilities, 2) are ≥ 25 feet in height and ≥ 15 acre-feet in storage, or 3) ≥ 50 acre feet storage and ≥ 6 feet in height. Visual inspection of sites was warranted as the NID may exclude low head dams or historical mill dams.

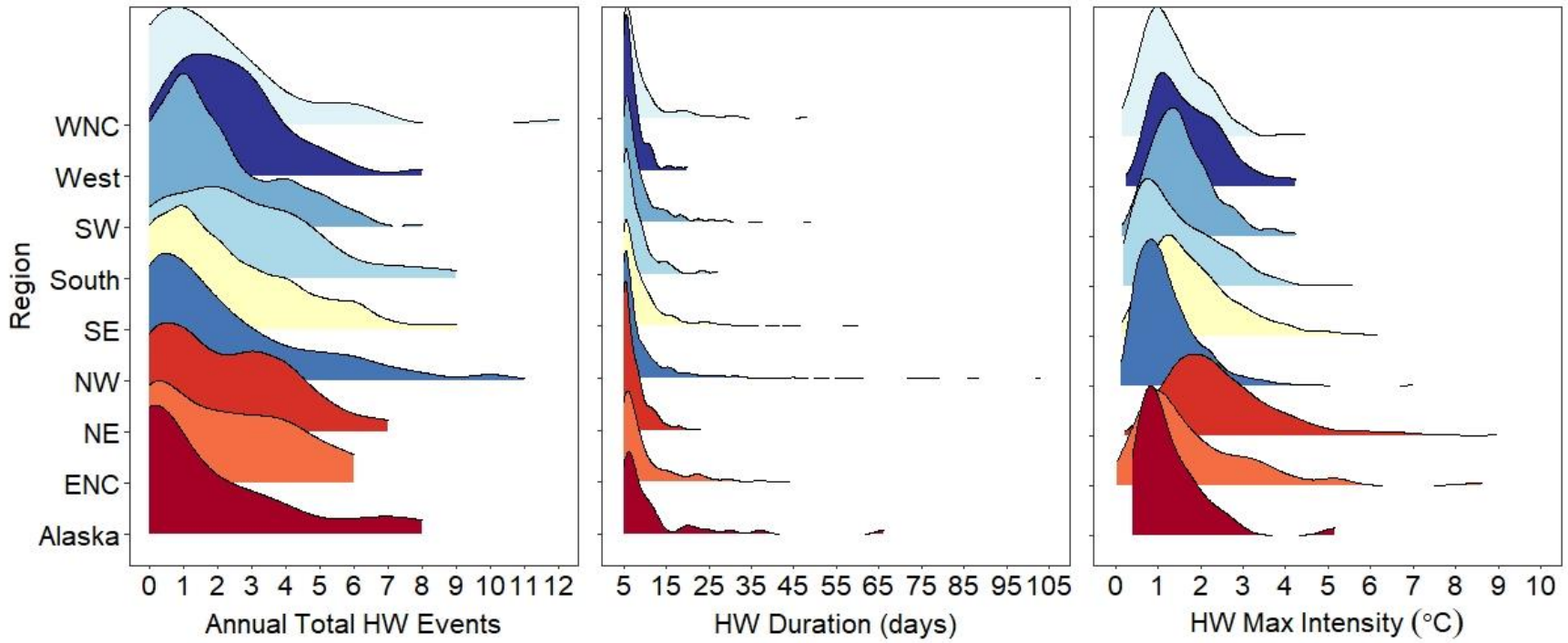

SI Figure 2.1 Regional density distribution of the annual total number of riverine heatwaves between 1996-2021 (left), heatwave duration (middle), and maximum heatwave intensity (right).

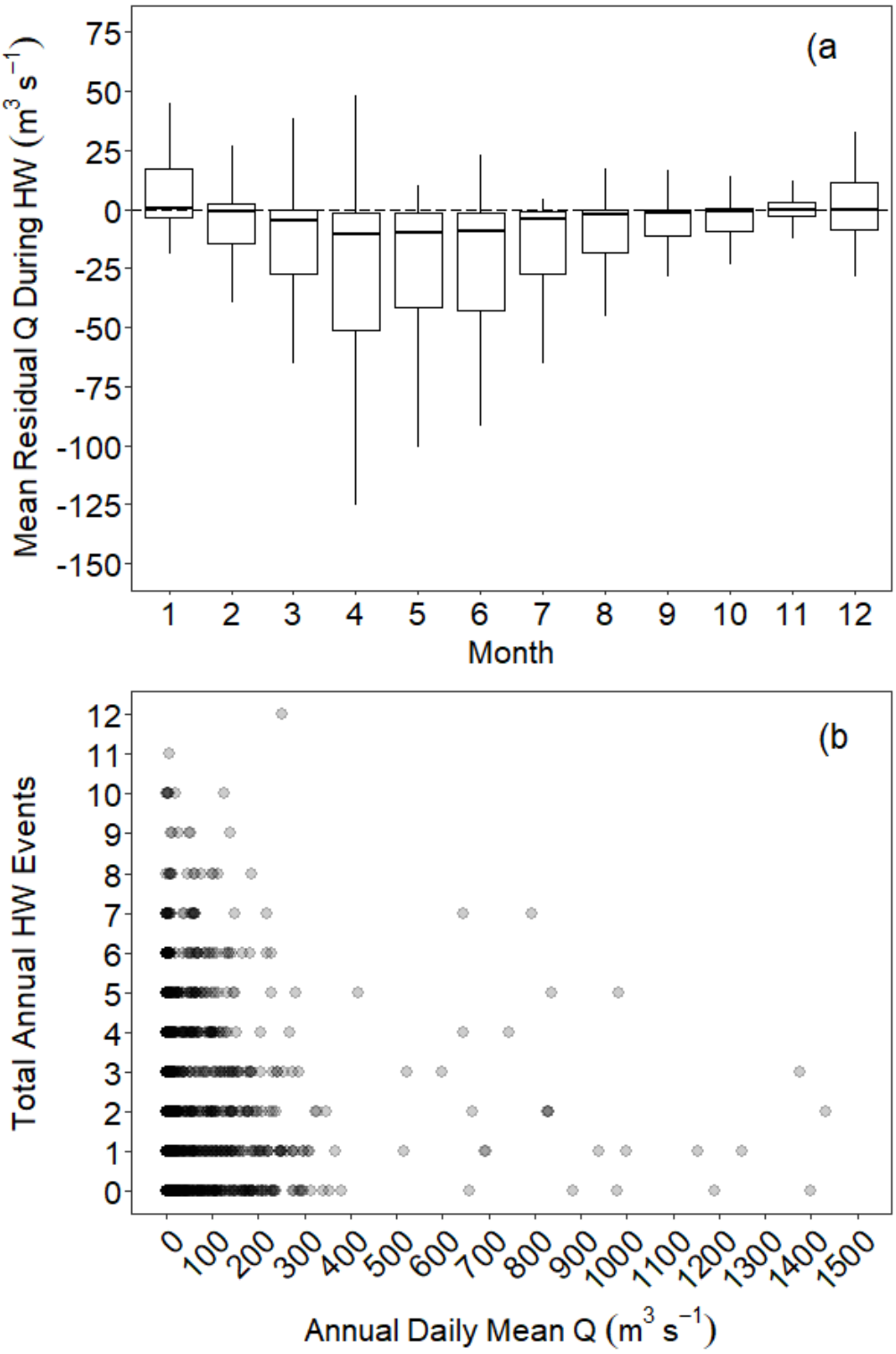

SI Figure 2.2 Boxplots of the mean residual discharge (Q) during each heatwave event grouped by month (a; 1 = Jan, 12 = Dec). The bold line within the boxplots represents the median and outliers have been removed. Scatterplot of the total annual number of riverine heatwave events as a function of annual daily mean discharge (b).

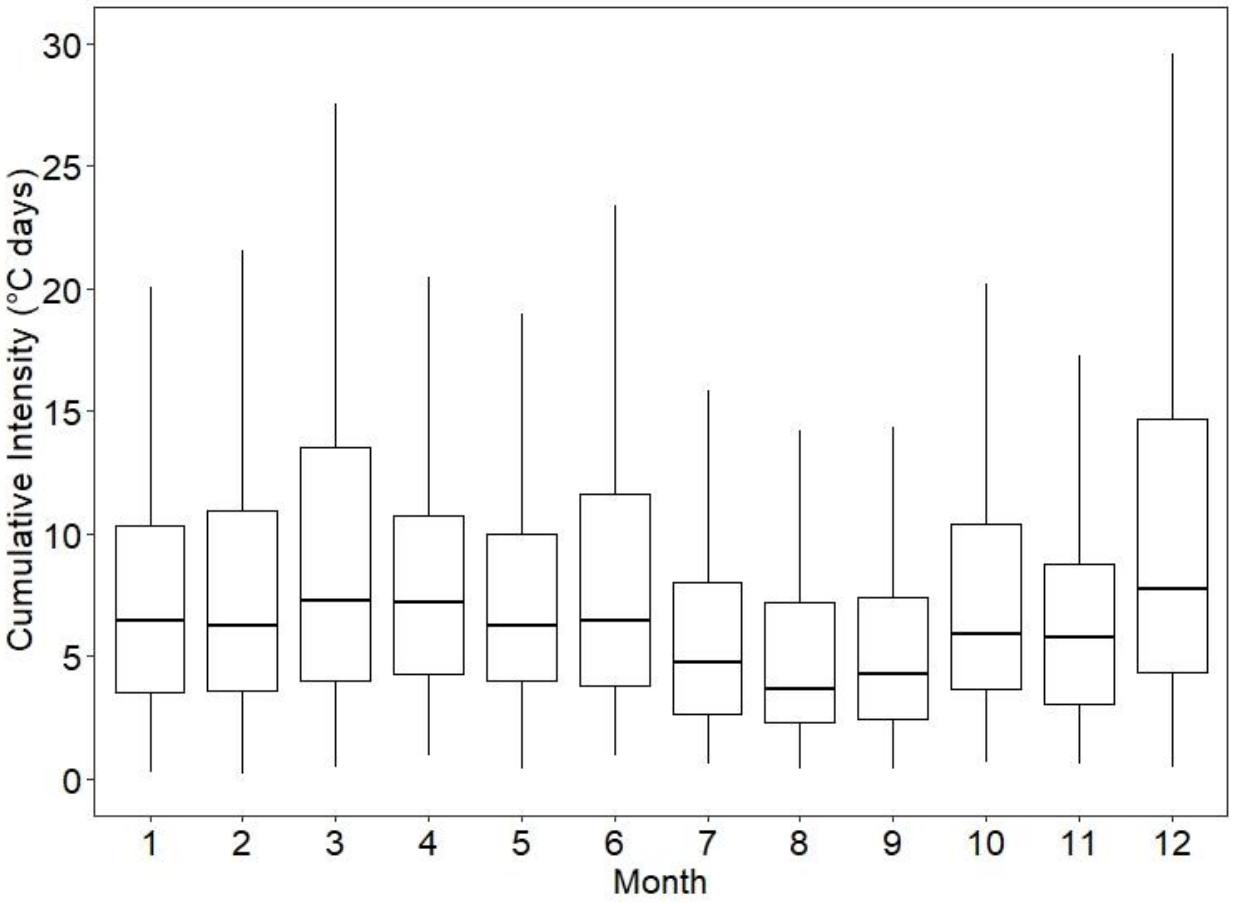

SI Figure 2.3 Boxplots of cumulative intensity above the 90th percentile threshold for heatwaves among all months.

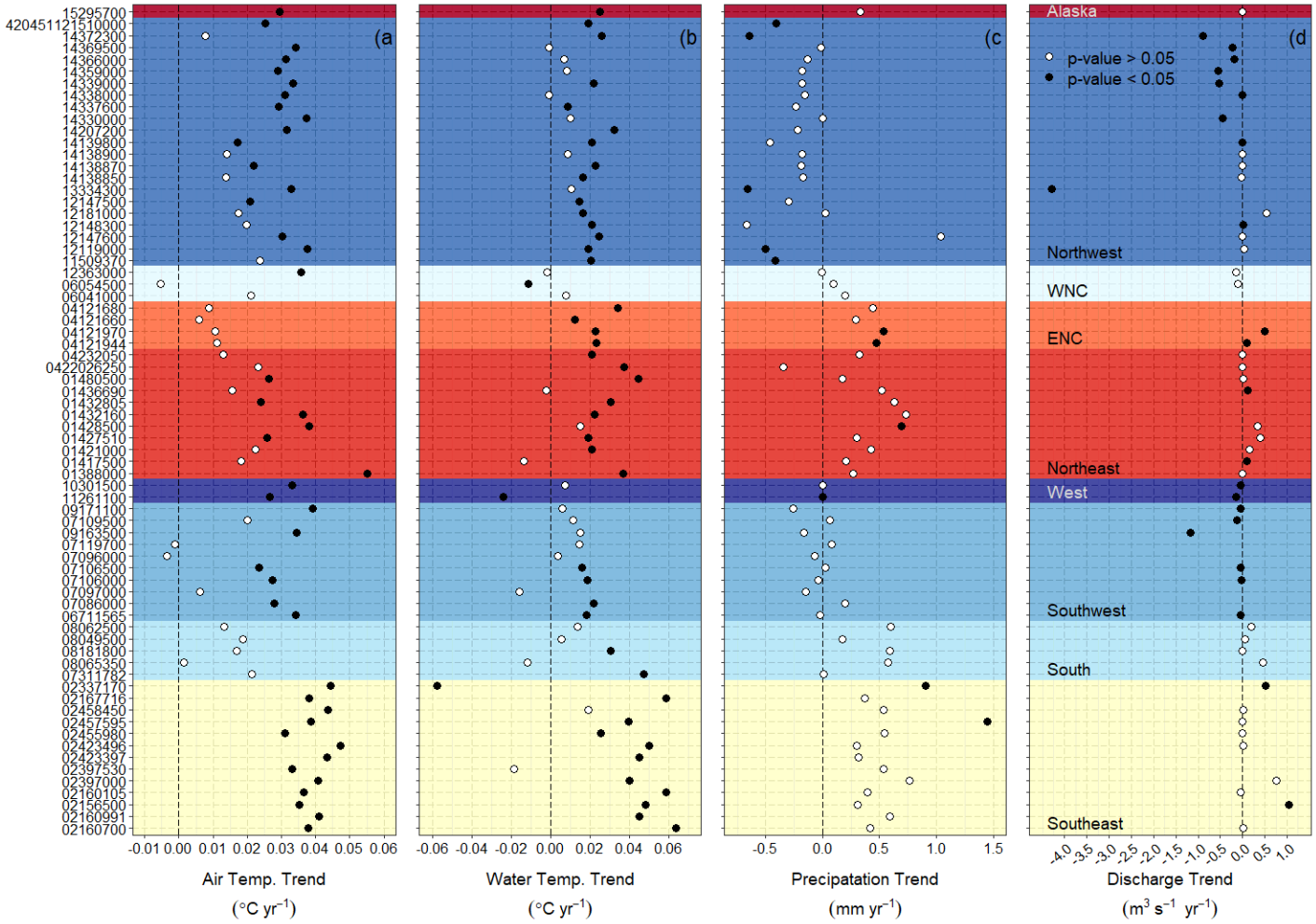

SI Figure 2.4 Sen's slope trend estimates for air temperature (a), water temperature (b), precipitation (c; all forms converted to water equivalent), and discharge (d) for all 70 sites (USGS site numbers on y-axis) throughout the U.S. Colors within the plots denote U.S. regions from Figure 1. Black dots represent statistically significant (p-value < 0.05) trends as determined using Seasonal-Kendall tests, while white dots represent non-statistically significant trends (p-value > 0.05). Significant trends close to zero are associated with sites that have a relatively low absolute mean value. WNC = West North Central, ENC = East North Central.

Appendix 2: Supplemental Information to Chapter 3

SI Table 3.1 Linear regression trends for 24-years of annual total duration (days year^{-1} ± SE) of estuarine heatwaves (EHW), low DO, and low pH events and associated p-values (p-val.). Statistically significant (p-value < 0.05) trends are bolded and italicized.

Estuary	Region	Reserve Code	Station ID	EHW	p-val.	Low DO	p-val.	Low pH	p-val.
Wells, ME	Northeast	WEL	IN	1.77 ± 1.12	0.138	-3.61 ± 2.93	0.249	-2.52 ± 2.45	0.325
Great Bay, NH		GRB	GB	0.56 ± 0.57	0.346	-0.83 ± 0.81	0.323	0.01 ± 1.13	0.990
Hudson River, NY		HUD	SK	0.82 ± 0.59	0.185	0.67 ± 0.56	0.251	-1.56 ± 0.91	0.114
			TS	-0.63 ± 0.95	0.518	-0.49 ± 0.92	0.606	***-1.53 ± 0.47***	***0.004***
Narragansett Bay, RI		NAR	PC	1.37 ± 0.85	0.127	***-2.08 ± 0.81***	***0.028***	-3.65 ± 2.16	0.120
Delaware, DE	Mid-Atlantic	DEL	BL	0.20 ± 0.30	0.510	***-0.94 ± 0.43***	***0.042***	-1.49 ± 1.01	0.159
			SL	-0.20 ± 0.37	0.584	0.13 ± 0.66	0.843	***-2.41 ± 1.08***	***0.038***
Chesapeake Bay, VA		CBV	TC	-0.13 ± 0.31	0.687	-0.82 ± 0.58	0.176	-0.25 ± 0.93	0.792
North Carolina, NC	Southeast	NOC	EC	0.05 ± 0.36	0.884	0.14 ± 0.61	0.817	0.24 ± 0.85	0.778
			RC	0.34 ± 0.61	0.585	-0.42 ± 0.91	0.648	0.01 ± 1.01	0.994
ACE Basin, SC		ACE	SP	0.59 ± 0.61	0.349	-0.50 ± 0.77	0.527	-2.37 ± 1.16	0.062
Jobos Bay, PR		JOB	09	***1.23 ± 0.47***	***0.018***	-3.04 ± 1.53	0.070	-0.75 ± 0.74	0.329
Apalachicola, FL	Gulf of Mexico	APA	EB	-0.66 ± 0.51	0.212	0.25 ± 0.63	0.697	-0.04 ± 0.63	0.952
			ES	-0.21 ± 0.57	0.715	-0.49 ± 0.41	0.258	0.13 ± 0.60	0.833
Padilla Bay, WA	West	PDB	BY	0.86 ± 0.63	0.190	0.06 ± 0.44	0.885	-2.59 ± 1.61	0.132
Elkhorn Slough, CA		ELK	AP	0.07 ± 0.73	0.927	***-1.14 ± 0.44***	***0.019***	***-4.07 ± 1.45***	***0.015***
			SM	-0.43 ± 0.82	0.607	-0.58 ± 0.59	0.338	***-3.03 ± 1.20***	***0.022***

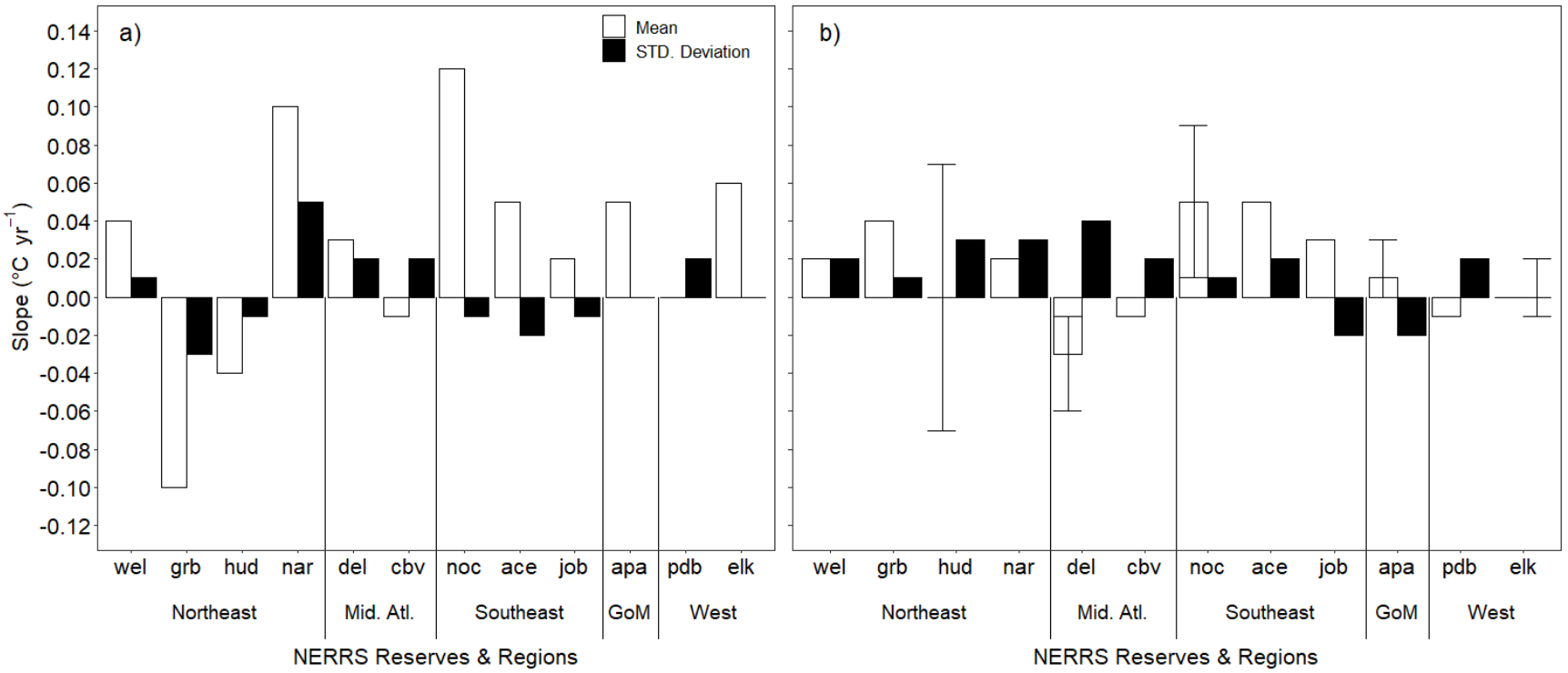

SI Figure 3.1 Slope of the linear regression between mean annual air (a) and water (b) temperature (white columns) and annual standard deviation (black columns) for each NERRS reserve. Error bars represent the range between multiple stations within a reserve.

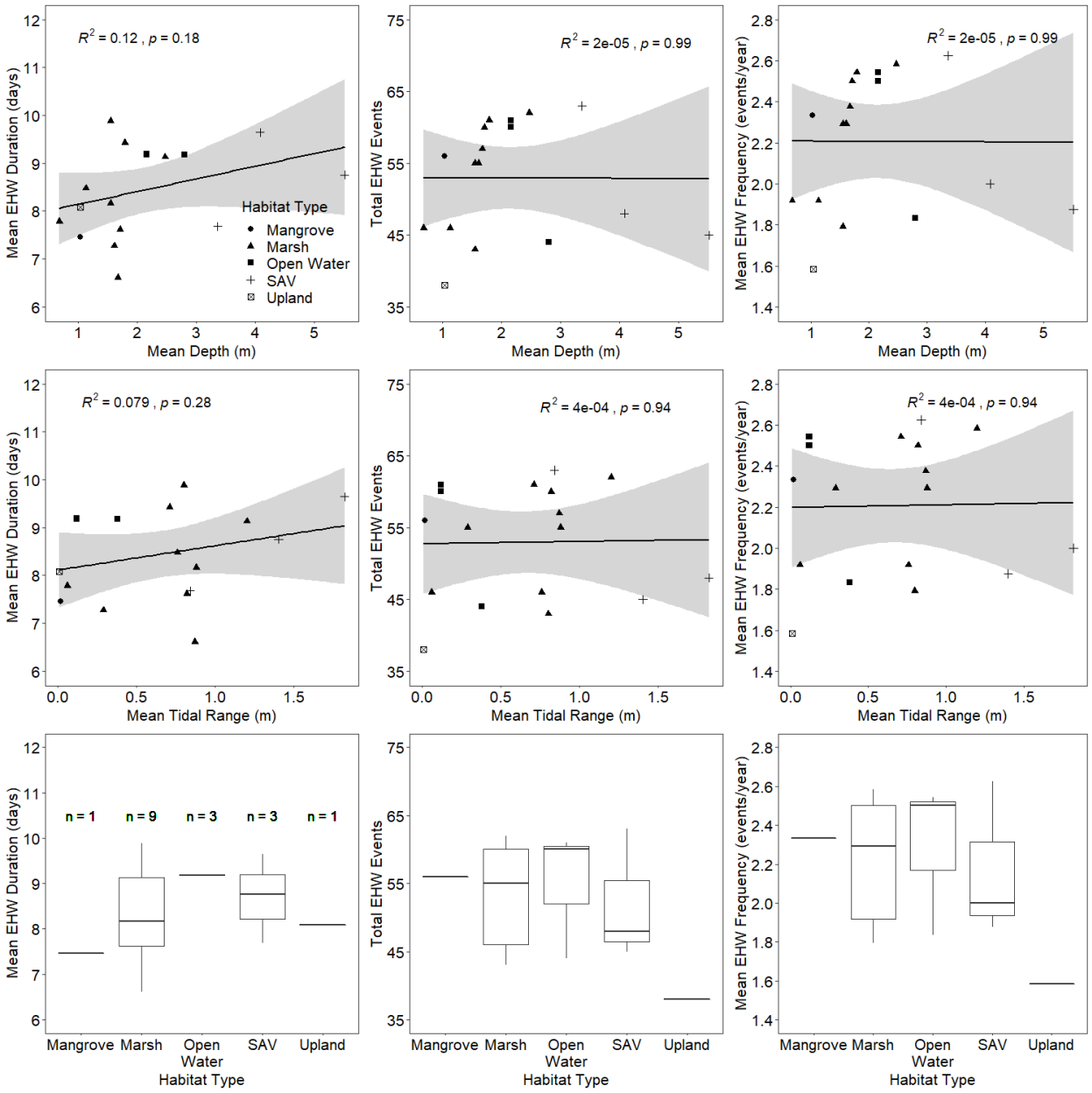

SI Figure 3.2 Linear regression and boxplot results for EHW characteristics as a function of NERRS station mean depth, mean tidal range (top and middle row respectively), and estuarine habitat type (bottom row).

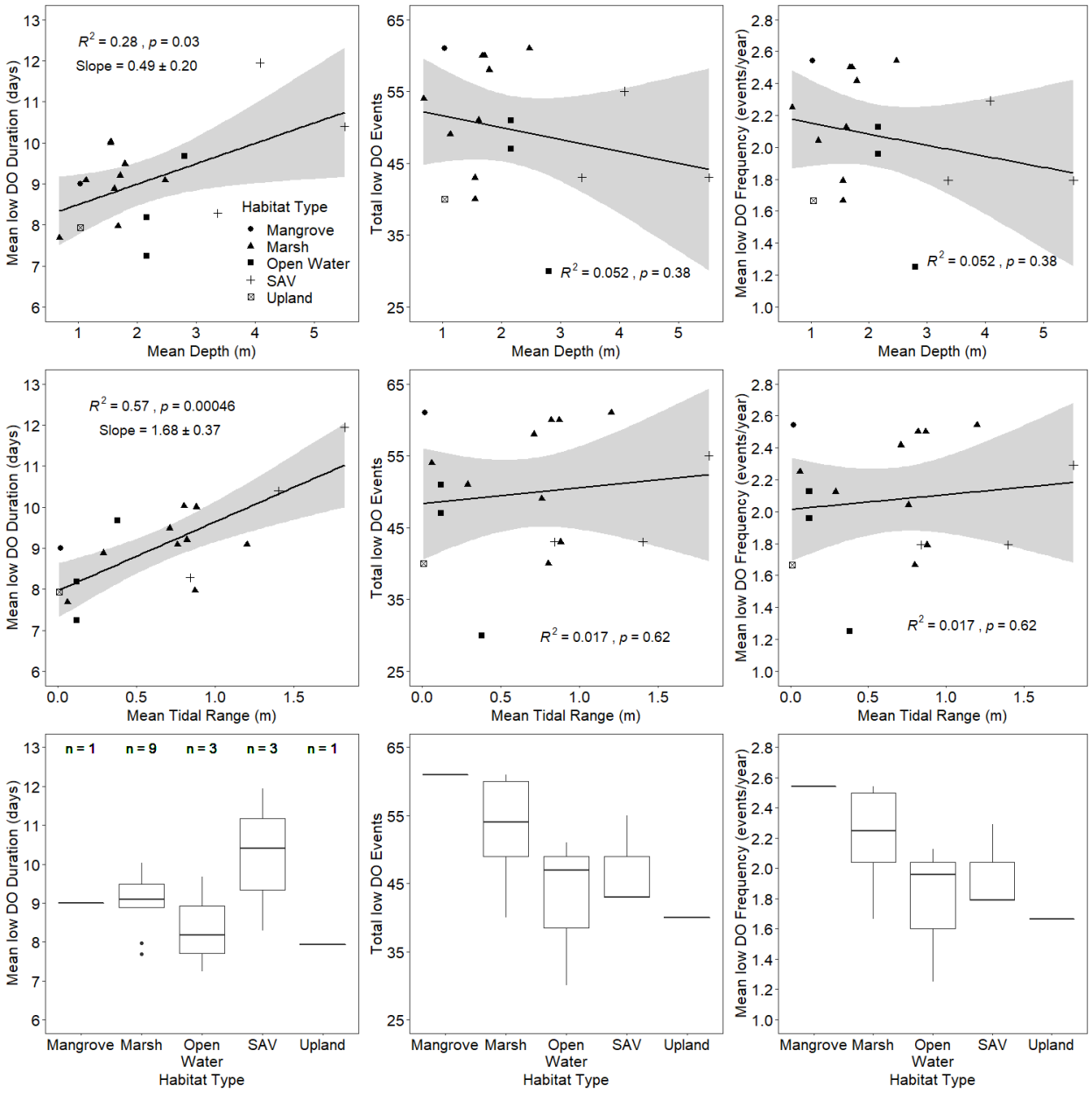

SI Figure 3.3 Linear regression and boxplot results for low DO event characteristics as a function of NERRS station mean depth, mean tidal range (top and middle row respectively), and estuarine habitat type (bottom row).

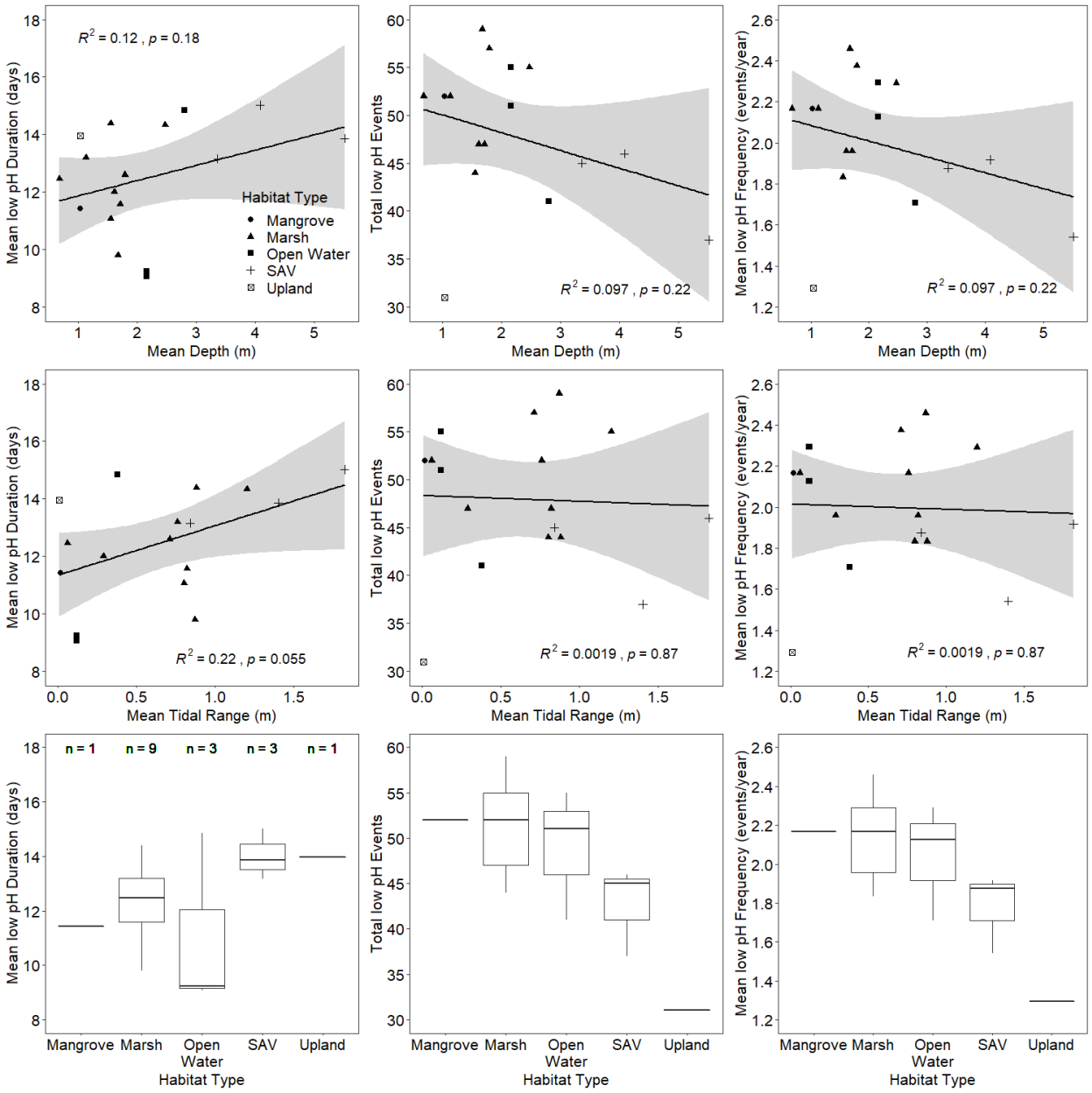

SI Figure 3.4 Linear regression and boxplot results for low pH event characteristics as a function of NERRS station mean depth, mean tidal range (top and middle row respectively), and estuarine habitat type (bottom row).

Appendix 3: Supplemental Information to Chapter 5

SI Table 5.1 Papers that provided seagrass recovery data used in this synthesis

Author & Pub Year	Journal	DOI
Abadie et al. 2019	*Frontiers in Ecology and Evolution*	10.3389/fevo.2019.00190
Alexandre et al. 2005	*Marine Ecology Progress Series*	10.3354/meps298115
Aoki et al. 2021	*Frontiers in Marine Science*	10.3389/fmars.2020.576784
Balsby et al. 2017	*Frontiers in Marine Science*	10.3389/fmars.2016.00285
Barañano et al. 2017	*Marine Biology Research*	10.1080/17451000.2017.1307989
Boese 2002	*Aquatic Botany*	10.1016/S0304-3770(02)00004-9
Boese et al. 2009	*Journal of Experimental Marine Biology and Ecology*	10.1016/j.jembe.2009.04.011
Bryars and Neverauskas 2004	*Aquatic Botany*	10.1016/j.aquabot.2004.09.001
Cabaço et al. 2005	*Marine Ecology Progress Series*	10.3354/meps298123
Cambridge 2002	*Bulletin of Marine Science*	+
Cardoso et al. 2010	*Marine Pollution Bulletin*	10.1016/j.marpolbul.2009.11.004
Collier et al. 2009	*Journal of Experimental Marine Biology and Ecology*	10.1016/j.jembe.2008.12.003
Creed et al. 1999	*Journal of Experimental Marine Biology and Ecology*	10.1016/S0022-0981(98)00188-9
Cyrus et al. 2008	*African Journal of Aquatic Science*	10.2989/AJAS.2008.33.3.4.616
Dawes et al. 1997	*Aquatic Botany*	10.1016/S0304-3770(97)00021-1
de Iongh et al. 1995	*Aquatic Botany*	10.1016/0304-3770(94)00438-R
Di Carlo and Kenworthy 2008	*Oecologia*	10.1007/s00442-008-1120-0
Eckrich and Holmquist 2000	*Marine Ecology Progress Series*	10.3354/meps201199
Eklöf et al. 2009	*Marine and Freshwater Research*	10.1071/MF09008
Eklöf et al. 2011	*PLoS ONE*	10.1371/journal.pone.0023229
El-Hacen et al. 2018	*Scientific Reports*	10.1038/s41598-018-34977-5
Frederiksen et al. 2004	*Aquatic Botany*	10.1016/j.aquabot.2003.10.002
Godet et al. 2008	*Diseases of Aquatic Organisms*	10.3354/dao01897
González-Correa et al. 2005	*Journal of Experimental Marine Biology and Ecology*	10.1016/j.jembe.2004.12.032
Greening and Janicki 2006	*Environmental Management*	10.1007/s00267-005-0079-4
Hammerstorm et al. 2007	*Marine Ecology Progress Series*	10.3354/meps07004
Heck and Valentine 1995	*Journal of Experimental Marine Biology and Ecology*	10.1016/0022-0981(95)00012-G
Kenworthy et al. 2002	*Journal of Coastal Research*	++
Kim et al. 2020	*Frontiers in Marine Science*	10.3389/fmars.2020.00500
Lee et al. 2007	*Marine Ecology Progress Series*	10.3354/meps342105
Lundquist et al. 2018	*Scientific Reports*	10.1038/s41598-018-31398-2
Macreadie et al. 2014	*Ecology and Evolution*	10.1002/ece3.933
McMahon et al. 2011	*Marine Pollution Bulletin*	10.1016/j.marpolbul.2010.11.001
Meehan and West 2000	*Aquatic Botany*	10.1016/S0304-3770(99)00097-2
Nakaoka and Aioi 1999	*Marine Ecology Progress Series*	10.3354/meps184097
Neckles et al. 2005	*Marine Ecology Progress Series*	10.3354/meps285057
Olesen et al. 2004	*Estuaries*	10.1007/BF02912039
Orth et al. 2020	*Science Advances*	10.1126/sciadv.abc6434
Park et al. 2009	*Estuarine, Coastal and Shelf Science*	10.1016/j.ecss.2008.10.003

SI Table 5.1 con't.

Author & Pub Year	Journal	DOI
Pergent-Martini et al. 2002	Bulletin of Marine Science	+++
Peterken and Conacher 1997	Aquatic Botany	10.1016/S0304-3770(97)00061-2
Peterson et al. 1987	*Fishery Bulletin*	++++
Plus et al. 2003	*Aquatic Botany*	10.1016/S0304-3770(03)00089-5
Preen 1995	*Marine Ecology Progress Series*	10.3354/meps124201
Preen et al. 1995	*Aquatic Botany*	10.1016/0304-3770(95)00491-H
Qin et al. 2016	*Aquatic Botany*	10.1016/j.aquabot.2016.01.002
Rasheed 1999	*Journal of Experimental Marine Biology and Ecology*	10.1016/S0022-0981(98)00158-0
Rasheed 2004	*Journal of Experimental Marine Biology and Ecology*	10.1016/j.jembe.2004.03.022
Rasheed et al. 2014	*Marine Pollution Bulletin*	10.1016/j.marpolbul.2014.02.013
Rollon et al. 1999	*Marine Pollution Bulletin*	10.1016/S0025-326X(99)00105-8
Ruesink et al. 2012	*Journal of Experimental Marine Biology and Ecology*	10.1016/j.jembe.2012.05.002
Sheridan 2004	*Estuarine, Coastal and Shelf Science*	10.1016/j.ecss.2003.10.004
Short 1983	*Journal of Experimental Marine Biology and Ecology*	10.1016/0022-0981(83)90159-4
Smith et al. 2016	*Marine Ecology Progress Series*	10.3354/meps11531
Soissons et al. 2014	*Marine Pollution Bulletin*	10.1016/j.marpolbul.2014.07.057
Soissons et al. 2016	*Ecological Indicators*	10.1016/j.ecolind.2016.01.030
Vaudrey 2010	*Aquatic Botany*	10.1016/j.aquabot.2010.08.005
Williams 1988	*Marine Ecology Progress Series*	10.3354/meps042063
Williams 1990	*Ecological Monographs*	10.2307/1943015
York 2015	*Scientific Reports*	10.1038/srep13167

+ Vol. 71, No. 3, November 2002, pp.1279-1289
++ Special Issue No. 37, Fall 2002, pp.75-85
+++ Vol. 71, No. 3, November 2002, pp.1227-1236
++++ Vol. 85, No. 2, January 1987, pp.281-298

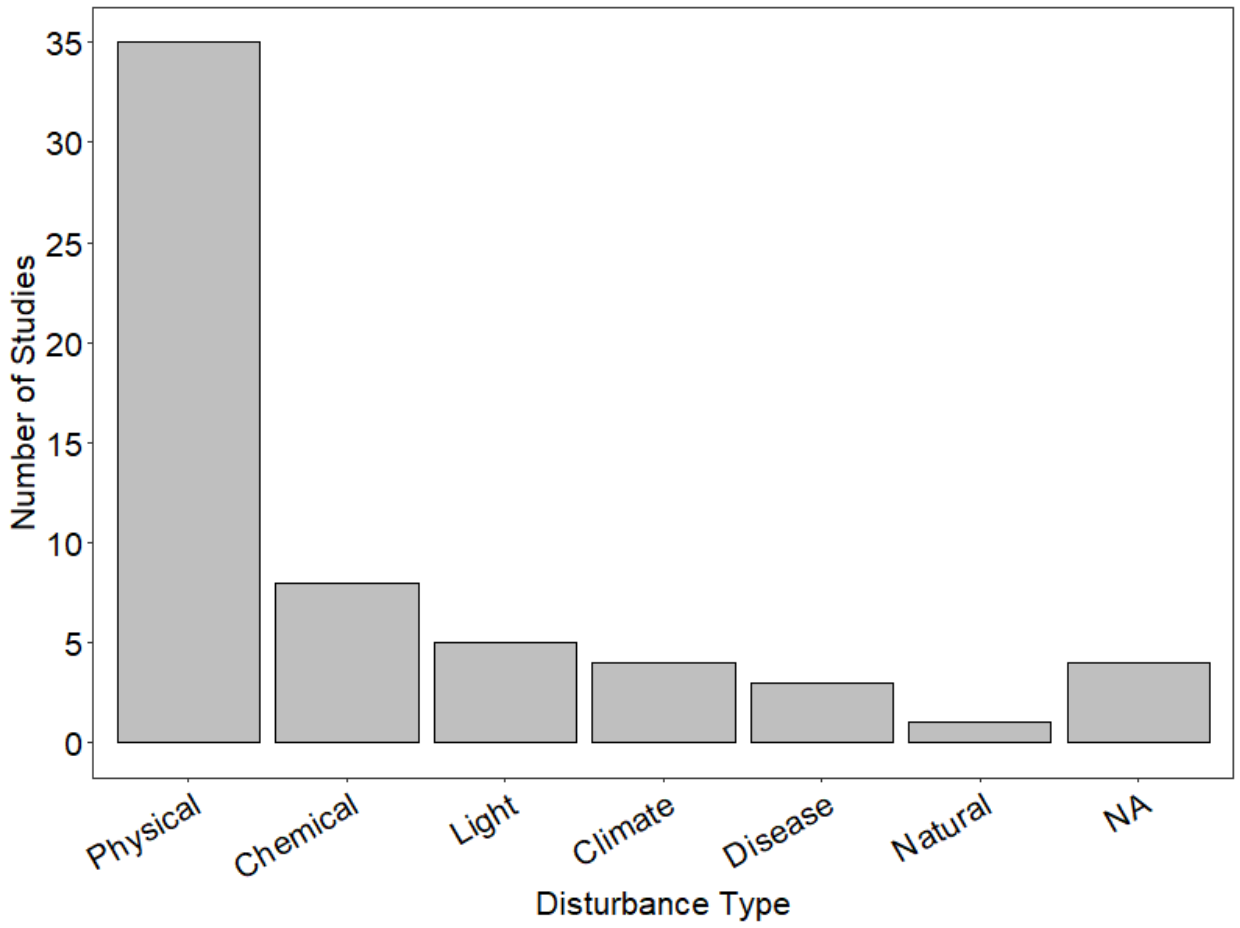

SI Figure 5.1 Seagrass disturbance classification cited among the 60 studies considered.

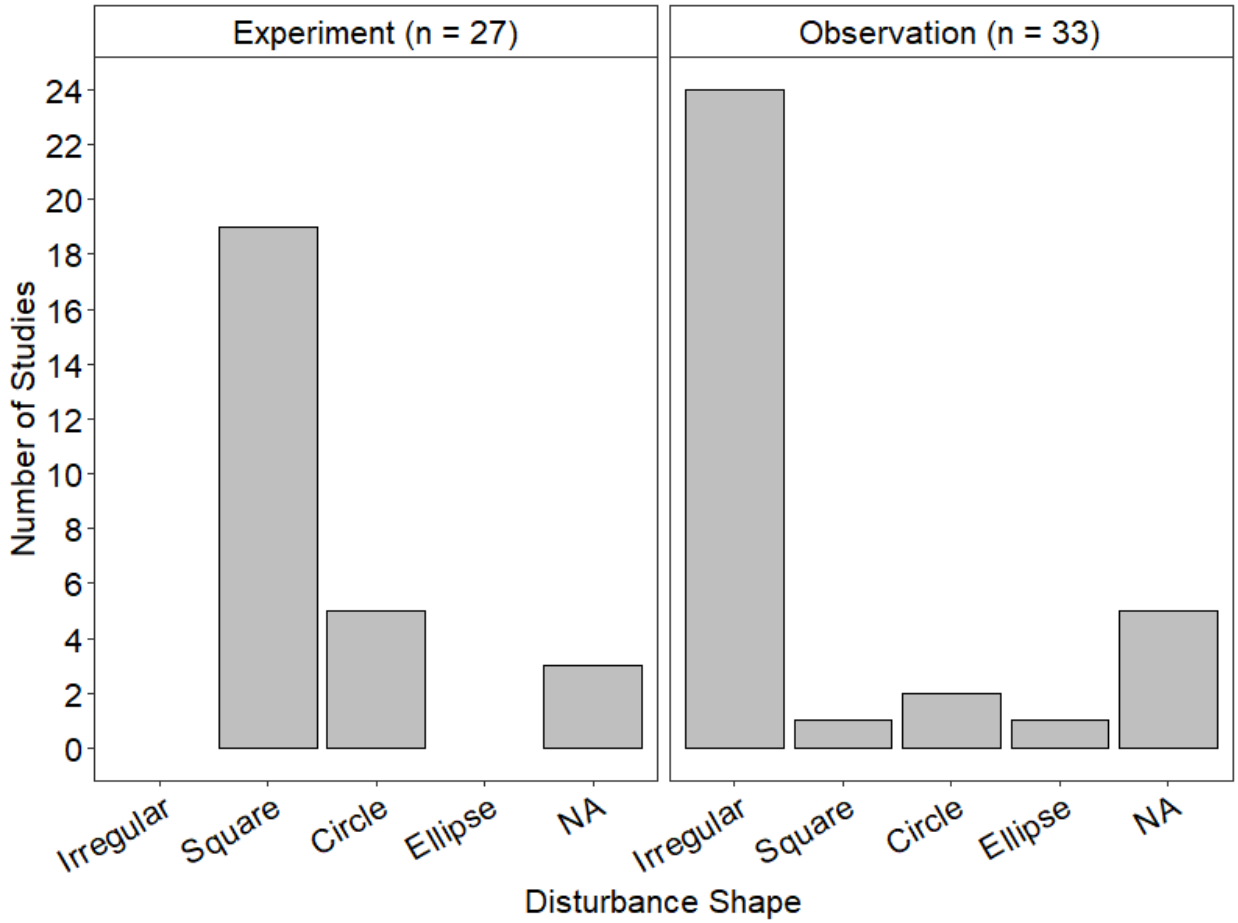

SI Figure 5.2 Recovery shape of the 60 studies considered in this analysis. Studies that did not indicate recovery shape in text or figures were classified as NA for missing data.

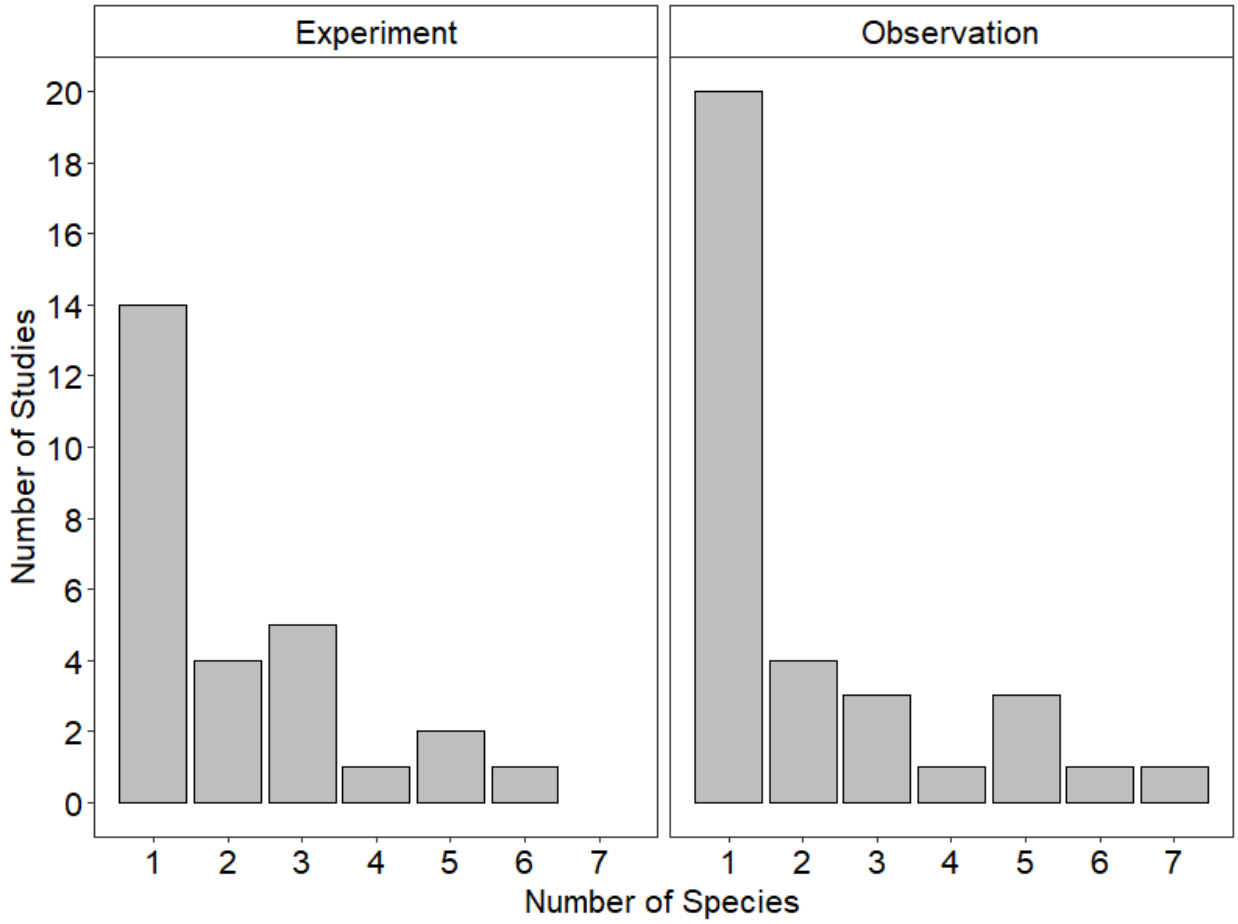

SI Figure 5.3 Number of seagrass species included in experimental (left) and observational (right) studies of seagrass recovery.

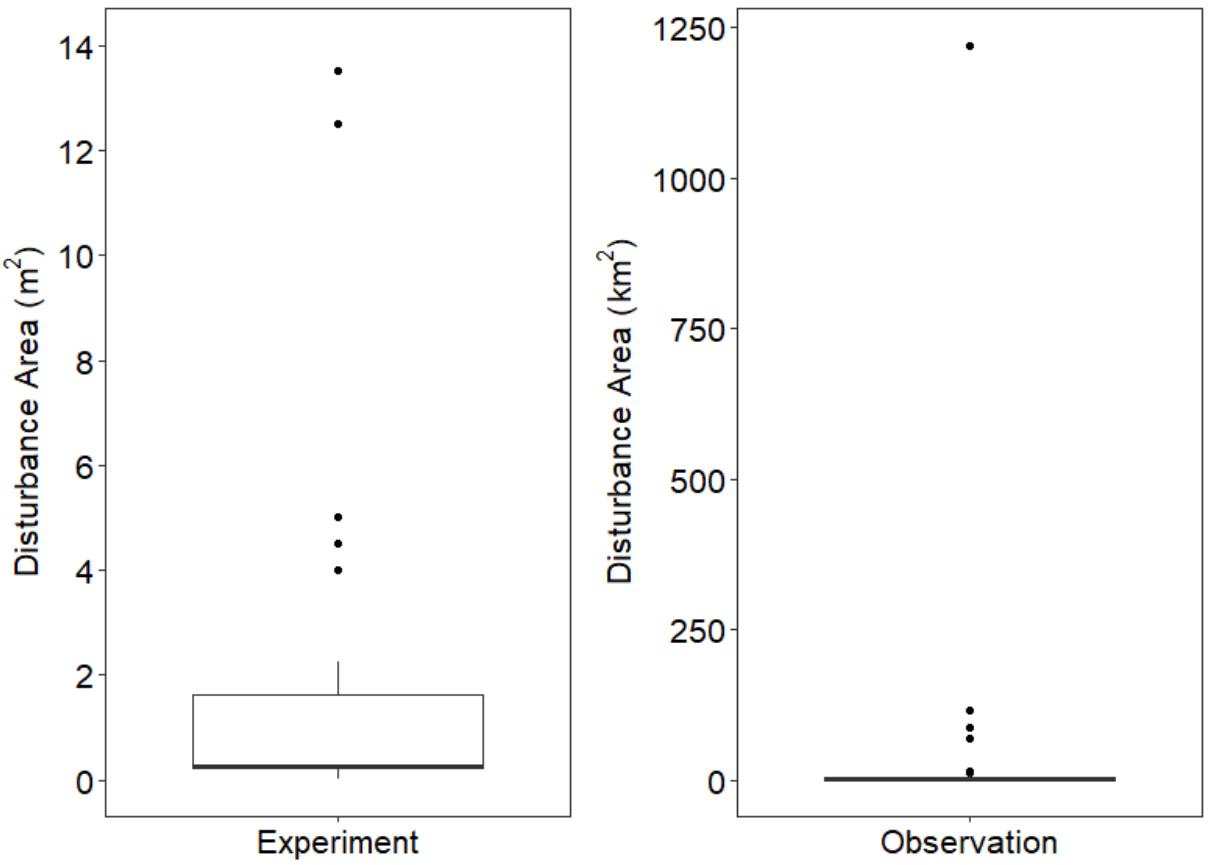

SI Figure 5.4 Disturbance area in experimental (left) and observational (right) studies of seagrass recovery. The experimental figure does not include the results of this study which had a disturbance area of 28.3 m^2.

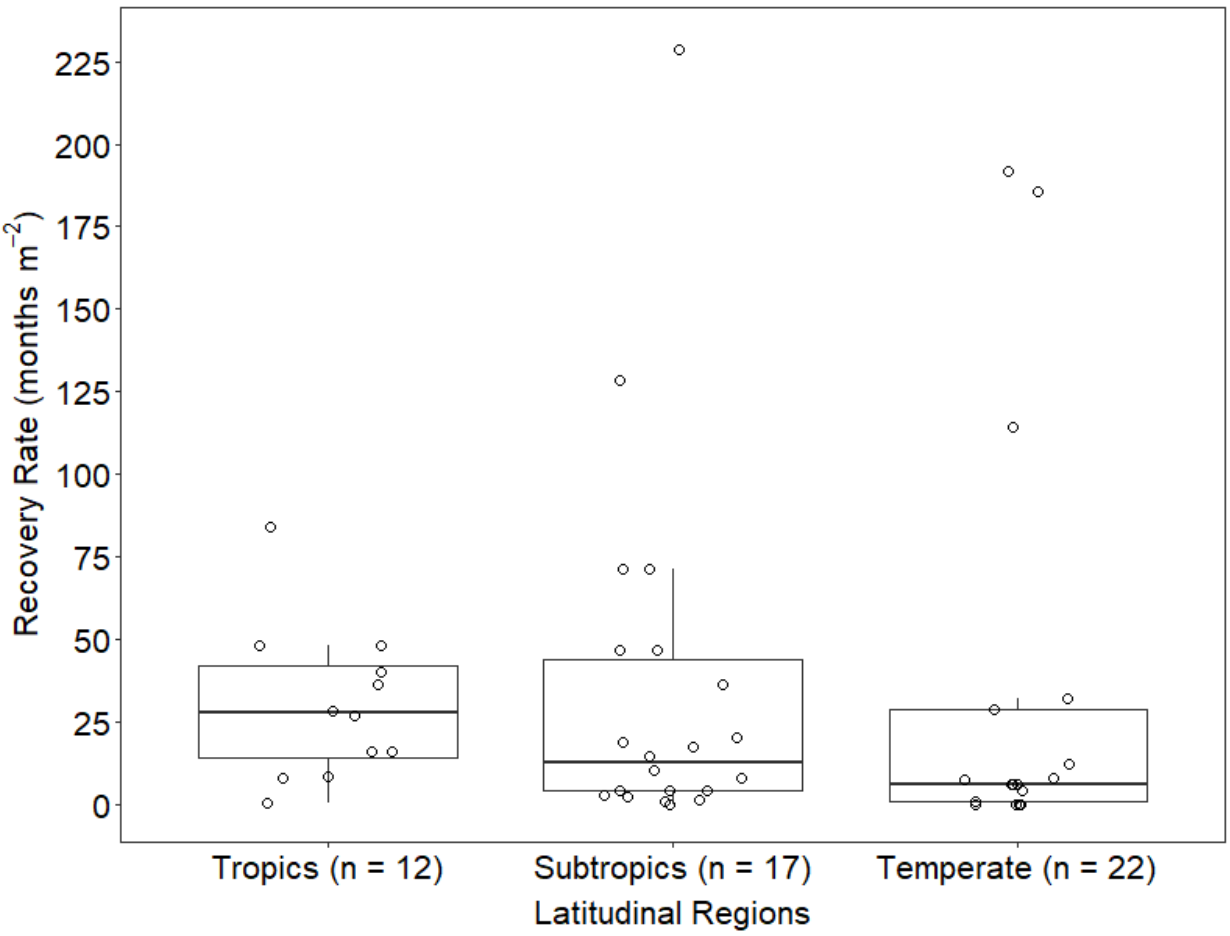

SI Figure 5.5 Range of seagrass recovery rates per latitudinal region. Dots represent individual experimental or observational studies that had ≥ 80% of the aboveground biomass disturbed and ≥ 90% recovery during the study period. Dots are jittered for visibility.